

---

International Conference on Case Histories in Geotechnical Engineering (1984) - First International Conference on Case Histories in Geotechnical Engineering

---

08 May 1984, 6:30 pm - 8:30 pm

## Guest Lecture – Foundation Engineering for Gravity Structures in the Northern North Sea

Ove Eide  
*Norwegian Geotechnical Institute, Oslo, Norway*

Knut H. Andersen  
*Norwegian Geotechnical Institute, Oslo, Norway*

Follow this and additional works at: <https://scholarsmine.mst.edu/icchge>



Part of the [Geotechnical Engineering Commons](#)

---

### Recommended Citation

Eide, Ove and Andersen, Knut H., "Guest Lecture – Foundation Engineering for Gravity Structures in the Northern North Sea" (1984). *International Conference on Case Histories in Geotechnical Engineering*. 1. <https://scholarsmine.mst.edu/icchge/1icchge/1icchge-theme4/1>

This Article - Conference proceedings is brought to you for free and open access by Scholars' Mine. It has been accepted for inclusion in International Conference on Case Histories in Geotechnical Engineering by an authorized administrator of Scholars' Mine. This work is protected by U. S. Copyright Law. Unauthorized use including reproduction for redistribution requires the permission of the copyright holder. For more information, please contact [scholarsmine@mst.edu](mailto:scholarsmine@mst.edu).

# Guest Lecture

## Foundation Engineering For Gravity Structures In The Northern North Sea

Ove Eide

Chief Engineer, Norwegian Geotechnical Institute, Oslo, Norway

Knut H. Andersen

Head, Analysis Group, Norwegian Geotechnical Institute, Oslo, Norway

**SYNOPSIS** During the past 10 years, 15 gravity structures have been installed in the northern North Sea. As new gravity structures are being designed for installation on softer soils and at greater depths, they still pose a great challenge to soil mechanics and foundation engineering. Great improvements have been made during the 10-year period. This applies to soil investigations, in-situ measurements, undisturbed sampling, laboratory testing and design analyses. Compared to structures on land, offshore gravity structures are characterised by large foundation areas, the installation method, and the cyclic wave loading state. The paper reviews investigation methods, site and soil conditions, construction principles, instrumentation and installation. The main emphasis, however, is given to current foundation design practice and experiences from full scale measurements.

### INTRODUCTION

Exploratory drilling for oil and gas on the Norwegian Continental Shelf started in 1966, and the first commercial discovery was made in 1968 in the Ekofisk area. Oil production started here in 1971 from the jack-up platform Gulftide.

Oil and gas fields in the northern North Sea are shown in Fig. 1, and the different continental shelves around Norway are shown in Fig. 2.

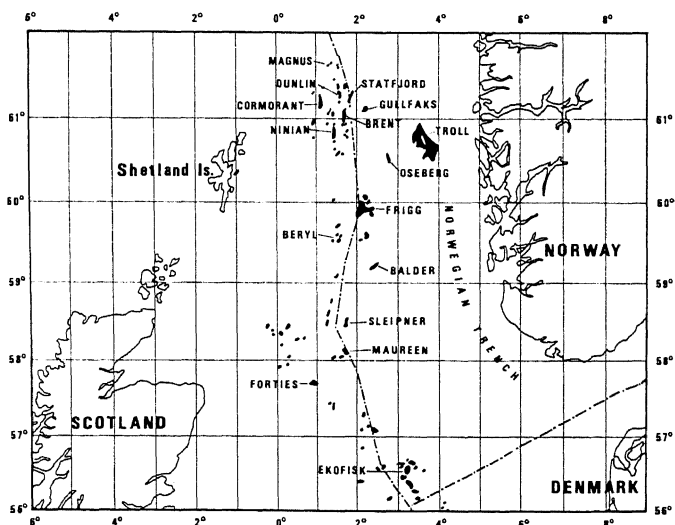


Fig. 1. Oil and gas fields in the northern North Sea.

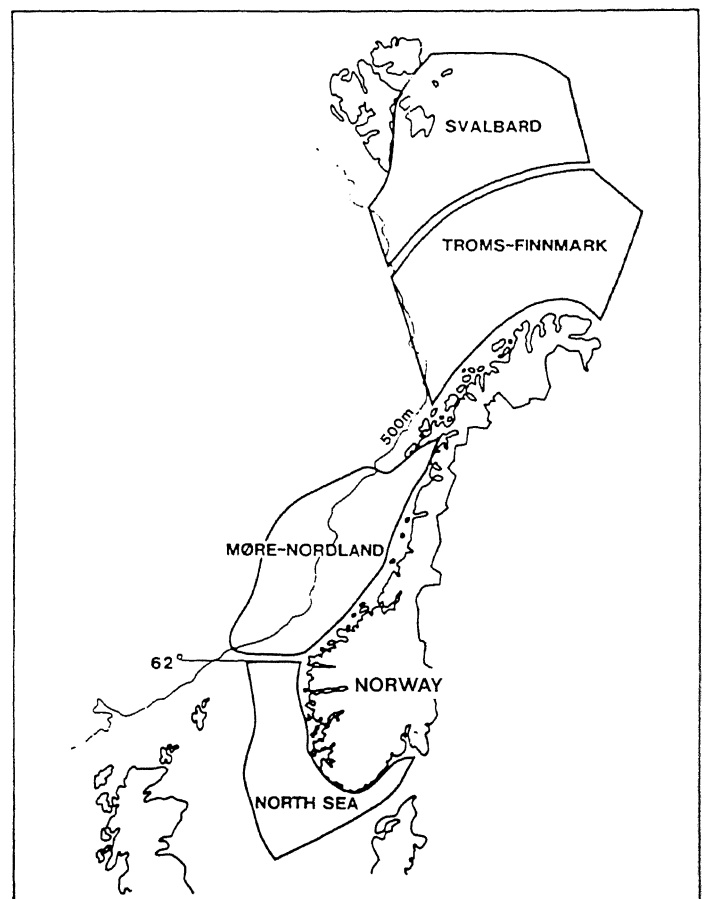


Fig. 2. The different continental shelves around Norway.

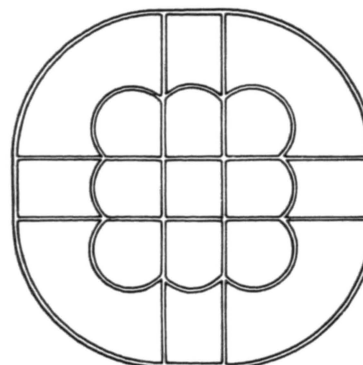
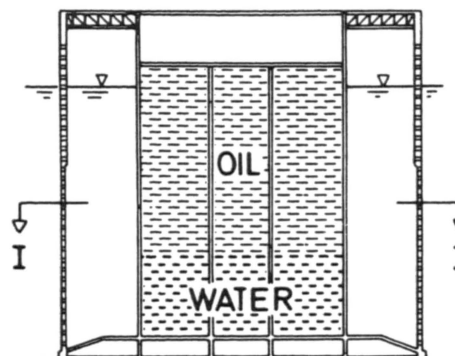
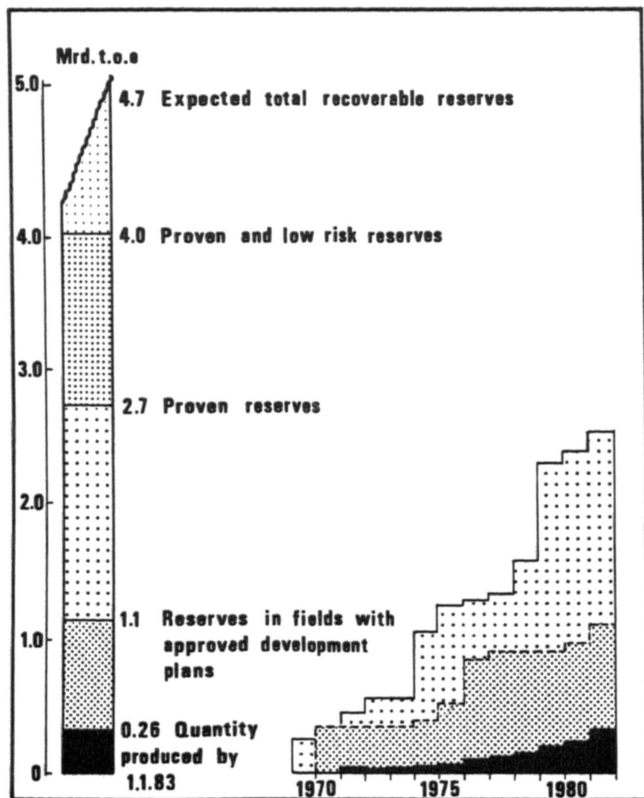
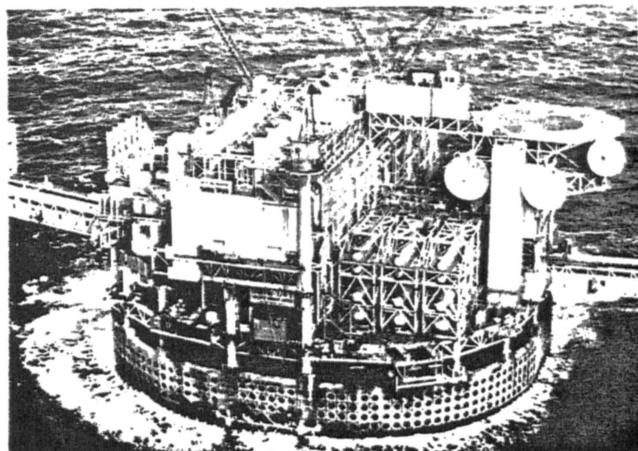
Reserves discovered and production in the Norwegian sector south of 62° are shown in Fig. 3.

The Ekofisk oil storage tank, Fig. 4, the first concrete structure to be placed in the northern North Sea, was ordered by Phillips Petroleum Company in May 1971 from the main contractor C.G. Doris (Marion, 1974). Construction work was carried out in Stavanger, Norway, by the contractors Selmer and Høyer Ellefsen, who later formed the company Norwegian Contractors together with Furuholmen.

The purpose of the tank was to store oil during bad weather conditions when offshore loading to a tanker was prohibited, and before the pipeline to shore had been laid. The capacity of the tank is one million barrels, i.e. 160 000 m<sup>3</sup>, corresponding to three days production. During storage, oil replaces sea water. The water is cleaned before it is pumped into sea again.

This pioneering work with concrete opened up the prospect of building concrete gravity platforms in the North Sea, and a great number of platform concepts were developed, at least 20 (New Civil Engineer special feature, 1973). Back in 1973 prognoses indicated that as many as 80 concrete platforms may be required in the next 20 years. This is certainly not the case, but in Norway concrete platforms have been continuously under construction since 1973, and it looks as though this will continue for many years to come.

The fixed offshore platforms may serve several different purposes, i.e. drilling, production and providing living quarters, and sometimes also oil storage. Loading into a tanker usually takes place from a separate loading buoy if the platform is not connected to a pipeline.



SECTION I-I

Fig. 3. Reserves discovered and production in the Norwegian sector south of 62°.

Fig. 4. The Ekofisk oil storage tank.

One reason for utilizing fixed platforms for oil and gas production in the North Sea is the great depth to the reservoirs, usually 3000 to 5000 m.

By diverting the wells, a very large area (many km<sup>2</sup>) can be covered from one platform location, as illustrated in Fig. 5.

The structure of a typical North Sea oil well is shown in Fig. 6.

The potential advantages of concrete gravity platforms compared to traditional steel jackets may be listed as follows:

- The structure can be completed near shore in calm waters and the deck and all fittings installed.
- There is a short installation period and limited risk during installation.
- The concrete will gain strength with time, and has few corrosion and fatigue problems, and consequently there will be less need for inspection.
- Conductors and risers are protected in concrete shafts.
- There is potential oil storage capacity with small additional cost.

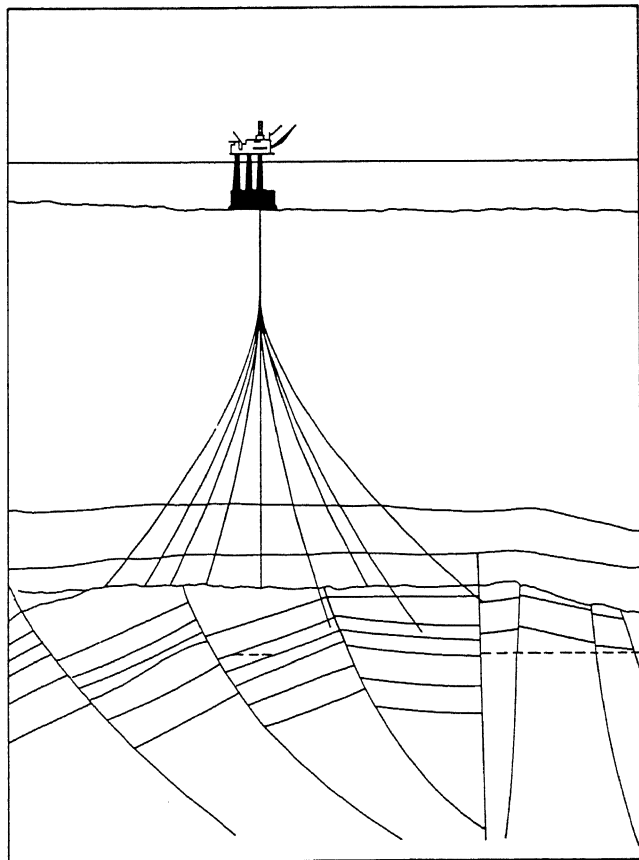


Fig. 5. Diversion of wells to deep reservoirs.

Costs are certainly a major competitive aspect, and the first concrete platforms were less expensive than steel jackets. This has, however, been evened out by improvements in the steel jackets, increased capacity of pile driving equipment and crane barges. The cost of the concrete structure or the jacket itself is, however, less than 10% of the total cost of the platform investment, which may be of the order of U.S. \$ 2 billion.

Up to 1983, 13 concrete and 1 steel gravity drilling and production platform have been installed in addition to the Ekofisk tank, as listed in Table I.

Figure 7 shows typical pictures of the different platforms. All the concrete platforms are single base structures, whereas the Maureen steel gravity structure is a tripod (The Oilman, 1983).

A major reason for Phillips Petroleum Company choosing the Tecnomare tripod platform for Maureen was that it provided an open space in the center, and the platform was to be installed over a pre-installed template. In fact, the structure was placed within 50 mm of the ideal position.

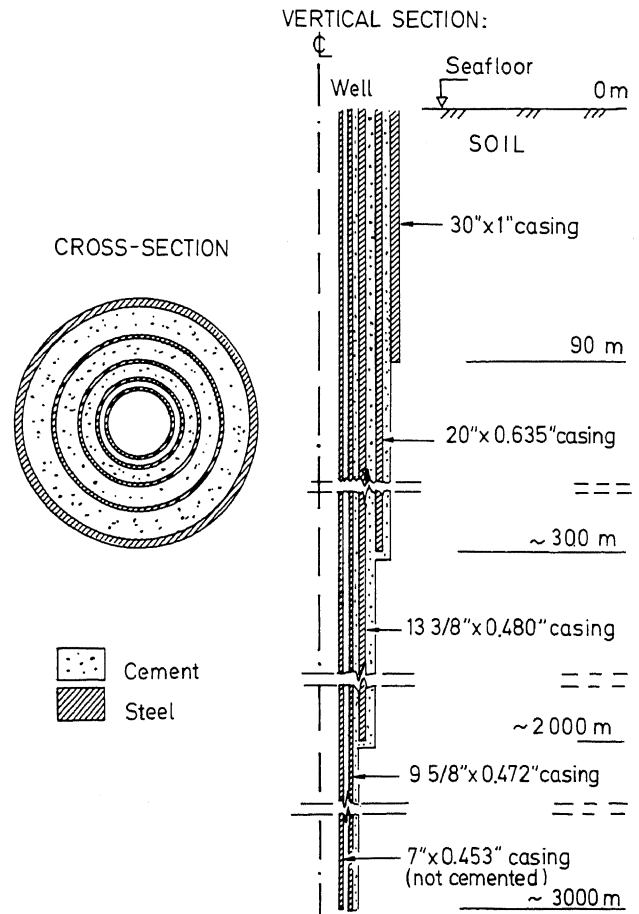
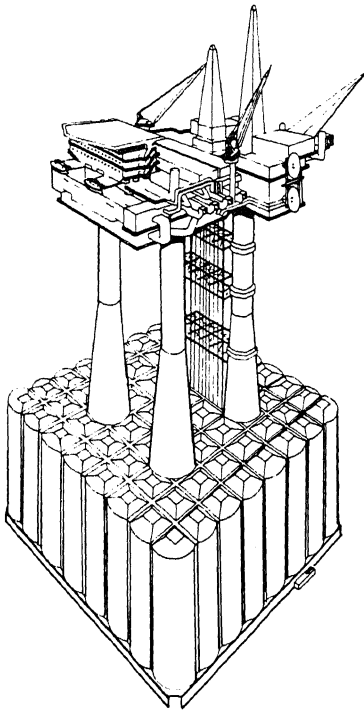
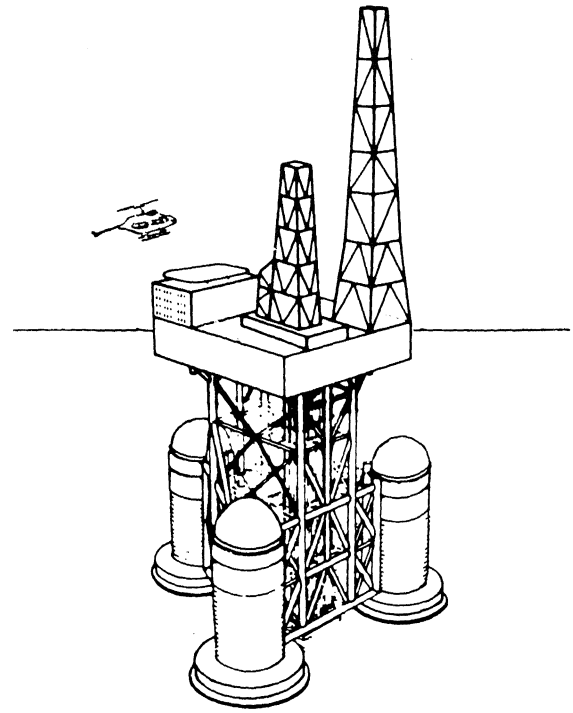


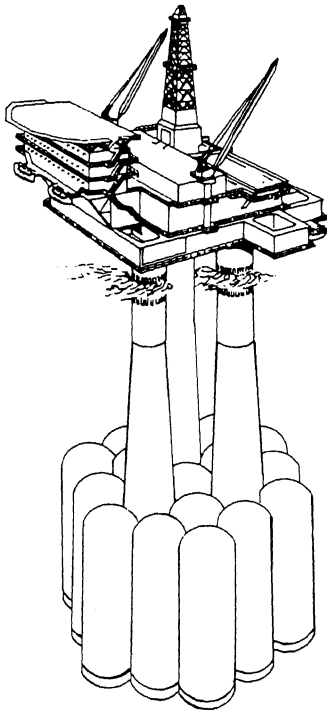
Fig. 6. Oil well configuration.



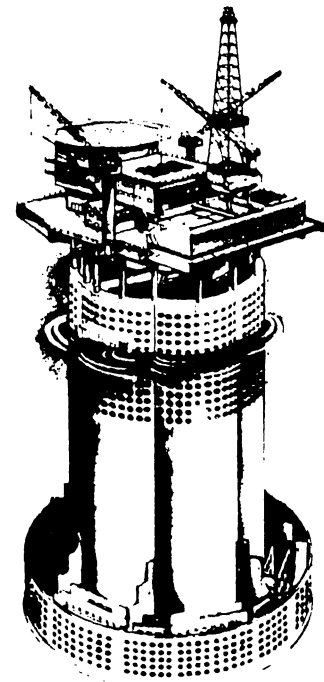
Cormorant A and Brent C, Sea Tank.



Maureen, Tecnomare



Brent B and D, Condeeeps



Frigg CDP-1, Doris.

Fig. 7. Examples of gravity platforms installed in the North Sea.

TABLE I. Gravity structures 1 to 15 are already installed in the North Sea, 16 to 18 are still to be installed.

No	Type	Name	Operator	Construction site	Sector	Year installed	Water depth m	Submerged weight, 10 <sup>3</sup> KN	Foundation area, m <sup>2</sup>	Skirts	Dowels	Soil properties
1	Doris	Ekofisk Tank	Phillips	Norway	Norway	1973	70	1.9	7,400	0.4 m concrete ribs	None	Fine dense silty sand
2	Con-deep	Beryl A	Mobil	Norway	U.K.	1975	120	1.7	6,200	3.0 m steel 0.5 m concrete	3	Fine dense silty sand (0 - 10 m) overlying very stiff silty clay
3	Con-deep	Brent B	Shell	Norway	U.K.	1975	140	1.7	6,200	3.5 m steel 0.5 m concrete	3	Stiff silty clay with interbedded sand layers
4	Doris	Frigg CDP-1	Elf	Norway	U.K.	1975	98	1.8	5,600	None	None	Fine dense silty sand (8 m) overlying stiff silty clay
5	Sea Tank	Frigg TP-1	Elf	Scotland	U.K.	1976	104	1.8	5,600	2.0 m concrete crete	None	Fine dense silty sand (3 - 7 m) overlying stiff silty clay
6	Doris	Frigg Manifold	Total	Sweden	U.K.	1976	94	1.8	5,600	None	None	Fine dense silty sand
7	Con-deep	Brent B	Shell	Norway	U.K.	1976	140	1.8	6,300	4.5 m steel 0.5 m concrete	3	Stiff silty clay with interbedded sand layers
8	Con-deep	Statfjord A	Mobil	Norway	Norway	1977	145	2.0	7,800	3.0 m steel 0.5 m concrete	3	Stiff silty clay (cover sand 2 - 10 cm)
9	Andoc	Dunlin A	Shell	Holland	U.K.	1977	153	2.0	10,600	4.0 m steel	4	Stiff silty clay with interbedded sand layers
10	Con-deep	Frigg TCP-2	Elf	Norway	Norway	1977	102	1.6	9,300	1.2 m steel 0.5 m concrete	3	Fine dense silty sand (3 - 6 m) overlying stiff silty clay
11	Doris	Ninian Central	Chevron	Scotland	U.K.	1978	136	3.2	15,400	3.8 m steel	None	Stiff silty clay with interbedded sand layers
12	Sea Tank	Cormorant A	Shell	Scotland	U.K.	1978	150	2.3	9,700	3.0 m concrete	None	Stiff silty clay with interbedded sand layers
13	Sea Tank	Brent C	Shell	Scotland	U.K.	1978	140	1.9	10,100	3.0 m concrete crete	None	Stiff silty clay with interbedded sand layers
14	Con-deep	Statfjord B	Mobil	Norway	Norway	1981	145	3.7	18,200	3.6 m steel 0.9 m concrete	4	Stiff clay (sand cover 0.2 - 1.5 m)
15	Techno-mare	Maureen	Phillips	Scotland	U.K.	1983	96	1.5	4,350	3.4 m steel	Guide piles	Stiff clay (sand cover 2 - 6 m)
16	Con-deep	Statfjord C	Mobil	Norway	Norway	1984	146	3.9	12,770	3.8 m steel	4	Stiff clay (sand cover 0 - 3 m)
17	Con-deep	Gullfaks A	Statoil	Norway	Norway	1986	133	3.9	11,000	0.4 m steel 0.4 m concrete	4	3 m moraine material above stiff clay
18	Con-deep	Gullfaks B	Statoil	Norway	Norway	1988	143	3.0	8,700	1.3 m concrete	None	Dense sand

The gravity structures, as listed in Table I, are all located on favourable foundation soils, either dense sand or very stiff clays. They have all been installed on the unprepared seabed, except that boulders have been removed by trawling in some cases.

It should be mentioned, however, that the first Condeep feasibility study for a platform on the Forties Field, a study paid for by BP, had soft, normally consolidated clay to 15 - 20 m depth. The foundation concept, which was judged to be feasible, utilized 20 m deep cylindrical concrete skirts (NGI, 1972).

Looking ahead, the next concrete gravity platform to be installed is Statfjord C in May this year. The Gullfaks A platform, which is now under construction, is scheduled for installation in 1986. A second concrete platform, Gullfaks B, has been ordered from Norwegian Contractors, and will be installed in 1988. These three are all conventional Condeep platforms and are included in Table I. The year of installation and depth of water for the various platforms are illustrated in Fig. 8.

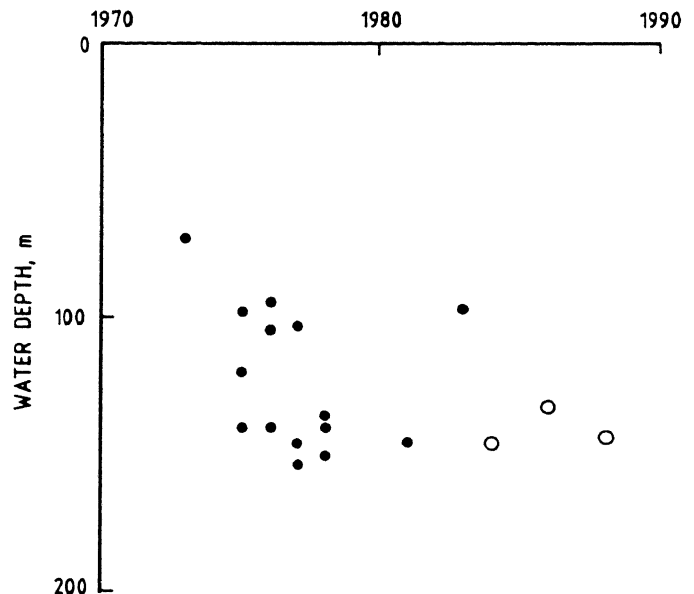


Fig. 8. Year of installation and depth of water for the various gravity platforms in the North Sea.

Other fields with potential for concrete gravity platforms now being studied are the Oseberg field for Norsk Hydro, and the Sleipner field for Statoil.

An essential part of designing a gravity type structure is meeting the foundation requirements. The size of the foundation slab and the loading conditions differ greatly from structures on land, and several new foundation design problems have had to be solved.

Both soil investigation and foundation design calculations have greatly improved during the 10 years since the Ekofisk tank was installed. The foundation designs for the earlier platforms were mainly based on static loading from the 100-year design wave, including degradation effects from cyclic loading, whereas today's practice is to perform analyses for large displacements due to cyclic design storm loading (Foss et al., 1979 and Andersen et al., 1982). Fortunately, lack of experience in the earlier days regarding the foundation behaviour of such structures has not resulted in any setbacks (Eide et al., 1979).

ENVIRONMENTAL CONDITIONS

The water depths at the different platform locations are given in Table I. There is a general increase in water depth northwards, from 70 m at the Ekofisk site to 153 at the Dunlin site.

Another typical feature is the deep Norwegian Trench, shown in Fig. 9. The maximum depth in the trench is 300 - 400 m. The oil and gas fields developed so far, are all located on the plateau west of the trench, along the border between Great Britain and Norway. The Troll field, which is the largest offshore gasfield the world, is located in the middle of the trench, and gravity platform concepts are now being developed for water of these depths, Fig. 10 (Schjetlein 1983).

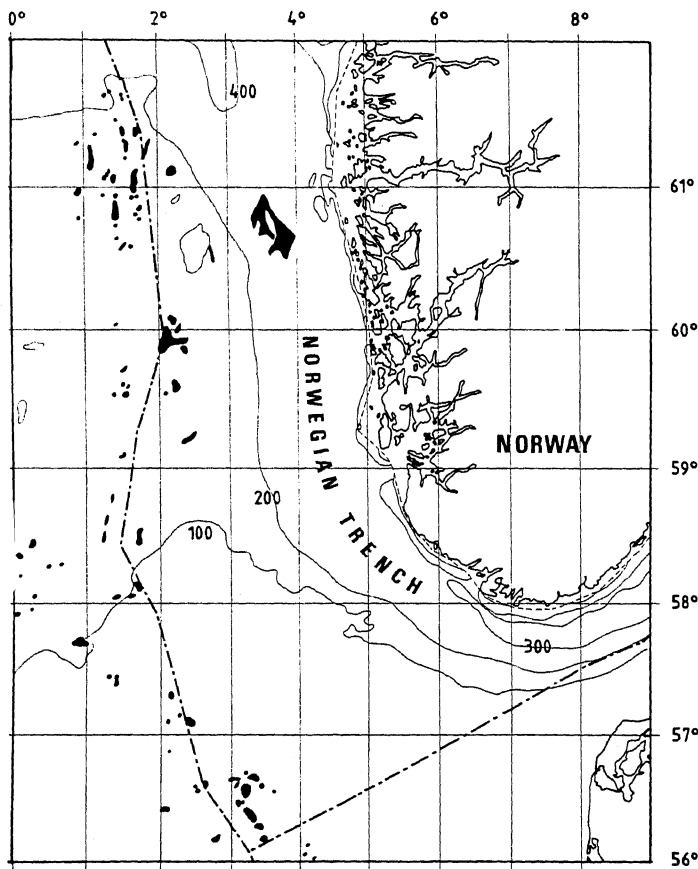


Fig. 9. Water depth contour lines in metres.

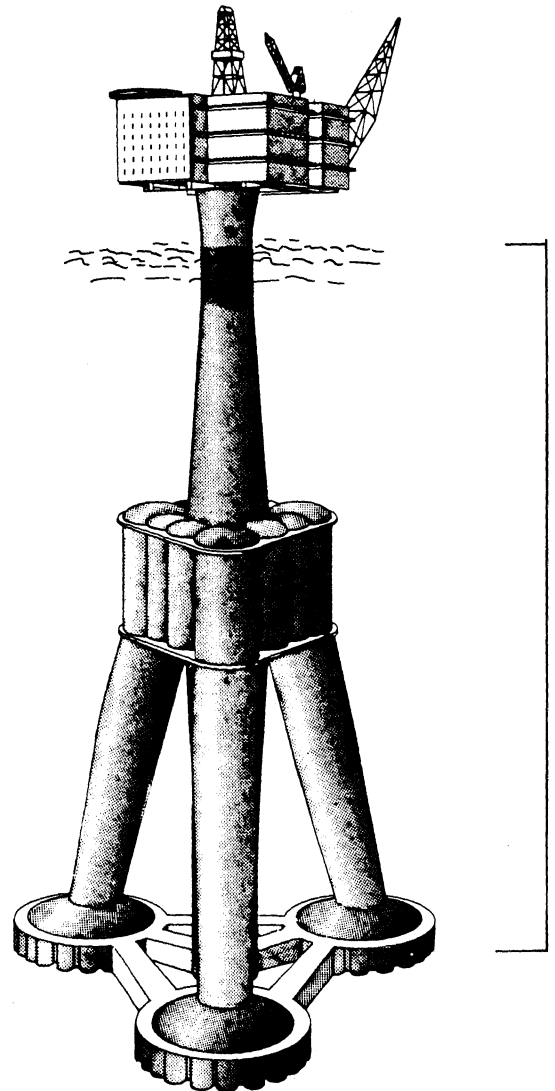


Fig. 10. Norwegian Contractors tripod Condeep T-300, proposed for the Troll field.

Meteorological observations are carried out on all the fields where platforms have been installed. The results of wind measurements on the Statfjord A platform in the period June 1980 to June 1982 are given in Table II, (Tryggstad, 1983).

TABLE II. Wind observations at Statfjord A, June 1980 - June 1982

Season	Speed m/sec.		Direction (°)
	Mean	Maximum	
Winter	10.0	30.9	330
Spring	8.6	30.9	150
Summer	6.4	15.4	340
Autumn	8.2	28.3	310

Waves used to be measured visually from weather ships, but are now mainly observed by wave rider buoys or radar on the platforms. At present, waves are measured in the Beryl, Brent, Ekofisk, Frigg, and Statfjord fields. Observations are made for 20 minutes every third hour.

The maximum wave heights used for design of platforms are shown in Fig. 11 (Huslid et al., 1982). The design wave height increases from 24 m at Ekofisk to 31 m in the Brent - Statfjord fields. The wave period is equally important when calculating wave loads on a gravity platform. Usually periods in the range of 15 to 20 sec. are considered for the 100-year design wave.

Actually, very little was known about the sea state for the design of platforms in the North Sea before oil activity started back in 1971. An illustration of this is that the design wave at Ekofisk was increased several metres during the period when the Ekofisk tank was being designed.

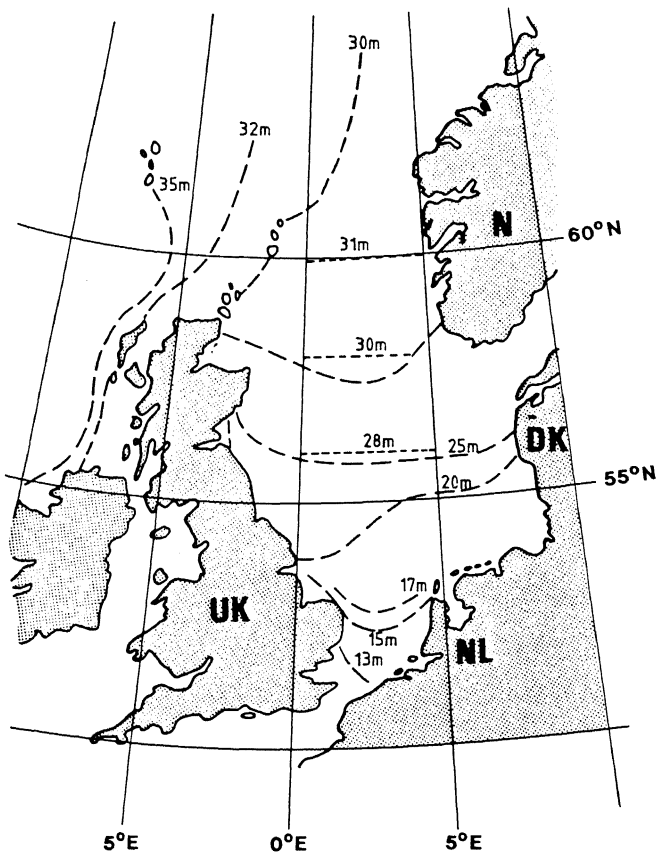
The Ekofisk tank was put to the test the first winter already. Five months after installation, on November 19, 1973, it was hit by a storm with a maximum wave height which, according to Det norske Veritas, was 23 m. The wave load was estimated to be between 70% and 90% of the design load (Clausen et al., 1975).

Another serious storm was experienced in the Frigg field on 24 November 1981. The wave load on the CDP-1 platform was estimated to have been almost equal to the design load. Even though the wave height did not reach the design value, the shape of the critical wave was particularly unfavourable and accounted for the high load on the structure.

A storm duration of 6 hours, and a Rayleigh distribution of wave loads have been assumed when designing the foundation of gravity structures for the North Sea (Schjetne et al., 1979).

The accumulated effect of storms over a period of time, and during the entire lifetime of the platform, must also be considered, both with regard to stability, cyclic displacements, dynamic behaviour, settlement and base contact stresses.

The tide was measured at the Troll field during two periods in 1980/1981. The tidal range is quite significant, and varies 0.5 m at spring tide, i.e. between half moon and new or full moon. The maximum tidal range is assumed to be somewhere between 1.5 and 2.0 m (Tryggstad, 1983).



- 50 year storm heights for a fully-developed storm lasting 12 hours (DOE 1978)
- ..... 100 year design wave heights (NPD 1977)

Fig. 11. Design wave heights according to the Department of Energy in U.K. and Norwegian Petroleum Directorate.



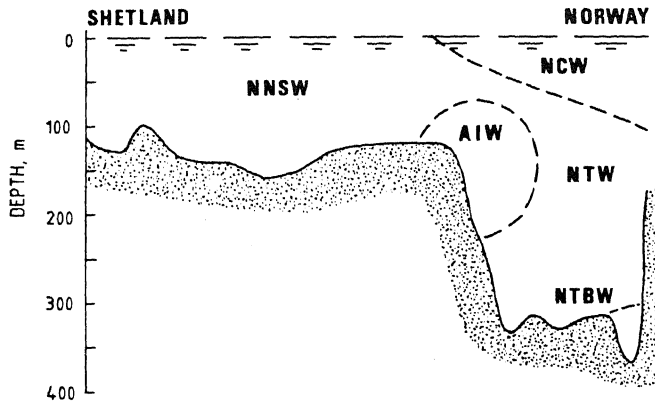


Fig. 12. Schematic distribution of water masses in the section from Shetland to Norway, N 60° 45' (Hackett, 1981).

Figure 12 shows the different water masses in a cross-section from Shetland to Norway at latitude N 60° 45' (Hackett, 1981).

- NNSW, Northern North Sea Water on the plateau to the west of the Norwegian Trench.
- AIW, Atlantic Inflow Water comes through the Faeroe - Shetland Channel, flowing southward along the western slope of the Norwegian Trench.
- NCW, Norwegian Coastal Water flows along the Norwegian coast from the Kattegat to the Barent Sea as a wedge of fresher water.
- NTW, Norwegian Trench Water flows northward under the Coastal Current, restricted to the west by the Shelf Edge Current.
- NTBW, Norwegian Trench Bottom Water along the bottom on the eastern side of the Norwegian Trench.

The current in the North Sea does not contribute very much to the environmental loads on a gravity platform, but it may be of great importance with regard to the scour potential around a platform. It is also of importance for towing conditions.

#### GEOLOGICAL CONDITIONS

When evaluating the foundation conditions in the North Sea, it is important to understand the geological history of the area (Løken, 1976 and Heiberg et al., 1982). During the Quaternary Period, i.e. the last 2 million years, the North Sea area was exposed to major climatic changes. These resulted in several cycles with drastic changes in geological conditions, which are reflected both in the bathymetry and in the geotechnical properties of the sediments laid down during this period.

In glaciated areas the changing sea level creates a very complex geological situation. Firstly, the world water balance is altered during glaciated periods, and the frozen water held in glaciers on the land surface causes eustatic lowering of the world-wide sea level. It has been estimated that the sea-level may have been lowered by 80 m during glaciations (West, 1968). Secondly, the weight of the ice, approximately 3000 m thick in central parts of Scandinavia during glacial maximum, caused isostatic depression of the landmasses. During deglaciation and removal of the ice load, a slow recovery took place, leading to upwarping of glaciated areas and downwarping of the marginal areas.

The eustatic variations occur simultaneously with the increase and decrease of the glaciers, whereas the isostatic variations are slow, and depend on the elastic properties of the earth's crust.

The actual change in sea level is the net difference between the eustatic and the isostatic variation. In central glaciated areas the isostatic upheaval after the glaciation was larger than the eustatic rise, which resulted in a net rise of land, such as most of the U.K., Norway, Sweden and the northern part of Denmark. The opposite situation is going on in areas such as southern England, Denmark, northern Germany and the Netherlands. This effect of land uplift and downwarping is still proceeding today, as shown in Fig. 13.

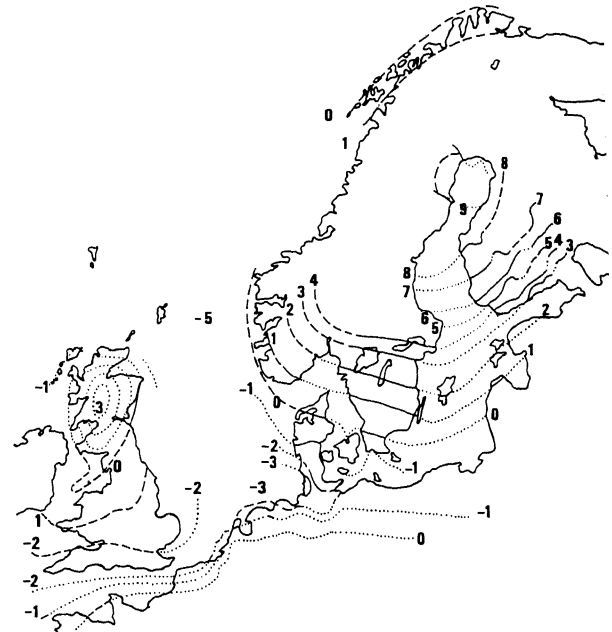


Fig. 13. Present uplift and downwarping in northwest Europe. Rate of change in mm. per year.

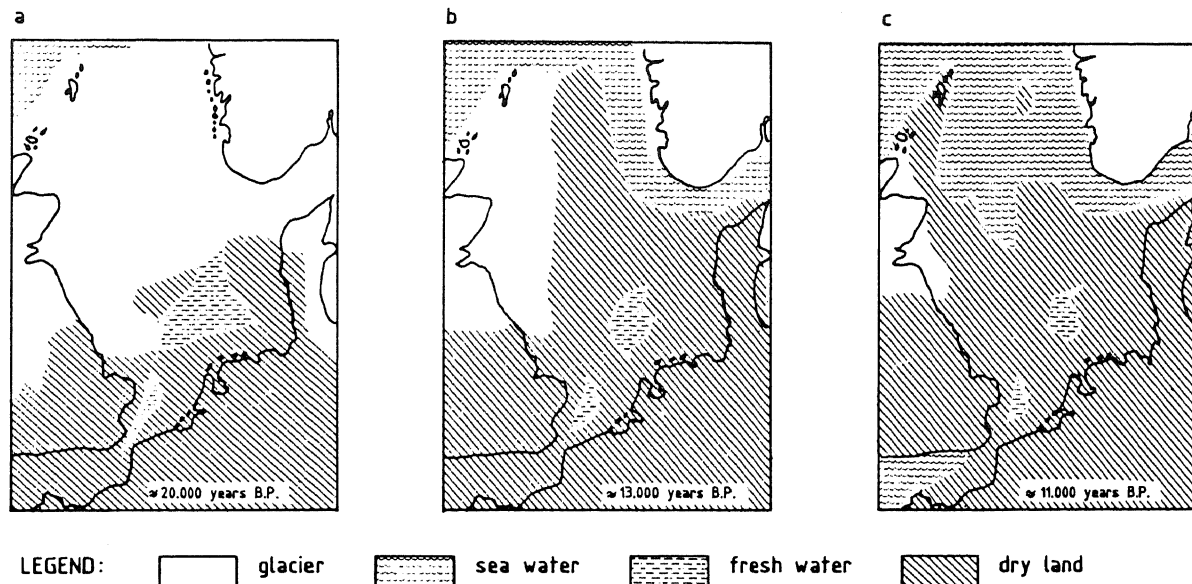


Fig. 14. Three stages of hypothetical deglaciation and shore line transgression in the North Sea (Løken, 1976).

During the last glaciation, at a maximum of about 20 000 years B.P., the ice sheet caused erosion and loading of the older sediments both in the plateau area and on the slopes of the Norwegian Trench. Just after the last glacial retreat, the plateau area and the channel shoulder were dry land. The sea level rose rapidly, and these areas were exposed to heavy erosion, which resulted in soft, loose sediments being deposited as a beach on the upper part of the slope. Only a very thin cover of sand, less than 0.5 m thick, is of recent age.

During the last glaciation, the northern areas of the North Sea and the Norwegian Trench were covered by a grounded ice sheet, Fig. 14a. At this stage the southern areas were dry land with ice-dammed lakes, exposed to permafrost and surface erosion by rivers and winds, in a similar manner to the arctic areas today.

As a result of a gradually changing climate from strongly arctic to somewhat milder, the thickness of the ice sheet decreased at the same time as the sea water level rose. This resulted first in buoyancy of the ice within the Norwegian Trench, followed by the breaking up of the floating ice by a calving front. Some fluctuations, both in the sea water level and in the location of the ice front, most probably occurred due to short climatic oscillations. For example, a radio-carbon dating from a vibro-core sample at 1.5 m depth at a site located between the Statfjord and Gullfaks areas gave an age of  $18\ 860 \pm 260$  years B.P. to a silty clay just below an upper layer of reworked till (Rokoengen et al., 1982).

About 13 000 years B.P. the Norwegian Trench must have been a wide, open fjord with drifting icebergs, from the calving ice front of the glacially eroded Norwegian landmass on one side and the dry land of the North Sea plateau, still more or less covered with ice sheets, on the British side (Fig. 14b).

As a result of the continuous improvement of the climate, the front of the melting ice sheets retreated, producing large amounts of sediments suspended in meltwater rivers, which carried the material out into the Norwegian Trench. Here beaches of gravel and sand were built up at the temporary shoreline near the top of the Trench slopes, whereas the finer material of silt and clay filled up the deeper western parts of the Norwegian Trench.

About 11 000 years B.P., the sea, encroaching from the north, gradually submerged the northern parts of the North Sea plateau. Most of the Norwegian land area and probably large parts of the Scotland and Shetland areas were still covered by ice. The major banks were small and large islands. The large shallow tidal flats in the central North Sea areas suffered shoreline erosion and reworking of the sediments under conditions similar to those in the German and Dutch coastal areas today.

During the following 2 000 years all the rest of the glacial ice melted away from the land areas, and the sea encroached further southwards. By about 8 500 years B.P. the shoreline was probably about 35 m lower than the present level. A little later the northern part of the North Sea and the southern part of the British Channel became connected.

The result of this geological history is that large areas of the North Sea, which are at present shallower than 150 m, have been dry land several times during the glacial periods. At the times when the glacial ice sheets were retreating, erosion took place on the banks, whereas re-sedimentation occurred in the depressions. This is the reason why erosion relics from glacial moraines are found as surface sand and gravel on the banks. Loose sand and silt deposits are found along the slopes of the Norwegian Trench, and in the middle of the trench more than 50 m of soft, normally consolidated clay occurs.

The depressions on the shelf plateau are in general filled with soft and normally consolidated marine clay and silt. Most of the remaining areas have a cover of uniform top sand over overconsolidated glacial clay. The shallow areas are usually more overconsolidated than the deeper areas.

Some special features which may affect the foundation of platforms adversely, should be mentioned.

Slope instability and submarine slides are well known from Norwegian fjords (Bjerrum, 1971) and very large submarine slides have occurred at Storegga, off Møre (Bugge et al., 1978). Up to now little data has been available on slope conditions in the North Sea, but a submarine slope stability study is running at NGI with particular concentration on the Western slope of the Norwegian Channel (Karlsrud and Edgers, 1982 and Edgers and Karlsrud, 1982).

Gasified sediments are found in the North Sea, and in most cases the gas is biogenic methane produced within the sediments. Only small traces of petrogenic gases, migrated upwards from deeper gas and oil reservoirs, have been found. The presence of such shallow gas can be recognized in seismic records as acoustic blanking, and it is very important to locate such zones before drilling and soil sampling are started.

Pockmarks are shallow, more or less circular depressions found in areas with soft and normally consolidated clays. The size of the pockmarks depends on the thickness of the soft clay layer, in such a way that in areas with a relatively thin top layer there will be many small pockmarks, whereas a thicker top layer results in fewer, but larger pockmarks, up to 15 m deep and 300 m wide. Size and distribution of pockmarks in the western part of the Norwegian Trench is given by Hovland (1981).

The explanation for the pockmarks is not quite clear, but they are probably caused by migrated gases.

Iceberg plough marks are found in areas of morainic material at water depths between 120 and 350 m. The typical size is 3 - 5 m in depth and 25 - 50 m in width and up to several km in length, but maximum values of four times as large have been measured. A special study of the effects of iceberg plough marks on the engineering of pipelines and gravity platforms is being undertaken by the Norwegian Continental Shelf Institute (IKU).

Rock boulders of all sizes up to 1.5 m in diameter are found, mostly lying on top of the stiff clay with little or no embedding, as found in the Statfjord area (Løken, 1976). These boulders are believed to have been rafted by ice and melted out of floating icebergs from Norwegian fjord glaciers at a stage illustrated approximately in Fig. 14c. These boulders were removed from the platform sites before the gravity platforms were installed.

A more serious problem, related to skirt penetration, is the rock boulders embedded at some depth in the sediment. Such boulders can be recognized in seismic records by their parabolic reflections.

## SITE INVESTIGATIONS

Site investigation for gravity platforms in North Sea are discussed by: Bjerrum, 1973; E 1974; McClelland, 1975; Ruiter, 1975; Høeg, 1982; Kjekstad et al., 1978; Andresen et al. 1979; Schjetne and Brylawski, 1979; and Lunn and St. John, 1979. It involves the following aspects:

- Continuous geophysical profiling
- Bathymetry and sea-bed inspection
- In situ soil testing
- Undisturbed sampling
- Laboratory testing on board
- Laboratory testing on shore
- Establishing engineering design parameters

Site investigations are usually carried out stages, starting with a preliminary investigation. The final investigation is carried out when the platform location is fixed in relation to the reservoir. In some cases the soil and foundation conditions will also influence the selection of the final location of the platform.

The instruments used for continuous geophysical profiling are shown in Fig. 15. In order to determine the type of soil material located between the different reflectors, the profile has to be calibrated against borings. Boreholes should preferably be located at the crossing points of profiles.

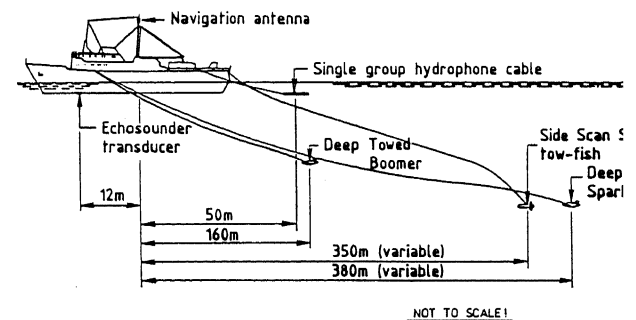
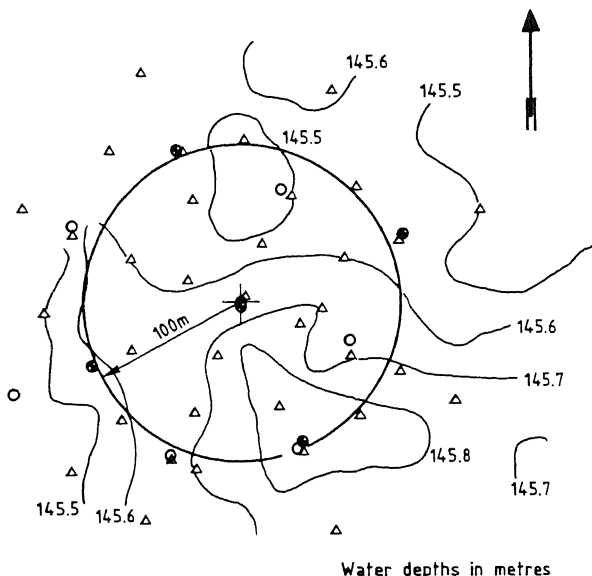


Fig. 15. Analog instrumentation layout.

At a potential platform site one may cover a 5-km<sup>2</sup> area with a 200 to 1000 m grid of high power sparker profiling. Detailed information close to the platform site is obtained using equipment giving less penetration and higher resolution, such as a multi-electrode sparker boomer. The actual platform area, of the order of 1 km<sup>2</sup>, may be covered with a 100 to 200 m grid, and the final area where detailed soil investigations are carried out (250 x 250 m) be surveyed with a grid spacing of approximately 25 m.

Simultaneously with the sparker-boomer survey one can carry out bathymetric mapping with a high precision echo-sounder and sea floor inspection with a side-scan sonar. The relative heights of a number of points on the sea floor can be determined with a differential pressure

meter on board a submersible. The contour map obtained in this way may have an accuracy of 5 to 10 cm (Fig. 16). The submersible helps locate sea floor obstructions such as boulders or shipwrecks.



**LEGEND:**

- △ Seacalf (CPT)
- Wilson (CPT)
- Borehole

Fig. 16. Site investigation for a gravity platform in the North Sea.

In situ soil testing. In 1972 an underwater rig was developed by Fugro-Cesco to perform cone penetration tests (Zuidberg, 1975). This equipment, known as the "Seacalf", has been used extensively. The penetration force (max. 200 kN) is hydraulically applied at the seabed. It is operated from the ship, and the reaction force is absorbed by the dead weight of the equipment.

A gravity structure requires good coverage of the upper soil layer by surface cone penetration tests (Fig. 16). The penetration depth obtained by "Seacalf" may be of the order of 10 - 15 m in dense sand and heavily overconsolidated clays, and up to 25 - 30 m in soft, normally consolidated clays.

Deep CPT tests have to be carried out inside the drillstring. This is done utilizing a seabed control unit, as shown in Fig. 17. Strokes of 1.5 to 3 m have been usual, but equipment which gives continuous penetration to great depths is also available now.

The piezocone is a piece of equipment which, in addition to cone resistance, measures pore pressure at the tip during penetration (Lacasse and Lunne, 1982). It gives valuable additional information about layering, and offers the possibility of measuring permeability in situ. This equipment is now being used in the North Sea.

Down-hole vane tests are carried out in soft clay deposits, such as in the Norwegian Trench, but usually not in stiffer soils.

Other in situ tests, such as pressuremeter readings, dilatometer readings and gamma logging have only to a small extent been used in the North Sea.

Hydraulic fracturing tests are carried out in order to determine the required conductor depth for mud circulation to deck level when drilling for the 20" casing.

Great improvements have been achieved in undisturbed sampling in the North Sea. To start with, percussion wire line sampling, as developed in the Gulf of Mexico, was the most common practice. Thin wall cylinders with internal diameters of 54 - 75 mm, are driven into the soil at the bottom of the drillstring by blows of a wire line operated hammer. The quality of the samples are usually poor as the driving causes disturbance.

Push sampling, using the weight of the drillstring to penetrate the tube, provides samples of better quality. The method can, however, only be used in fairly soft material due to the limited penetration force.

The sea-bed jacking units shown in Fig. 17 make it possible to transmit higher penetration forces to the drill pipe. The sample can thus be cut with a constant rate of penetration and with one stroke, even in dense material. Piston samplers are now available for sampling in soft materials offshore.

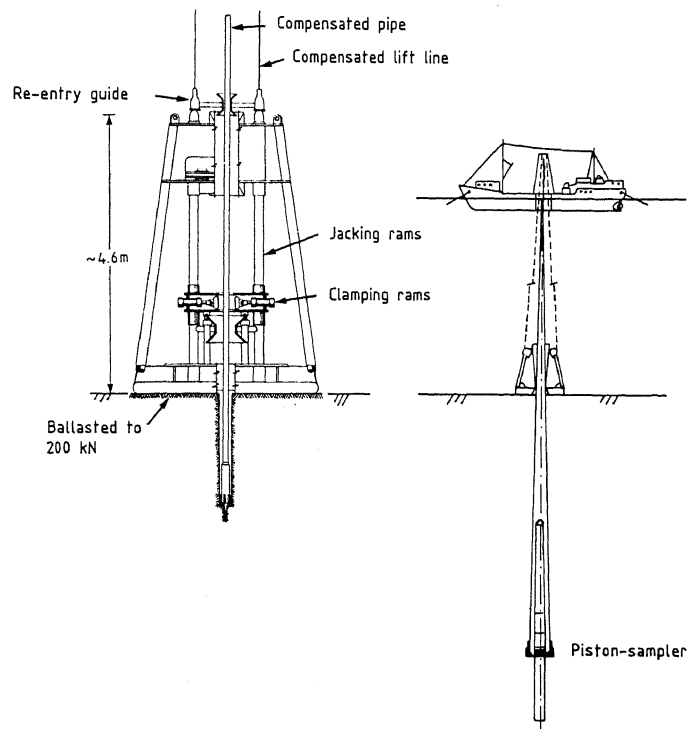


Fig. 17. Sea bed control unit for sampling and in-situ testing.

A laboratory on board the vessel where samples can be x-rayed, extruded, classified, tested, photographed and sealed, serves several purposes such as:

- enabling continuous updating of the soil properties in order to modify the sampling or boring program.
- checking the disturbance of each sample immediately after recovery.
- obtaining shear strengths and water contents as quickly as possible after sampling.

The practice at NGI has been to extrude stiff clay samples as soon as possible to prevent swelling by sucking water from cuttings or free water in sand layers. The samples are then waxed and sealed for transportation to laboratories on shore. Soft clay samples are, however, kept in the cylinders to avoid unnecessary handling and disturbance.

X-ray inspection of the samples in the tube on board the ships has proven very useful. It gives immediate information about the quality of the sample and type of material regarding layers, gas etc, Fig. 18.

Onshore laboratory testing. Andresen et al. (1979) describe the details of the static and cyclic testing techniques followed by the Norwegian Geotechnical Institute once the samples have been brought ashore. The specified laboratory procedures and data evaluation attempt to account for offshore sampling

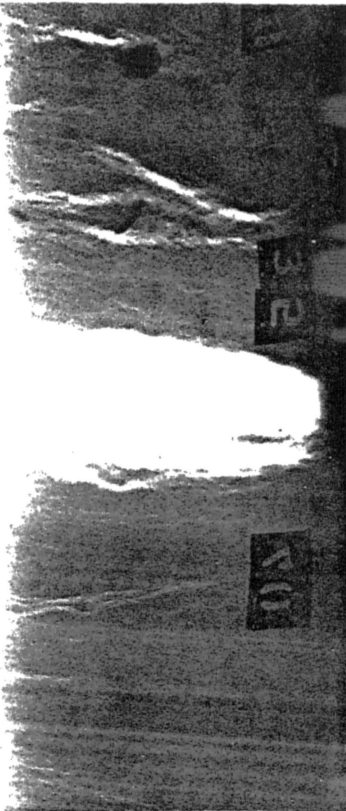


Fig. 18. X-ray of a sample from a depth of 90 m. Fissured clay with elongated fissures. Some sand and gravel. The large void may be due to stress release or gas expansion.

disturbance and the effect of the release of high in-situ stresses on the soil specimens.

When establishing design parameters and profile for foundation design analyses, most emphasis placed on the test results from undisturbed samples (Kjekstad and Lunne, 1979). In situ test results give valuable additional information about homogeneity and variation in soil conditions. Substantial efforts have been focused on correlating cone penetration resistance and sleeve friction with strength, deformation characteristics of sands and clay, and this is made use of in the evaluation of design parameters. Lately piezocone test results are also utilized.

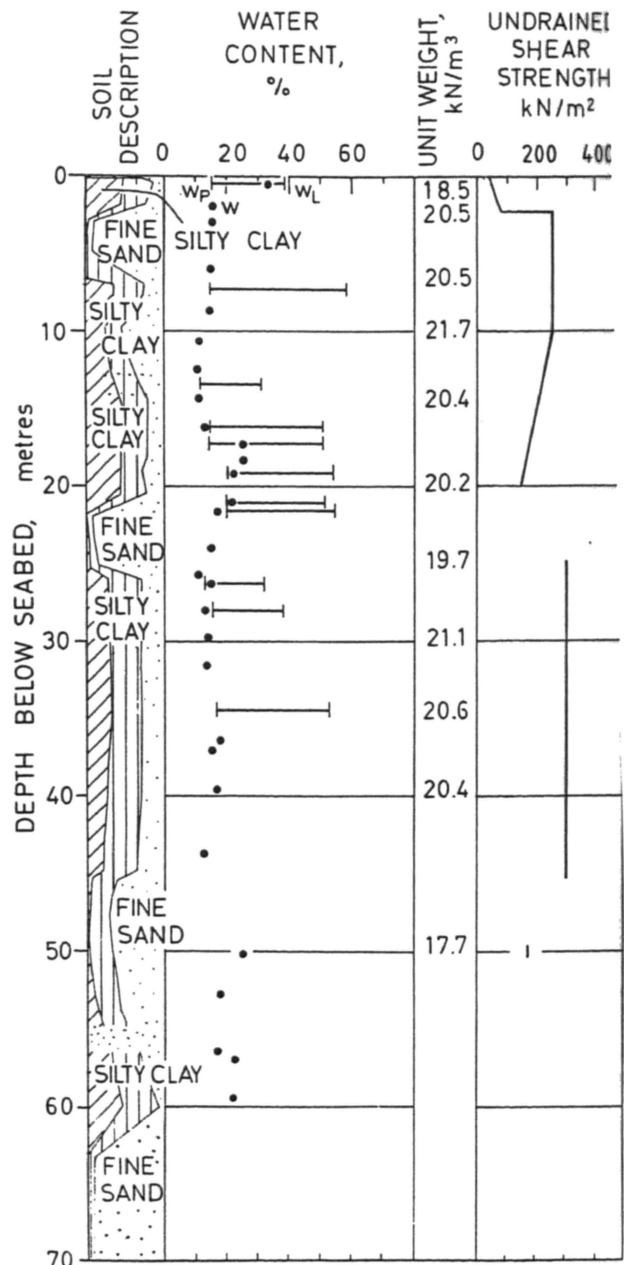


Fig. 19. Borehole profile, Brent B site.

**NORTH SEA SOIL CONDITIONS**

The soil conditions in the North Sea are quite complex as a result of the geological history outlined previously. It is important for foundation evaluation to understand the geology at the site, and such a study is therefore normally included.

The mechanical properties of the soil are a result of geological events, i.e. sedimentation, mechanical pushing by ice, preloading by glaciers, freezing, drying or chemical effects, gradients and shear stresses from wave actions (Bjerrum, 1973).

The phenomenon which has caused concern and discussion is that less stiff clays can be found below highly overconsolidated layers (Fig. 19). A possible explanation of this may be that consolidation in the deeper layer has been prevented by permafrost. There is no indication that cementation plays an important role for the soil properties.

The soil structure is always studied and reported and illustrated by photos. Highly overconsolidated clays are in some cases fissured, which may influence shear strength properties. Different types of fissures are recognized, as illustrated in Fig. 20.

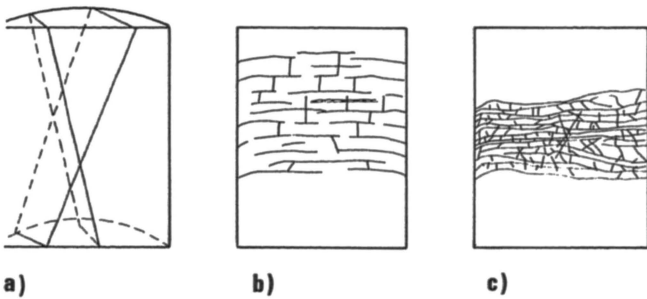


Fig. 20. Typical fissures found in overconsolidated silty clays in the North Sea (Heiberg et al., 1982).

Steeply inclined, open fissures as shown in Fig. 20a, usually reveal lower strength when tested on large diameter triaxial samples, than on smaller samples or in classification tests employing a fall cone, torvane or pocket penetrometer.

Types b) and c) in Fig. 20 are more or less dense fissuring found in some glacially activated profiles in the North Sea. Sometimes type b) is found above type c) in the same borehole profile. The fissures may have been caused by stress release after unloading from a grounded ice sheet, or possibly by permafrost. Slickenside fissures, possibly caused by syneresis, have been observed less frequently. The borehole profile in Fig. 19 may serve as an illustration of the soil conditions described.

Most of the sands at water depths less than 150 m are very uniform in grain size distribution and very dense. The dense packing may be attributed to the sedimentation processes, reshaping by wave loading or mechanical preloading by glaciers. The borehole profile from

the Ekofisk site, shown in Fig. 21, may illustrate this type of soil. As previously mentioned, loose sand may be found on the surface of the western slope of the Norwegian Trench, and flow slides have been experienced in some Norwegian fiords (Bjerrum, 1971).

The gravity platforms in the North Sea have so far had their foundation sites on competent soils, dense sand and very stiff clays. Eight of the platforms are on sites with stiff, silty clay below 0.2 - 3 m. In the other six cases there are dense, silty, fine sand layers to depths greater than 3 m, as indicated in Table I.

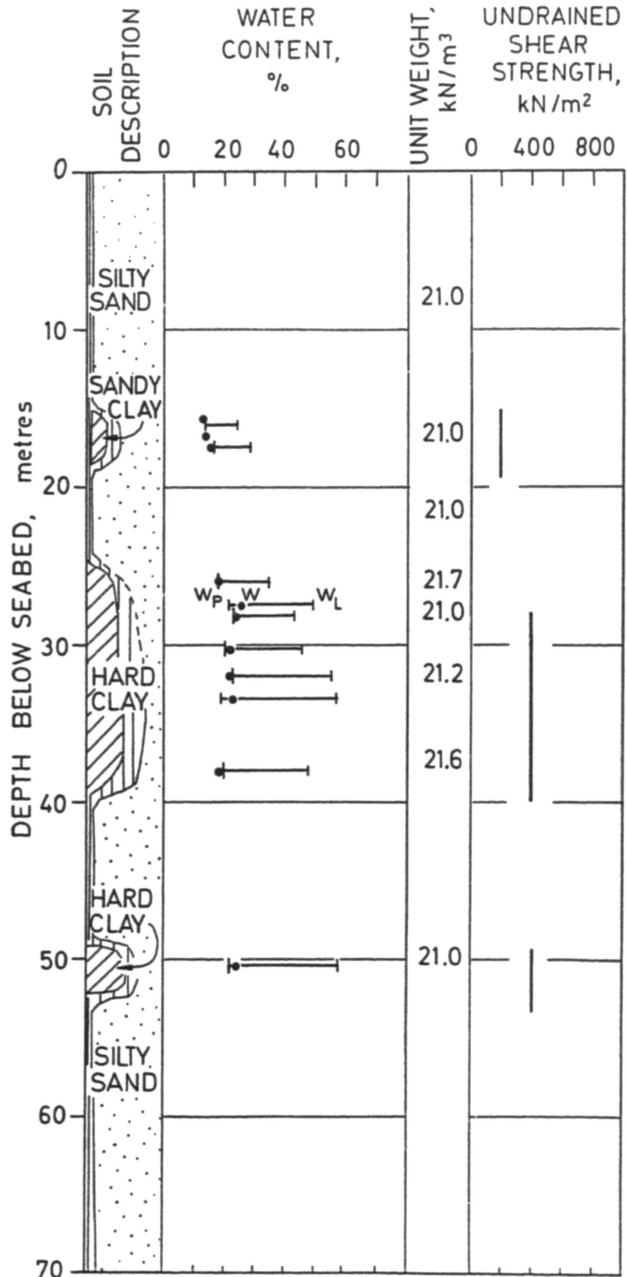


Fig. 21. Borehole profile at the Ekofisk site.

At most of the platform sites the sea-bed is extremely flat with only small differences in elevation over the foundation slab area. The maximum slope of the sea-bed has been experienced in the Frigg field for the TP-1 and TCP-2 platforms, where the slope was 0.6°, giving a 1 m difference in elevation over the base area with its length of approximately 100 m. On all the other sites the maximum difference in sea-bed elevation has been from 0.1 to 0.4 m.

Fixed platforms are now being considered for the Troll field in the middle of the Norwegian Trench, with a water depth of 340 m and soft, normally-consolidated clays to great depths (Fig. 10; Dybwad et al., 1980; Schjetlein 1983). The soil conditions are illustrated by the borehole profile in Fig. 22. Last summer a very comprehensive soil investigation was carried out at the site, utilizing piezocone, field vane and piston sampler for taking undisturbed samples (Moeyes and Hackley, 1983). For the first time in the North Sea, X-ray inspection of the samples in the tube was done on board the ship. This proved very useful in checking the quality of the sample.

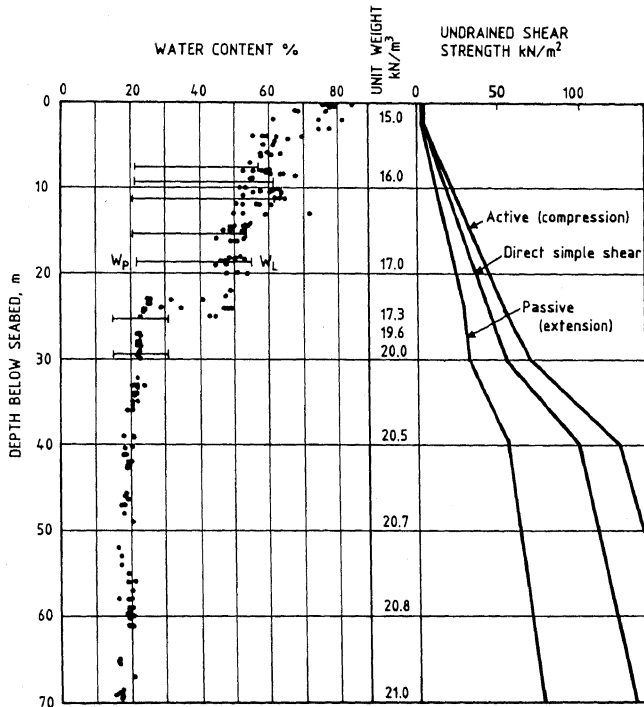


Fig. 22. Borehole profile in the Norwegian Trench.

### CONSTRUCTION OF CONCRETE GRAVITY PLATFORMS

All the concrete gravity platforms have been constructed according to the same basic principles (Fig. 23; Gerwick, 1975; Mo, 1976; Derrington, 1976; and Werenskiold, 1976):

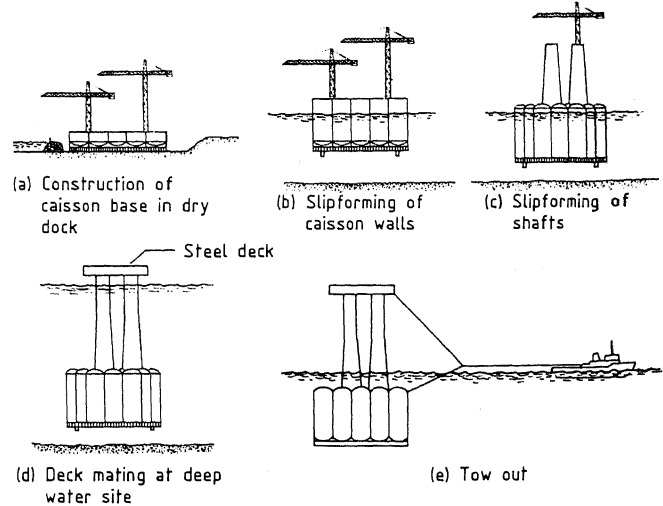


Fig. 23. Construction sequence for concrete gravity structures (Mo, 1976).

- Base section is constructed in dry dock
- Floating out to deep water construction site
- Slipforming caisson and towers
- Deck mating with the structure submerged
- Towing to the site and installation

Main factors in the design are:

- Floating stability
- Capacity of carrying deck load during towing out
- Wave loading
- Foundation
- Load cases for structural design

The design of the base sections may vary with regard to the following features:

- Flat base slab contra spherical domes
- Cantilevered slab or not
- Type of skirts if any
- Dowels or not

Typical base sections and skirt geometry are shown in Figs. 24 and 25.

The advantage of the spherical domes is that they can withstand higher contact stresses and be forced to penetrate into the ground. The cantilevered slab gives advantages regarding wave loading and scour. The design of the skirt system may be the most important item to play with when adjusting a gravity platform to the site and soil conditions.

he purpose of the skirt system is to:

Confine any soft top soil layers and bring the foundation level down to more competent soils.

Improve hydraulic conditions at the edges, and reduce the hazard of scour.

Facilitate conditions for grouting the base area.

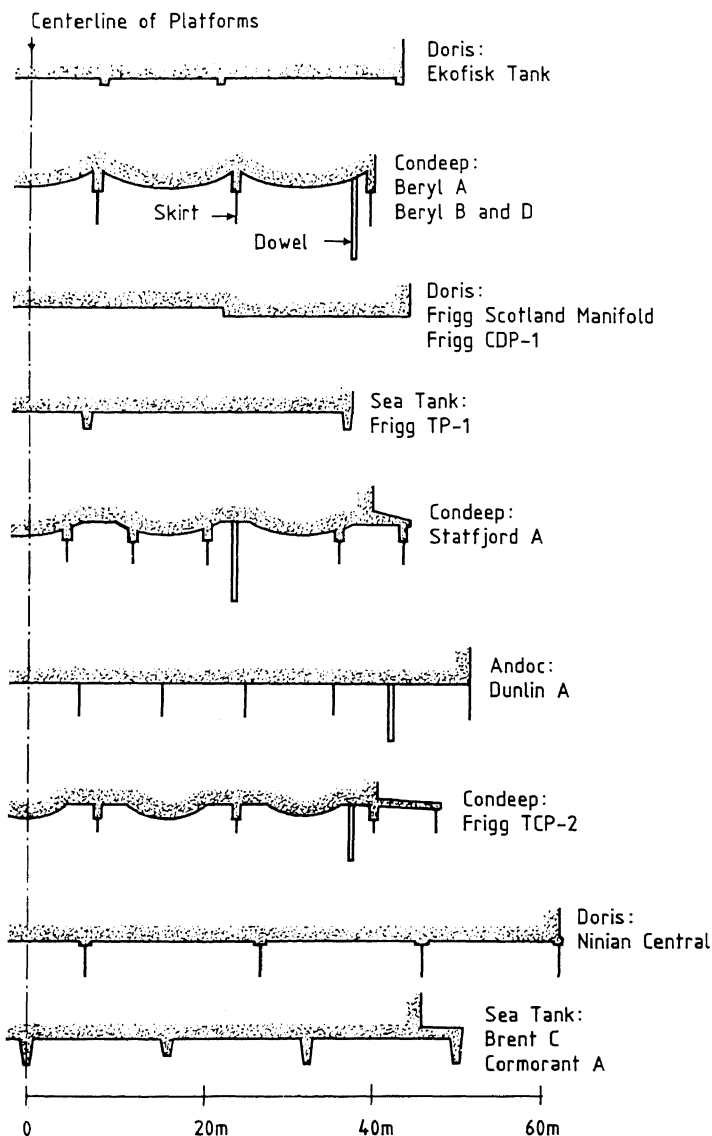


Fig. 24. Cross-section through caisson bases of different concrete gravity structures.

All the Condeep platforms and the Howard-Doris Ninian Central platform are equipped with steel skirts, mainly 3 - 4 m deep. The Sea Tank platforms are equipped with wedge-shaped, 2 - 3 m deep concrete skirts. The Ekofisk tank and the two other Howard-Doris platforms have virtually

no skirts. For the Norwegian Trench with its soft clay conditions, skirts as deep as 20 - 30 m are now being considered.

The purpose of the dowels are to:

- Keep the platform in position prior to skirt penetration.
- Prevent damage on steel skirts at touch down.
- Avoid skidding.

On the Ekofisk tank and the CDP-1 platform skidding during installation has been reported.

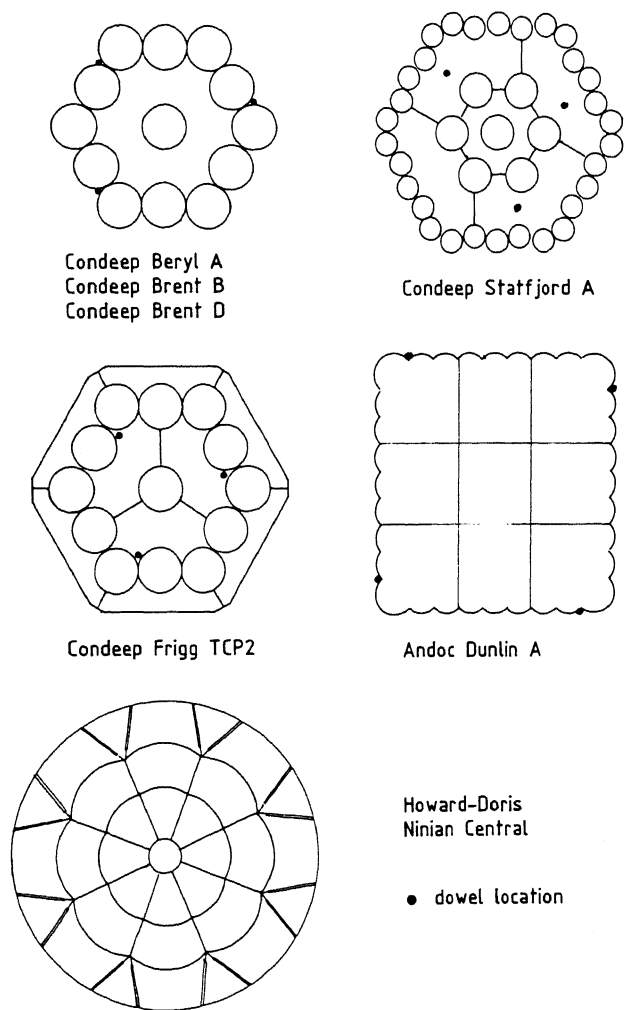


Fig. 25. Geometry of steel skirts for some concrete gravity platforms.



All the Condeep platforms have been equipped with a sub-base drainage system (Eide et al., 1982). Different type of filter systems have been built into the base, depending on the structure and the top soil conditions. The systems have been operated by a suction pressure 10 to 20 m below LAT. The drainage system employed at the Statfjord B platform is shown in Fig. 26.

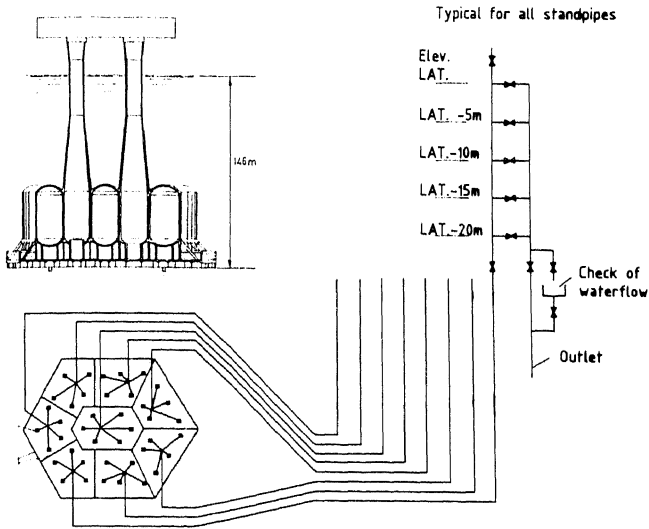


Fig. 26. Base drainage system employed at Statfjord B.

The purpose of the drainage system is to speed up consolidation and improve the stability shortly after installation as illustrated in Fig. 27. The drainage system also reduces generation of excess pore pressure during storms.

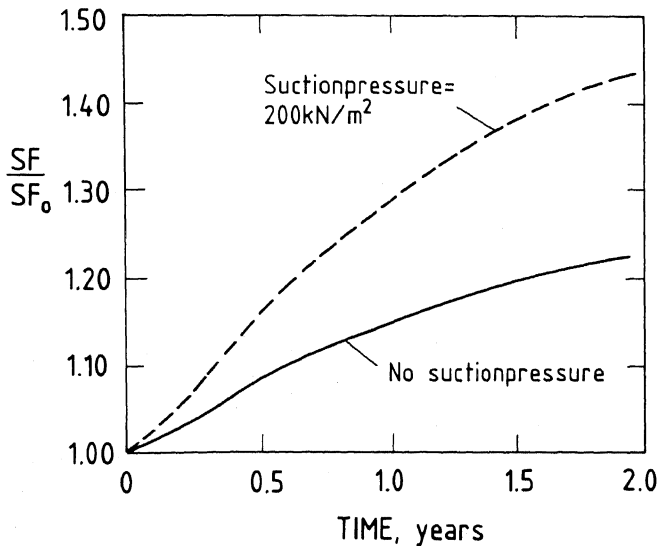


Fig. 27. Increase in safety factor FS against bearing capacity failure versus time after platform installation for Statfjord B.

A platform removal system has been required for the more recently built platforms. The drainage system may be used for this purpose, as the water pressure in the skirt compartments can be increased in order to pull the skirts out of the ground after the platform has been deballasted.

Construction of gravity platforms as described here requires a deep water site, especially for the deck mating operation. Furthermore, the towing route to the site must have a sufficient depth of water. The deep Norwegian fiords and the west coast of Scotland offer these possibilities.

The building site and the towing route for the first 13 gravity structures are illustrated in Fig. 28, and in addition the Statfjord B and the Maureen platform are now in position. Of the 13 structures, eight have been built in Norway, five in Scotland, one in Holland and one in Sweden. Two of the structures built in Scotland and the one built in Holland were towed to Norway for deck mating.

Of the 15 structures 11 are located in the British sector and four in the Norwegian sector. By 1988 three more concrete platforms will be installed in the Norwegian sector.

The towing time to the sites has been of the order of one week, depending on weather conditions. Installation has to take place in the summer season from May to September.

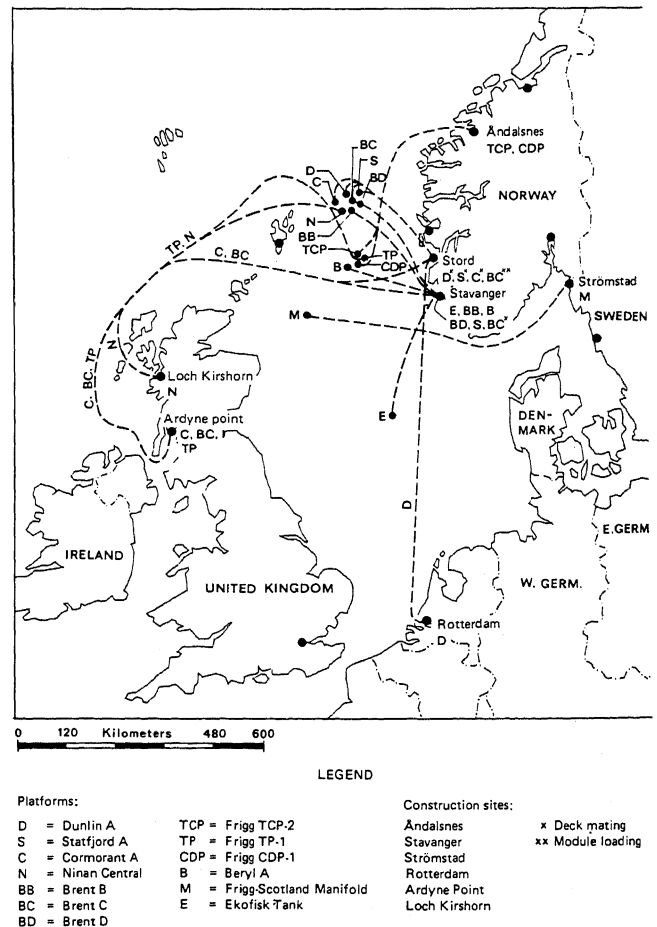


Fig. 28. Platform construction sites, approximate towing routes and final positions.

## STRUMENTATION

strumentation is included for two reasons. The first is to obtain correct and safe installation of the platform. The other is to check performance during operation (DiBiagio et al., 1976; DiBiagio and Høeg, 1983).

Some sensors which have to be placed in the base of the caisson during construction work in the dry dock, will be submerged in sea water for two years or more before installation of the platform. This makes special requirements of the sensors, and as they are not accessible for maintenance or replacement, they are usually duplicated. It is also very important that measurements during installation are available in such a form that the installation personnel can make immediate decisions. This makes special requirements of the data acquisition system. Some of the instruments for the installation phase may also continue to be used in the operational phase.

The main control measurements for the installation phase are as follows:

Position determined by acoustic transponders or electronic distance measurements.

Draught determined from sea water pressure measurements near the base.

Base clearance determined by echo sounders and special mechanical devices.

Axial stresses and bending moments in dowels determined by strain gauges.

Ballast water level in different cells controlled by pressure transducers.

Tilt measurement controlled by biaxial inclinometers.

Water pressure in skirt compartments controlled by means of differential pressure transducers.

Contact pressure against spherical domes measured by earth pressure cells.

Strain in reinforcing steel in spherical domes giving total loads on domes.

Short term settlements have been measured by means of a closed hydraulic system with reservoir on the platform and transducer on the sea floor. During skirt penetration inspections along the periphery of the base have been carried out by a submarine taking video tapes or immediate checking on board the platform.

For performance measurements during the operational phase, the following are recorded:

Skirt water pressure, in order to study the effect of the drainage system. In addition, the amount of drainage water is measured.

Earth pressure cells, in order to study load distribution, both static and dynamic.

- Inclinometers, to study long-term tilt effects. In addition optical levelling on deck is done twice a year.
- Settlements, usually recorded relative to a reference point at 50 to 60 m depth.
- Pore water pressure in the soil at different levels below the platform base.
- Accelerations at caisson and deck level.
- Long term horizontal displacement due to predominant storm direction.

Possible scour of the sea bottom near the platform is monitored by a submarine. Reference sticks are set up in order to improve these inspections.

As an example case, the instrumentation of the most recently installed concrete gravity platform in the North Sea, the Statfjord B Condeep platform is given in Tables III and IV and illustrated in Fig. 29 (DiBiagio and Høeg, 1983).

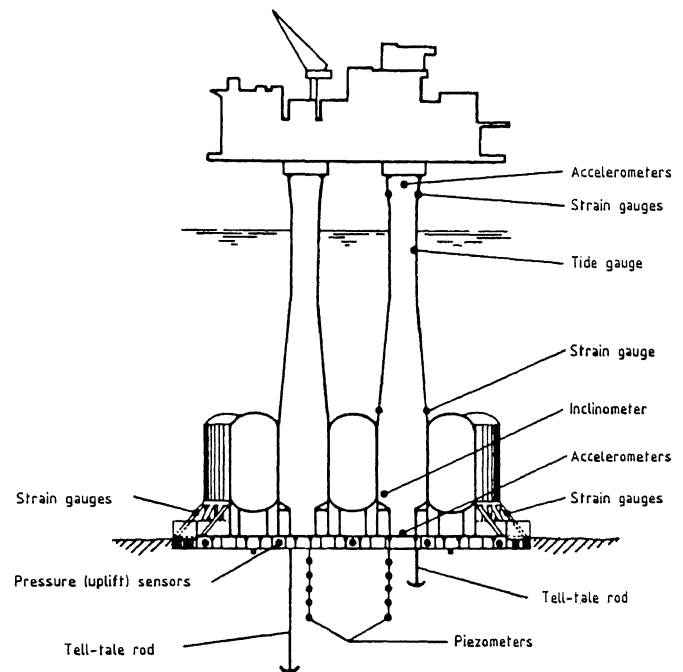


Fig. 29. Instrumentation for monitoring the long-term performance of Statfjord B (DiBiagio, 1983).

## STRUMENTATION

strumentation is included for two reasons. e is to obtain correct and safe installation the platform. The other is to check performance during operation (DiBiagio et al., 1976; Biagio and Høeg, 1983).

e sensors which have to be placed in the base-ction during construction work in the dry ck, will be submerged in sea water for two ars or more before installation of the plat- rm. This makes special requirements of the nsors, and as they are not accessible for intenance or replacement, they are usually plicated. It is also very important that asurements during installation are available such a form that the installation personnel n make immediate decisions. This makes spe- al requirements of the data acquisition stem. Some of the instruments for the stallation phase may also continue to be used the operational phase.

e main control measurements for the stallation phase are as follows:

Position determined by acoustic transponders or electronic distance measurements.

Draught determined from sea water pressure measurements near the base.

Base clearance determined by echo sounders and special mechanical devices.

Axial stresses and bending moments in dowels determined by strain gauges.

Ballast water level in different cells controlled by pressure transducers.

Tilt measurement controlled by biaxial inclinometers.

Water pressure in skirt compartments controlled by means of differential pressure transducers.

Contact pressure against spherical domes measured by earth pressure cells.

Strain in reinforcing steel in spherical domes giving total loads on domes.

ort term settlements have been measured by ans of a closed hydraulic system with reser- ir on the platform and transducer on the sea oor. During skirt penetration inspections ong the periphery of the base have been rried out by a submarine taking video tapes r immediate checking on board the platform.

r performance measurements during the opera- onal phase, the following are recorded:

Skirt water pressure, in order to study the effect of the drainage system. In addition, the amount of drainage water is measured.

Earth pressure cells, in order to study load distribution, both static and dynamic.

- Inclinometers, to study long-term tilt effects. In addition optical levelling on deck is done twice a year.
- Settlements, usually recorded relative to a reference point at 50 to 60 m depth.
- Pore water pressure in the soil at different levels below the platform base.
- Accelerations at caisson and deck level.
- Long term horizontal displacement due to pre- dominant storm direction.

Possible scour of the sea bottom near the plat- form is monitored by a submarine. Reference sticks are set up in order to improve these inspections.

As an example case, the instrumentation of the most recently installed concrete gravity plat- form in the North Sea, the Statfjord B Condeep platform is given in Tables III and IV and illustrated in Fig. 29 (DiBiagio and Høeg, 1983).

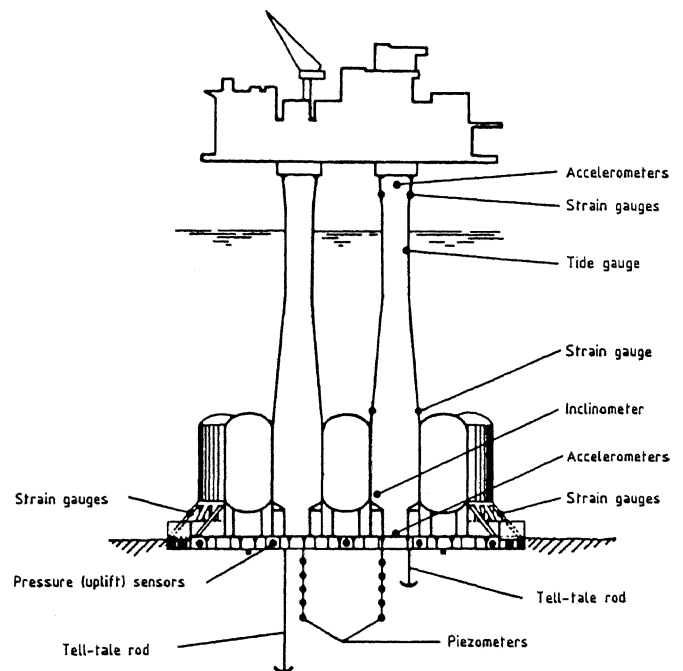


Fig. 29. Instrumentation for monitoring the long-term performance of Statfjord B (DiBiagio, 1983).

TABLE III. Summary of Instrumentation for Monitoring Installation. Mobil - Statfjord B Condeep Platform

Measurement	Number of instruments	Type
Wave height	1	Waverider buoy
Wind speed and direction	1	Anemometer
Clear tow path	3	Sidescan sonar
Under keel clearance	4	Echosounder
Draught	2	Pressure sensor
Touchdown	4+[4]	Pressure sensor
Penetration depth	5	Special device
Water pressure under base	10+[10]	Pressure sensor
Inclination	2	Servo-inclinometer
Ballast water level	43	Pressure sensor
Short-term settlement	1+[1]	Pressure sensor

Total .... 76+[15]

Note: Numbers in brackets [ ] denote redundant instruments

TABLE IV. Summary of Performance Monitoring Instrumentation. Mobil - Statfjord B Condeep Platform

Measurement	Number of instruments	Type
Wind speed and direction	1	Anemometer
Inclination	2	Servo-inclinometer
Long-term settlement	2	Tell-tale rod
Water pressure under base	10+[10]	Pressure sensor
Pore water pressure	10+[10]	Pressure sensor
Tidal variations	1+[1]	Pressure sensor
Strain top/bottom tower	16+[16]	Strain gauges
Strain in inclined braces	14+[14]	Strain gauges
Linear acceleration	4	Servo-accelerometer
Angular acceleration	5	Servo-accelerometer

Total .... 65+[51]

Note: Numbers in brackets [ ] denote redundant instruments. Wave data is obtained from a neighbouring platform.

The strain gauges at top and bottom of one tower are used to determine the forces and moments that are caused by environmental loads above that level, and the long term creep in the concrete. The strain gauges on the inclined struts around the base are used to obtain information about long term load distribution and cyclic forces during storm periods.

## INSTALLATION PHASE

Installation of the platforms from a floating position above the final location has been carried out by ballasting, i.e. sluicing water into the different cells. Platform installation may be divided into five different phases.

### Positioning

This is maneuvering the platform in a floating position to the exact location where it is intended to be installed. The orientation of the platform is also checked. For free-standing platforms, the usual requirements have been that the centre of the platforms should be within a 50 m diameter circle, and the orientation should be within  $\pm 5^\circ$ . Where the platforms have been placed close to other already installed platforms, special requirements have existed.

### Touch Down

This is the time when the lowest part of the structure touches the sea bottom. Touch down is the start of dowel penetration for platforms with dowels, or skirt penetration for platforms with just skirts. Touch down is recorded either by instrumented dowels or by other appropriate systems.

### Skirt penetration

It is necessary to calculate the skirt penetration resistance, and the need for eccentric ballasting to achieve vertical penetration. On the basis of experience, this can now be done with considerable confidence, both for steel concrete skirts (Lunne and Kvalstad, 1982).

The wall friction and point resistance for steel skirts have been correlated to cone penetration resistance,  $q_c$ . For clay profiles with some interbedded sand layers the following relations have been found:

$$\begin{aligned} \text{wall friction} & f = 0.03 q_c \\ \text{point resistance} & t = 0.4 q_c \end{aligned}$$

For clay profiles with less sand, values approximately 50% higher have been back-calculated.

For sands where piping has not been observed back-calculations gave:

$$\begin{aligned} \text{wall friction} & f = 0.003 q_c \\ \text{point resistance} & t = 0.6 q_c \end{aligned}$$

Where piping occurred much less penetration resistance was observed.

Penetration resistances for some platforms equipped with steel skirts are shown in Fig.

The main concern during skirt penetration is to avoid piping below the skirts and to keep the platform vertical. To avoid piping it has been necessary to provide an evacuation system to remove the water trapped within the skirt compartments. The evacuation capacity was designed for the expected penetration rate in order to avoid large overpressures in the skirt compartments.

Platform designers have used large pipes to evacuate directly into the sea. One structure has holes in the skirts at various levels. The most recently installed Condeep platforms evacuated water directly from the skirt compartments into the cells. The amount of water was regulated so that the penetration rate maintained zero pressure change in the skirt compartments.

On some of the platforms the water pressure in each skirt compartment could be regulated separately. Both overpressure and suction-pressure could then be applied when the penetration rate due to ballasting approached zero. The purpose of this system was to adjust the tilt of the platform, and by use of suction-pressure in the skirt compartments additional penetration force can be mobilized.

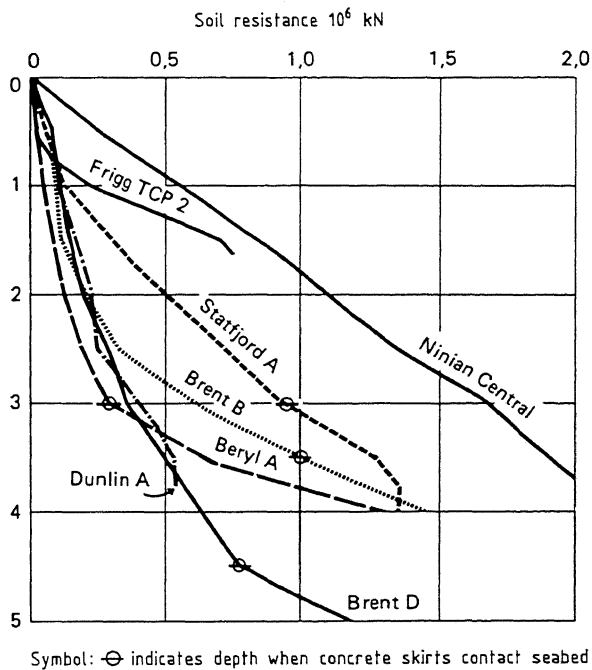


Fig. 30. Observed skirt penetration resistance for platforms equipped with steel skirts.

Base Seating

This phase has been particularly important for the Condeep platforms which had spherical-shaped bottom domes. The main object of the instrumentation is to check the base contact stresses which should not exceed some allowable value. Ballasting is then terminated and grouting executed.

For platforms with flat base slabs, penetration is to be stopped with an appropriate space between the slab and the sea floor in order to permit grouting.

Finally, ballasting takes place after grouting.

Sub-base Grouting

Grouting of the space between sea floor and the base is carried out for the following reasons:

- To avoid further penetration and to keep the platform vertical.
- To ensure uniform soil stresses on the slab and to avoid overstressing of any structural elements during continued ballasting and environmental loading.
- To avoid piping from water pockets below the base during environmental loading.

Grouting is especially important with uneven or sloping sea floors. The evacuation of displaced skirt water and excess grout material has either taken place directly into the sea or through a valve where grout quality can be checked (Boon et al., 1977; Ground Engineering, 1978).

A typical time schedule for the installation phase is shown in Fig. 31.

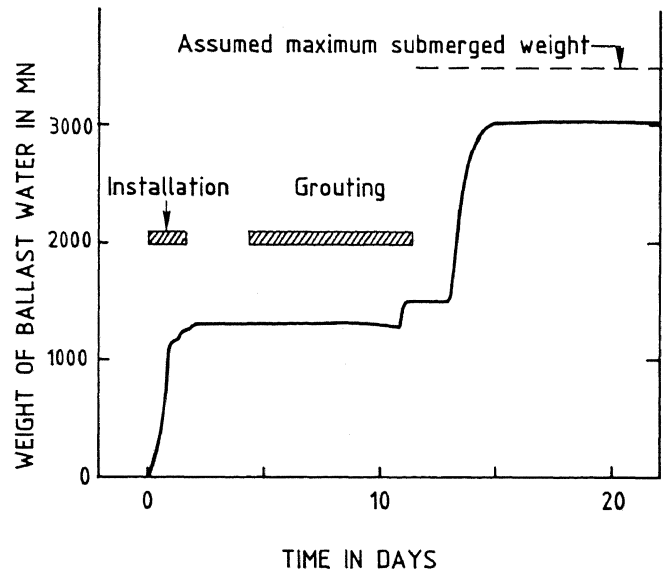


Fig. 31. Time schedule for installation and grouting of Statfjord B.

Installation of all the gravity platforms has taken place without any major problems, but each platform has had some minor events, including the following:

Ekofisk Tank

The major concern was related to contact stresses between the base and the soil, and the problem was raised just prior to tow out. Phillips had not been able to document the bathymetry to the satisfaction of Det norske Veritas who acted as certifying authority. Unevennesses greater than 30 cm might have caused unacceptable local stresses against the base section. Preparation for grouting was improvised, but turned out not to be necessary, as the observed unevenness around the periphery was less than 10 cm.

### Beryl A

The first conductor was installed with the water level in the drill shaft 20 m below mean sea level. This was a temporary low water level as the cell pressures had not yet been regulated to their final value. Even with 3.5 m deep skirts, piping took place, and approximately 400 m<sup>3</sup> of silt and fine sand was washed into the cell through the 1" wide annulus around the conductor, and it all happened in a couple of minutes. The additional settlement due to this event was 2 cm, and regrouting had to be carried out. The intact instrumentation proved very useful during this event.

### Brent B

During grouting of the last compartment a serious leakage took place into the minicell, probably from a broken, embedded grout pipe. The leakage was 200 m<sup>3</sup>/h at its maximum, and the skirt water pressure dropped more than 40 m before it was regulated back to normal by giving access to sea water. The leakage was stopped by adding various sorts of fiber material to the water which was sluiced into the skirt compartment, and grouting was finally completed.

### Frigg TP-1

The seafloor here slopes 0.6°, and the platform was grounded against the slope. Narrow tolerances were given due to a bridge connection to an already existing platform. This made it necessary to pull and rotate the platform with the concrete skirt partly embedded. Some sort of "bulldozing" took place (Foss and Warming, 1979).

The capacity to apply eccentric ballasting was not sufficient for vertical penetration and some tilt of the platform had to be accepted.

During the grouting operation grout of the order of 600 - 700 m<sup>3</sup> was lost out onto the sea-bed. This was due to piping taking place during skirt penetration and insufficient skirt depth.

### Cormorant A and Brent C

During grouting the same type of problem as was experienced with TP-1 was encountered. A step-by-step grouting procedure helped to solve the problem, but on Cormorant A the total volume injected was 7500 m<sup>3</sup>, compared to the theoretical value of 4900 m<sup>3</sup>.

### SOIL PRESSURE ON DOMES KN/m<sup>2</sup>

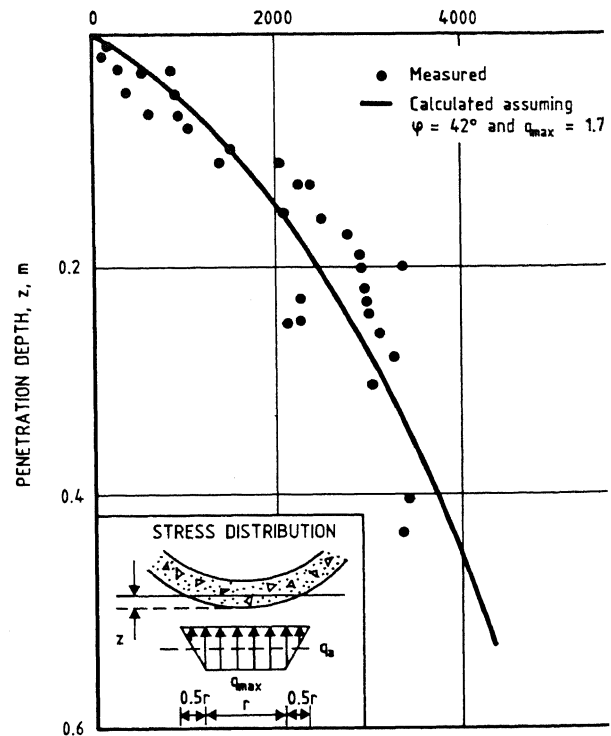


Fig. 32. Soil pressure on domes as a function of penetration depth. Comparison measured and calculated values. Frigg TCP-2 Condeep platform (Kjekstad, 1978).

### Frigg TCP-2

The slope of the sea-bed here is the same as TP-1, 0.6°, corresponding to 1 m difference elevation over the base diameter. Due to the cylindrical cells the Condeeps have great capacities for eccentric ballasting, and the domes at TCP-2 were made especially strong in order to be able to penetrate. The platform could then be made to penetrate vertically. Actually, request from Elf, the platform was installed at a slope of 0.1° to the slope of the sea-bed. The maximum eccentricity during penetration was 25 m. Contact stress as a function of penetration depth is shown in Fig. 32 (Kjekstad and Stub, 1978).

ent D

marine inspection during skirt penetration showed that some local piping still took place at a skirt penetration depth of 1.5 - 2.0 m. The full penetration depth of skirts here was 3 m.

Due to a local sand layer, high contact pressures were developed at one dome, and this determined when ballasting should be stopped and grouting started. The platform continued to penetrate another 10 - 12 cm after ballasting was stopped. The high contact pressure at the critical dome dropped off due to punch-through failure in the local upper sand layer. The reduction in dome contact stresses with increased penetration depth took place during one day as shown in Fig. 33.

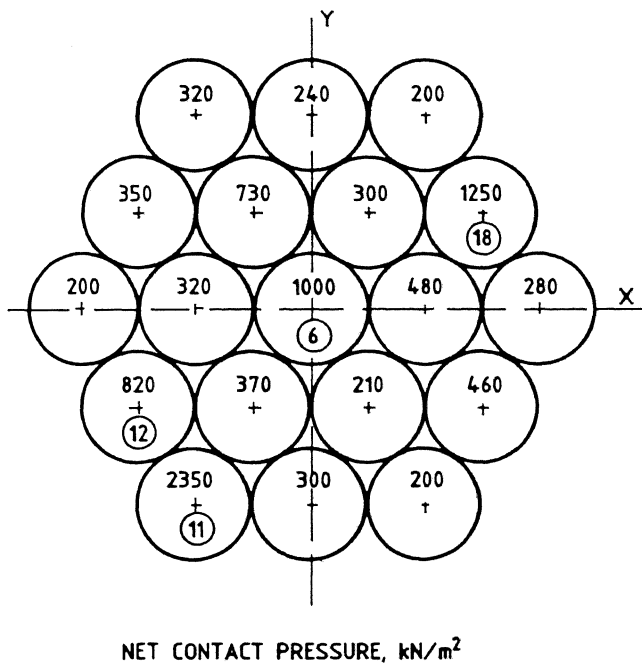
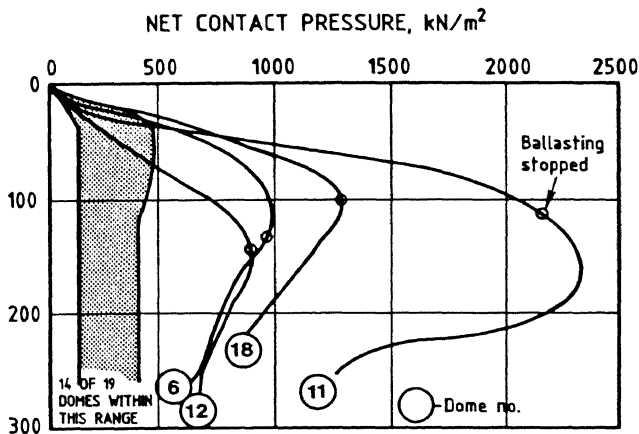


Fig. 33. Dome contact stresses during installation of Brent D Condeep platform.

Ninian Central

The Ninian Central Howard-Doris platform was ballasted centrally and allowed to tilt during the skirt penetration phase. When the final penetration depth of 3.7 m was reached on the one side, penetration was 2 m less on the other side, corresponding to an inclination 51'. With further centric ballasting the structure rectified itself, and at final ballasting the inclination was only 6', corresponding to 0.2 m difference in elevation over the base area.

Statfjord A

At Statfjord A a still more pronounced delayed skirt penetration took place after ballasting was terminated than that experienced at Brent D. The additional penetration after ballasting was stopped, was of the order of 0.2 - 0.3 m. This is assumed to be due to relaxation of the skirt wall friction due to rate effects. This rate effect is estimated to have been of the order of 20%.

Statfjord B

Contrary to the other Condeep platforms Statfjord B has a flat base slab. The reason is that the base area had to be extended in order to obtain adequate foundation stability. The cantilevered slab is supported by inclined struts (Fig. 34) and the basement is used for storage of sand ballast. Statfjord B is the largest gravity platform installed in the North Sea, with a base area of 18,200 m<sup>2</sup> and submerged weight of 3.7 · 10<sup>6</sup> kN.

Due to the flat base it was important to control the skirt penetration, and to stop at a certain depth. On the basis of previous experience this was handled very efficiently. During the skirt penetration phase water was sluiced both from the skirt compartments and from open sea in such a way that no differential skirt water pressure developed.

The experience from Brent D and Statfjord A was that skirt penetration continues after the stopping of ballasting, and this was not acceptable for Statfjord B. Instead of waiting for long term penetration to occur, the principle used was to unload, as illustrated in Fig. 35.

The most expedient penetration force to regulate is the skirt water pressure. One meter of differential skirt water pressure corresponds to 1.8 · 10<sup>5</sup> kN penetration force. The penetration force applied is shown in Fig. 36. The maximum total penetration force was 1.8 · 10<sup>6</sup> kN, which consisted of 1.3 · 10<sup>6</sup> kN ballast water and 0.5 · 10<sup>6</sup> kN suction force.

In order to demonstrate the efficiency of unloading by reducing suction, this principle was applied 20 cm above the preset penetration depth. During the eight-hour stop, no further penetration took place. The same procedure was employed at the final penetration depth (Fig. 37).

The platform was installed with an inclination less than 0.01° (1:6000), and the average skirt penetration depth differed less than one centimeter from the preset value.

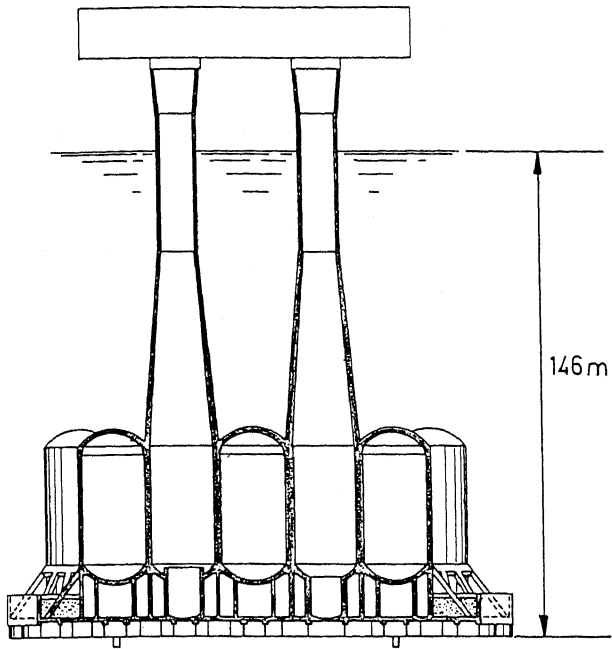


Fig. 34. Statfjord B Condeep platform.

PENETRATION RESISTANCE

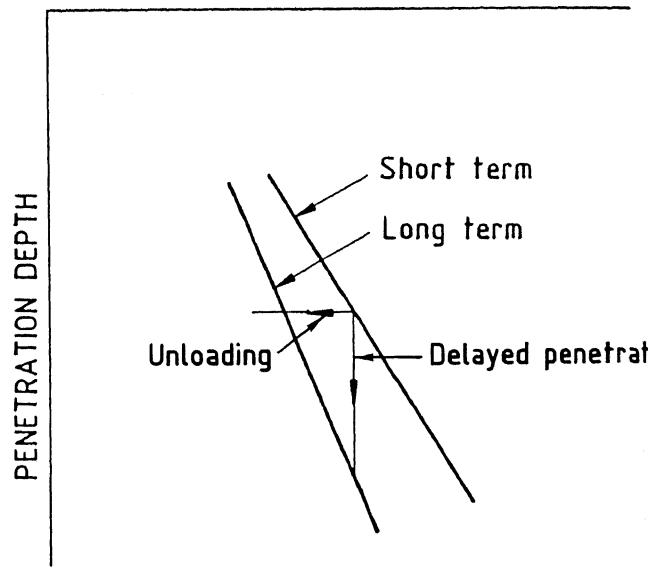


Fig. 35. Unloading required to avoid delayed skirt penetration.

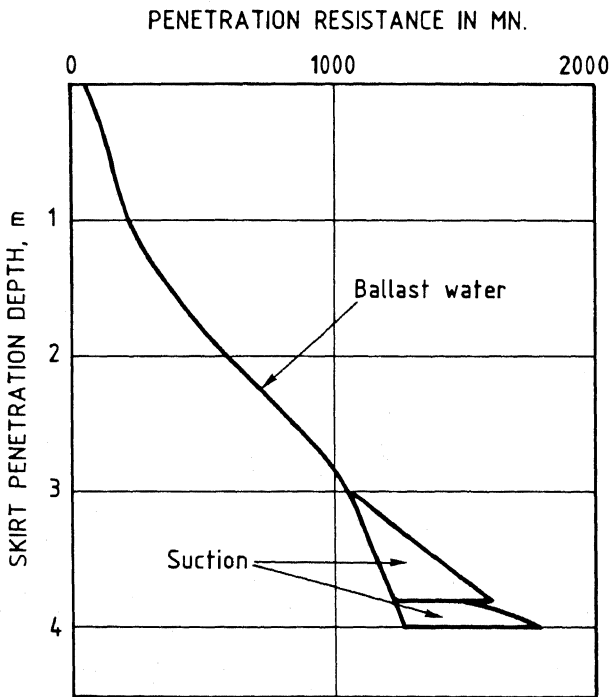


Fig. 36. Observed skirt penetration resistance during installation of Statfjord B Condeep platform.

TIME IN DAYS

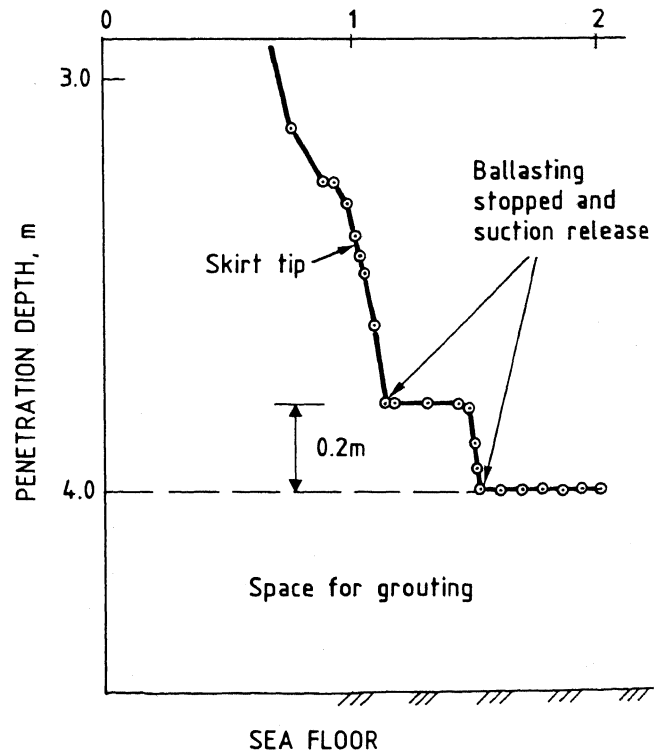


Fig. 37. Time scale for the final skirt penetration at Statfjord B.



## FOUNDATION DESIGN ANALYSES

described in the previous text, foundation engineering plays an important role when planning and controlling the installation of the platform. In addition, the foundation engineer has to ensure that the foundation behaviour will be satisfactory after the platform has been installed. The platform and its soil foundation will then be subjected to severe environmental loading. The major geotechnical problems to be considered for this phase, are:

- stability of the soil foundation
- soil stiffness for dynamic analyses and calculation of cyclic displacements
- settlements and permanent displacements
- base contact stresses
- piping and erosion

Each of these problems will be dealt with in more detail in the following by defining the problem, describing calculation procedures and representing observed behaviour.

## STABILITY

### General

The geotechnical design analyses have to ensure that the soil has a bearing capacity sufficient for carrying the weight of the platform and the cyclic forces from the environmental loading.

The stability analyses have to consider the following factors:

Horizontal and moment forces constitute an important part of the driving forces. The analytical method must be able to deal with this kind of loading in a realistic manner.

The wave load period is typically of the order of 10 - 20 seconds. This may introduce dynamic (inertia) effects. Further, undrained shear strength of soil may depend on time to failure.

The soil foundation will consolidate under the weight of the platform. The amount of consolidation prior to the arrival of the design storm will influence the undrained shear strength to be used in the analyses.

The cyclic loading from the waves in the design storm induces cyclic shear stresses in the soil which will generate pore pressures in the soil and reduce the effective normal stresses. The "cyclic strength" of the soil may thus be smaller than the original undrained static strength. The static strength may also be reduced by the cyclic loading.

- Depending upon the soil conditions, drainage may occur during the design wave and during the design storm. This will influence whether the design wave may be assumed to act under drained or undrained conditions and the effect of cyclic loading on soil strength.
- Smaller storms may also generate pore pressures which later drain away. This "precycling/drainage" will influence the soil behaviour under subsequent cyclic loading.

- For tripod platforms the vertical and horizontal forces and the local moments are not the same on the front pod and the rear pods.

The factors mentioned above are discussed in more detail in the following:

### Stability Analysis Procedure

The stability analyses are usually performed as limiting equilibrium analyses in which equilibrium between driving and resisting forces is controlled (e.g. Morgenstern and Price, 1965; Janbu, 1973; Lauritzsen and Schjetne, 1976). Various potential failure surfaces have to be analysed to find the most critical one. The procedure by Lauritzsen and Schjetne (1976), Fig. 38, is tailor-made for stability analyses of gravity platforms. The base is transformed into a square with the same area. The vertical load is applied on the "effective foundation area". The effective foundation area is defined in the same way as in bearing capacity formulas (e.g. Hansen, 1970, Meyerhof, 1953). The horizontal force is distributed over the whole foundation area. If the ratio between horizontal skirt spacing and skirt depth is large, it must be considered whether the horizontal part of the sliding surface may go up between the skirts.

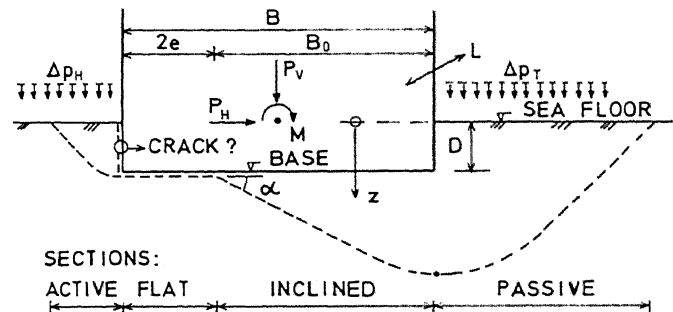


Fig. 38. Principles of slip surface method (Lauritzsen and Schjetne, 1976).

The analysis is performed with the forces from the design wave. Even if the wave loads are of a dynamic nature, the analysis is usually performed as a quasi-static analysis. The dynamic (inertia) effect is taken into account by multiplying the static wave forces with dynamic amplification factors which depend upon the dynamic characteristics of the platform and the soil. For current North Sea designs the dynamic amplification of the forces has been relatively small (of the order of 10%). For platforms in greater depths of water or on other soil conditions, the dynamic amplification may become larger.

The load duration is so short that even for sand it may be realistic to assume that the soil is undrained during the action of the design wave (Andersen et al., 1982). However, for sand one should be careful in relying on high undrained shear strengths which depend upon large negative pore pressures. These may drain away locally. For clays, it is assumed that undrained conditions prevail during the design wave.

Soil strength from laboratory tests must be determined from specimens subjected to the same stress and loading conditions as occur in situ (Fig. 39). The analysis can be performed as a total stress analysis or as an effective stress analysis with pore pressure parameters representative of the in situ loading conditions.

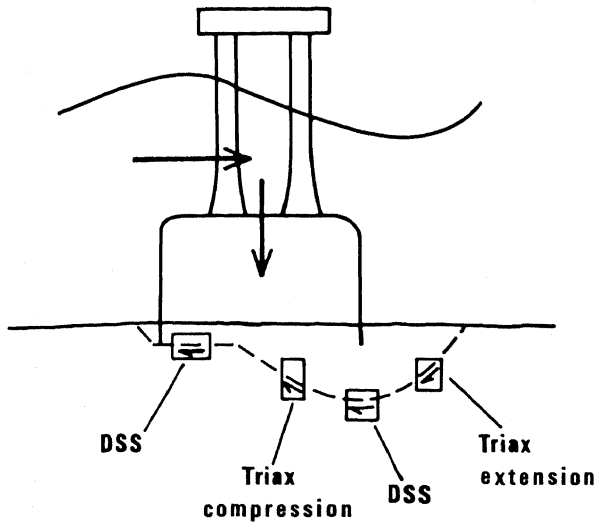


Fig. 39. Typical elements along a potential failure surface beneath an offshore gravity platform.

#### Analyses of Tripod Platforms

The analyses described in the previous section are valid for gravity platforms in general and cover both single base and tripod type platforms. The tripod type platforms, however, require some additional considerations.

Figure 40 shows schematically a tripod platform and the forces that it transfers to the soil.

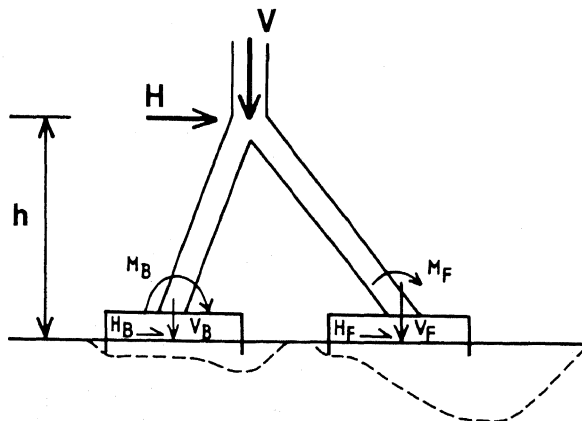


Fig. 40. Forces on a tripod platform.

The forces are a static vertical force due to the submerged platform weight and a cyclic horizontal wave force acting a distance,  $h$ , above the sea bottom. These forces are transferred to the

soil through the three pods. In Fig. 40 it is assumed that two of the pods are symmetrical around an axis in the load direction. They will then have identical loads.

The problem to be solved is to find how the horizontal force and the moment are distributed among the various pods. Assuming the two back pods to have the same forces, there are 6 unknowns, namely  $M_F$ ,  $H_F$ ,  $V_F$ ,  $M_B$ ,  $H_B$  and  $V_B$ . To determine these unknowns, there are three equations:

- (1) • vertical force equilibrium,  $\Sigma V = 0$
- (2) • horizontal force equilibrium,  $\Sigma H = 0$
- (3) • moment equilibrium,  $\Sigma M = 0$

To be able to solve the problem, it is therefore necessary to make three assumptions. These are:

- (4) & (5) • there is failure in the soil beneath both the front pod and the back pods.

The last assumption is that:

- (6) • the structure will find the most efficient way of distributing the loads among the pods. This means searching for the load distribution which gives the highest total failure load.

The assumptions have been proposed by Lauritzen (1983) who has also formalized a procedure to perform tripod stability analyses. Their validity is being checked by means of model tests and finite element analyses.

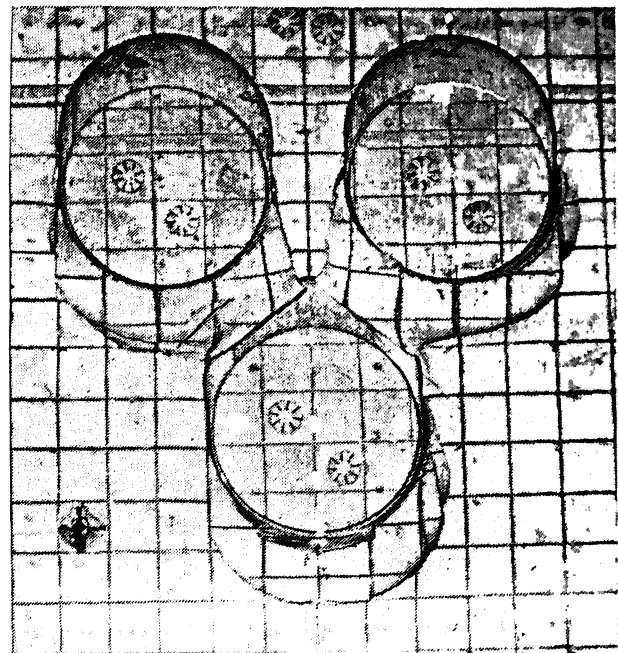


Fig. 41. Illustration of interaction between the failure zones beneath the various pods for a tripod platform. Results from model test carried out by Danmarks Ingeniørakademi. The figure is a photograph of the soil surface after the platform model has been removed.

another factor which has to be considered when calculating the bearing capacity of a tripod foundation, is interaction through the soil. The failure surfaces from the three pods may overlap, and the bearing capacity may be influenced. An example is shown in Fig. 41, which shows the foundation beneath a tripod model test after failure. How far apart the pods must be to avoid interaction depends upon the failure mode of the pods.

#### Consolidation Effects on Stability

When designing the platform it is assumed that the design storm may arrive during the first autumn after the platform has been installed. If the platform is to be towed out and installed safely, this has to be done during the summer, before severe storms may be expected. Then open spaces between the base and the soil will be grouted, and the platform will be ballasted to its full weight. These operations should be completed before the design storm is expected.

In the case of sand foundations, drainage will occur relatively rapidly, and it is reasonable to assume that the soil consolidates under the weight of the platform before the design storm arrives. As an example, pore pressure measurements in the sand beneath the Ekofisk tank during ballasting which increased the vertical pressure by 60 kPa in the course of approx. 55 days did not show any excess pore pressure in the sand due to this operation (Eide et al., 1979).

For clays consolidation goes much slower. For the Brent B Condeep platform on silty, sandy, stiff to hard clay interbedded with layers of fine, silty sand, pore pressure and settlement observations have shown that consolidation was completed for approx. 10 months (Andersen and Vas, 1980). For the Statfjord A Condeep platform on silty, sandy, very stiff to hard clay with only one sand layer at a depth of 31 - 35 m, observations have shown that consolidation was taken more than 3 years to complete (Lunne and Kvalstad, 1982). For soft clays it is expected that consolidation may even take much longer than 3 years to be completed.

If a platform is installed late in the summer on a site where clay layers are important for the stability, it must therefore be assumed that the design storm occurs before any consolidation takes place in the clay. However, if the platform is installed early in the summer, it may be assumed that some consolidation occurs. For some platforms in the North Sea 3 months of consolidation has been assumed in design. The amount of consolidation and the corresponding increase in effective stresses may be calculated by ordinary consolidation theory as for structures on land. Experience from the North Sea is that consolidation occurs faster than assumed in design (Lunne and Kvalstad, 1982). If the strength increase due to consolidation is to be relied upon in design, however, it is vital that the platform is installed early in the summer and that no delays occur.

#### Design Storm Loading

The platforms have to be designed such that the soil is able to withstand the design force after being subjected to the cyclic loading from the other waves in the storm. In the North Sea it has often been assumed that the design storm duration is 6 hours and that the design wave arrives at the end of the storm when the effect of cyclic loading on the soil strength is most severe. A typical 6 hour design storm composition is shown in Table V. Laboratory tests have shown that cyclic loading will tend to generate excess pore pressures in the soil, and the effective normal stresses and the shear strength of the soil will be reduced (e.g. Andersen, 1983).

TABLE V. Storm compositions for various storm durations (Hansteen, 1981)

3-hr. duration		6-hr. duration		24-hr. duration	
No. of cycles	% of max. force	No. of cycles	% of max. force	No. of cycles	% of max. force
1	100	1	100	1	100
2	95	2	96	2	96
4	88	4	89	4	96
8	81	8	82	8	86
15	74	15	77	15	81
30	67	30	70	30	76
50	59	50	64	50	71
90	51	90	58	90	66
200	41	200	49	200	60
500	23	500	37	500	52
		900	20	900	44
				1800	34
					19

Clay foundations will be undrained during a design storm and the cyclically induced excess pore pressure will accumulate from cycle to cycle during the storm. In fact, drainage may be so slow that the excess pore pressure generated during one storm does not dissipate before the next storm arrives. For clays it may therefore be necessary to analyse the accumulated effect of cyclic loading from several successive storms.

With sands drainage will occur much faster than for clays. Some drainage may therefore occur during the design storm and make the effect of cyclic loading less severe than if it had occurred under completely undrained conditions. However, even in sand the cyclic storm loading may induce some excess pore pressure.

#### Field Observations of Excess Pore Pressures Induced by Storm Loading

An example illustrating that storm loading does induce excess pore pressure in the clay beneath a gravity platform is shown in Fig. 42. The example shows pore pressure observations in the soil beneath the Brent B Condeep platform during a major storm with a significant wave height of 10.3 m the first winter, some 3.5 months after installation. The maximum wave is roughly twice the significant wave height, and the maximum wave forces were estimated to give a moment of  $8.6 \cdot 10^5$  kNm (43% of the design moment) and  $1.54 \cdot 10^5$  kN (31% of the horizontal design

force). The storm has its maximum intensity when the difference between the maximum and the minimum pore pressures in Fig. 42 are greatest.

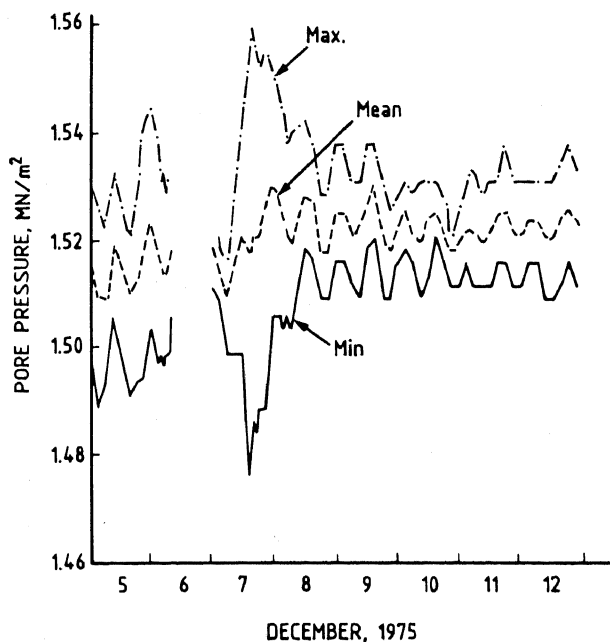


Fig. 42. Pore pressure measured in the soil beneath the Brent B Condeep platform during a storm with a significant wave height of 10.3 m. Depth = 4 m beneath sea floor (Andersen and Aas, 1979).

The average pore pressure then increases by approx. 10 kPa. Similar pore pressure increases were also recorded in piezometers at other depths. This is a relatively modest pore pressure increase, but it is of the same order of magnitude as expected from laboratory test results and theoretical analyses. Laboratory test results also show that the amount of cyclically induced pore pressure increases strongly with increasing cyclic shear stress. Further, the soil beneath the Brent B platform has experienced some consolidation under the weight of the platform during the 3.5 months from installation to the arrival of the storm (Fig. 78), and this has caused some increase in the soil strength. Thus there are reasons to expect a considerably higher cyclically induced excess pore pressure during a design storm arriving soon after a platform has been installed. These observations indicate that cyclic storm loading generates excess pore pressures in the clay beneath gravity platforms and that the effect of cyclic loading on soil behaviour must be taken into account in the stability analyses of gravity platforms on clay.

The pore pressure measurements beneath the Brent B Condeep platform also produce some evidence of the effect of consolidation under the weight of the platform on the soil strength and the effect of cyclic loading. The second winter after the platform was installed, there was a major storm with the same significant wave height of 10.3 m as the first winter. It is interesting to note that while a pore pressure of 10 kPa was

generated the first winter, there was no tendency to pore pressure generation the second winter. The main reason is most probably that the soil strength increased due to the consolidation which took place between the two storm periods. The soil was actually fully consolidated before the second winter period (Fig 78).

Another example of field observations which shows that storm loading may also induce excess pore pressures in sand foundations, is the observations on the Ekofisk tank. The Ekofisk tank is located on a very dense, fine sand. Figures 43a and 43b show pore pressure measurements in the sand beneath the platform during major storm 4.5 months after installation. The significant wave height during this storm was 11 m. The maximum wave height was estimated to be 21 m, corresponding to 90% of the 24 m design wave. Figures 43a and 43b show that the average pore pressure increases by 10 - 20 kPa during this storm. These observations indicate that generation of excess pore pressures during a storm must be considered and taken into account in stability analyses even for structures placed on very dense sand deposits.

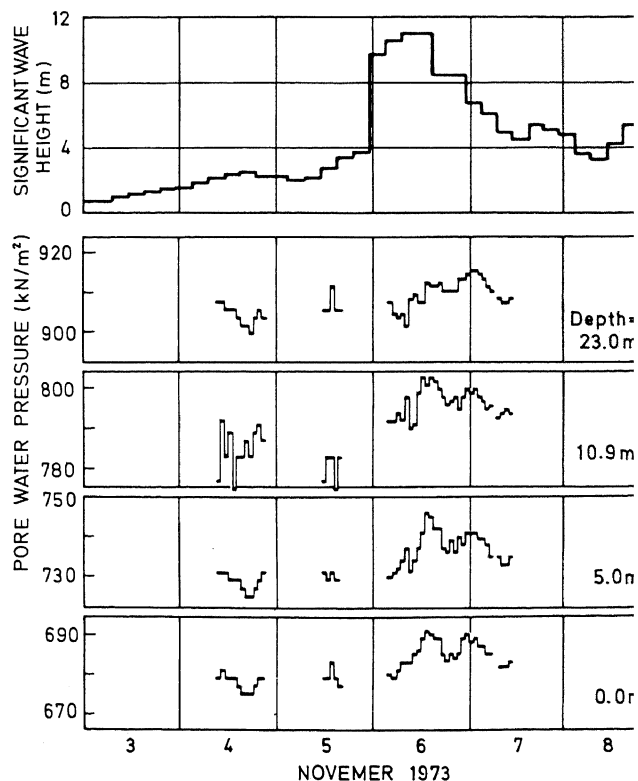
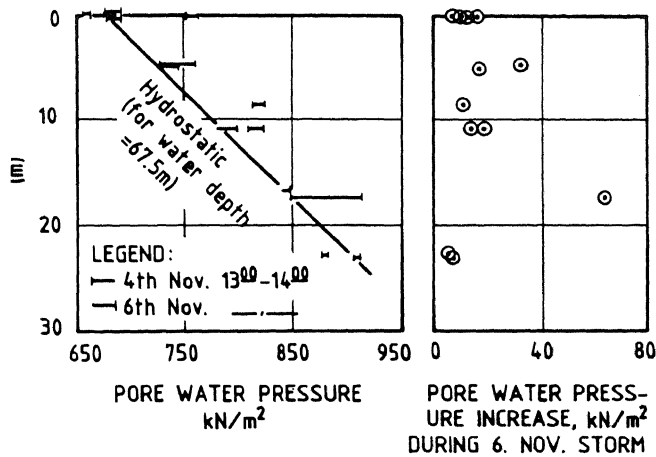


Fig. 43a. Pore water pressure observations in the soil beneath the Ekofisk tank before and during the 6th November storm for typical gauges (Clausen et al., 1975).



g. 43b. Pore water pressure versus depth in the soil beneath the Ekofisk tank. The increase in pore water pressure is taken as the rise in pressure from 4th November at 1300 - 1400 hours to 6th November at 1300 - 1400 hours (Clausen et al., 1975).

Cyclic Loading Effects on Bearing Capacity as Observed in Plate Loading Tests

As observed in laboratory tests and evidenced by the field observations, storm loading will induce excess pore pressures in the soil beneath gravity platforms. This will reduce the effective normal stresses and the shear strength of the soil. Fortunately, none of the North Sea gravity platforms have experienced foundation bearing capacity problems. Therefore there are no field observations showing the effect cyclic loading will have on the bearing capacity of the soil. The problem has been modelled in centrifuge model tests (e.g. Rowe and Craig, 1979). To provide additional data and experience, NGI has carried out field plate loading tests. The purpose of these tests was to provide a check of bearing capacity analyses based on triaxial and simple shear laboratory tests. The model plate was 1 x 1 m and equipped with skirts. The soil was a stiff, overconsolidated clay. Figure 44 shows that for the cyclic load sequence applied to the plate in this case, large cyclic displacements occurred for cyclic forces constituting only 70% of the foundation capacity for monotonic static loading.

Figure 45 shows that cyclic loading also causes a reduction in the bearing capacity for subsequent static loading. The reduction in static bearing capacity in Fig. 45 is extreme, since the foundation had been subjected to very severe cyclic loading. However, more moderate cyclic loading will also reduce the static bearing capacity.

Figures 44 and 45 illustrate two different failure situations. The failure in Fig. 44 is associated with large displacements that occur during cyclic loading. Figure 45 shows the effect of cyclic loading on the bearing capacity for subsequent monotonic static loading.

The plate loading test results indicate that the bearing capacity of the soil may be significantly reduced by cyclic loading and show that it is essential to take the effect of cyclic loading into account when calculating the bearing capacity of the soil beneath a gravity platform.

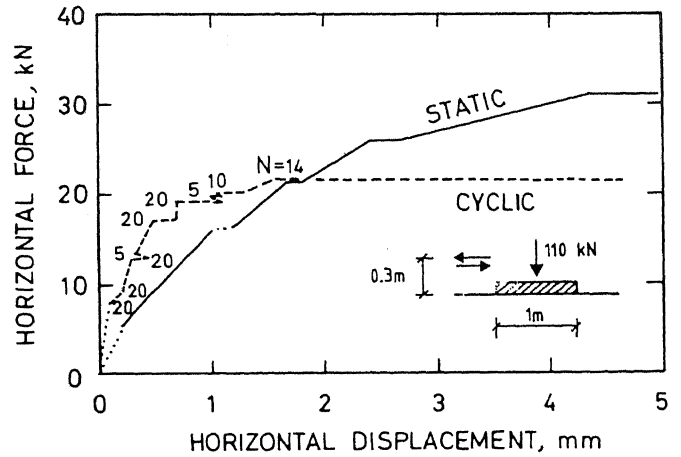


Fig. 44. Results from in situ cyclic and static plate loading tests on a stiff clay at Haga (Stenhamar and Andersen, 1982). For the cyclic tests, the figure presents the cyclic displacement amplitude as a function of the cyclic force amplitude. The cyclic test was run by applying 20 cycles with a force amplitude of 8 kN, 20 cycles with 9 kN and so on with increasing cyclic force amplitude. The number of cycles, N, at the various force amplitudes are given in the figure.

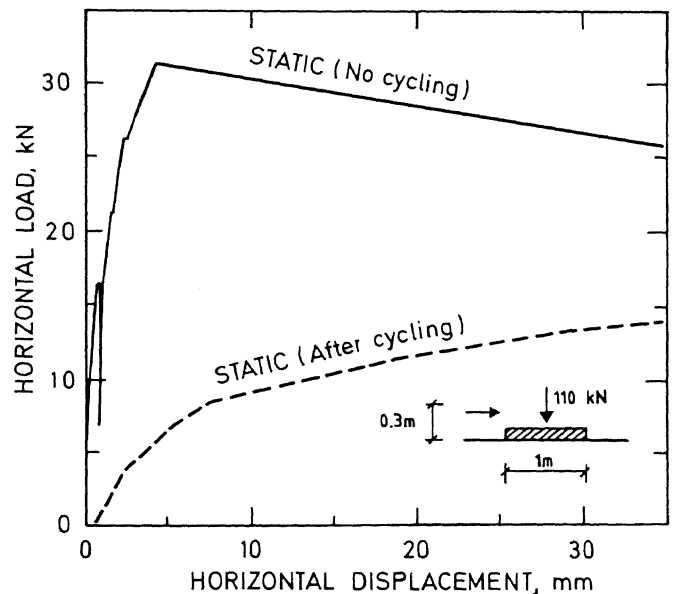


Fig. 45. Results from in situ plate loading tests showing the reduction in static bearing capacity due to cyclic loading. The test with previous cyclic loading had been subjected to the cyclic load sequence in Fig. 44.

Effect of Cyclic Loading on Soil Strength in General

Calculation of the bearing capacity of the soil beneath a gravity platform has to be based on soil strength determined in laboratory tests on small soil specimens. To be able to interpret the laboratory test results and to determine a soil strength which accounts for the effect of cyclic loading, it is necessary to first consider what happens to the soil when it is subjected to cyclic loading. This is illustrated by means of the stress paths in Fig. 46.

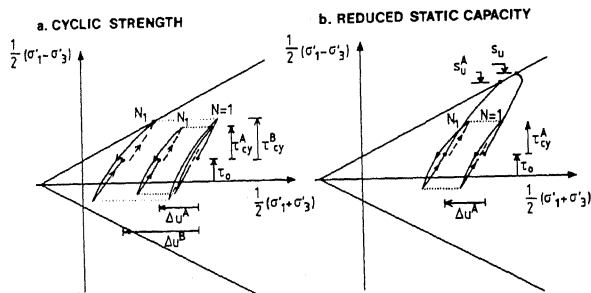


Fig. 46. Behaviour of soil subjected to cyclic loading.

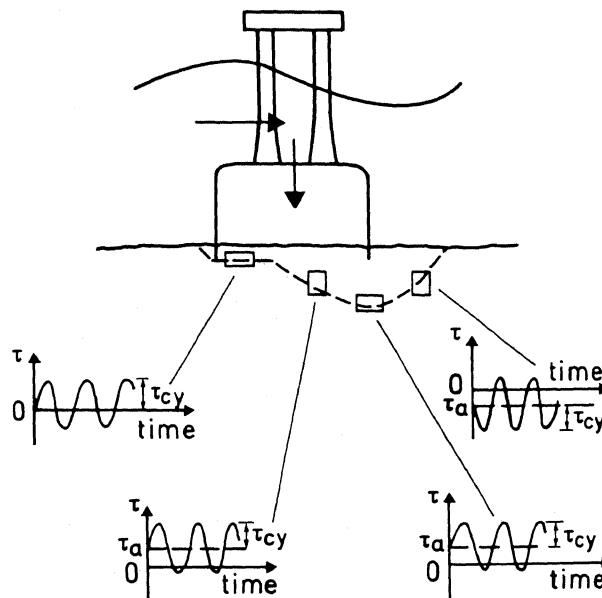
As mentioned previously, cyclic loading will induce an excess pore pressure in the soil which leads to reduced effective normal stresses. A soil element with a cyclic shear stress amplitude of  $\tau_{cy}^B$  will thus move towards the failure envelope as indicated in Fig. 46a. After a certain number of cycles,  $N_1$ , the failure line is reached. The soil element will then experience large shear strains and be in a state of cyclic failure. The failure mode may take the form either of large cyclic shear strain amplitudes or large permanent shear strains, depending on the combination of cyclic and average shear stresses that the soil element has been subjected to.

If the cyclic shear stress amplitude is smaller, e.g.  $\tau_{cy}^A$  in Fig. 46a, a much smaller pore pressure will be generated after the same number of cycles,  $N_1$ . However, if cycling is continued, this element will also reach the failure line unless the cyclic shear stress is very small. The "cyclic strength" of a soil element is therefore not a material constant, but depends upon the number of cycles that it is subjected to.

If cycling is stopped before the element has reached the failure line, the cyclic loading will influence the static strength that can be mobilized under subsequent monotonic static loading. This is illustrated in Fig. 46b. The static stress path for the element which has been subjected to cyclic loading will reach the failure line at a lower shear stress than for an element which has not been subjected to previous cycling. The shape and the slope of the static stress paths may also change due to the cycling, and the reduction in static strength due to cycling may be smaller than the percentage reduction in effective stresses. The reduction in static strength will depend upon both the average shear stress and the cyclic shear stress amplitude during cycling. Like the cyclic strength, it will also depend upon the number of cycles.

Cyclic Soil Strength

The elements in the soil beneath a gravity platform will be subjected to a variety of stress paths and combinations of average and cyclic shear stresses (Fig. 47). The average shear stress,  $\tau_a$ , is composed of 1) the initial shear stress in the soil prior to the installation of the platform,  $\tau_o$ , and 2) a shear stress which is induced by the submerged weight of the platform  $\Delta\tau_a$ . The initial shear stress has been acting under drained conditions. The shear stress due to the weight of the platform will first act under undrained conditions, but as the soil consolidates under the weight of the platform, this shear stress will also act under drained conditions. The cyclic shear stress,  $\tau_{cy}$ , is induced by the cyclic wave forces. In a storm, the wave height varies continuously from one wave to another, and the cyclic shear stress will also vary from cycle to cycle.



- Triaxial tests
- Simple shear tests

Fig. 47. Example of loading of soil elements along a potential failure surface in the foundation beneath an offshore gravity platform. Simplified.

The data presented in the following are from laboratory tests on clay specimens with both  $\Delta\tau_a$  and the cyclic loading applied under undrained conditions. With sand it will as discussed previously be more representative to apply  $\Delta\tau_a$  drained, and it is also necessary to evaluate the effect of partial drainage during cyclic loading. The following section will first present the results from tests in which the cyclic shear stress is kept constant throughout the test. Afterwards it will be shown how the cyclic

Soil strength can be determined for conditions where the cyclic shear stress varies from one element to another, as happens during a storm.

Examples of measured cyclic strengths of clay specimens loaded with symmetrical, constant, cyclic shear stresses under simple shear conditions, are presented in Fig. 48. The number of cycles to failure depends upon the magnitude of the cyclic shear stress and the overconsolidation ratio. At a given ratio between cyclic shear stress amplitude and undrained static shear strength, the higher the overconsolidation ratio is, the sooner cyclic failure is reached. It is therefore important to prepare the laboratory specimens to the same overconsolidation ratio as in situ.

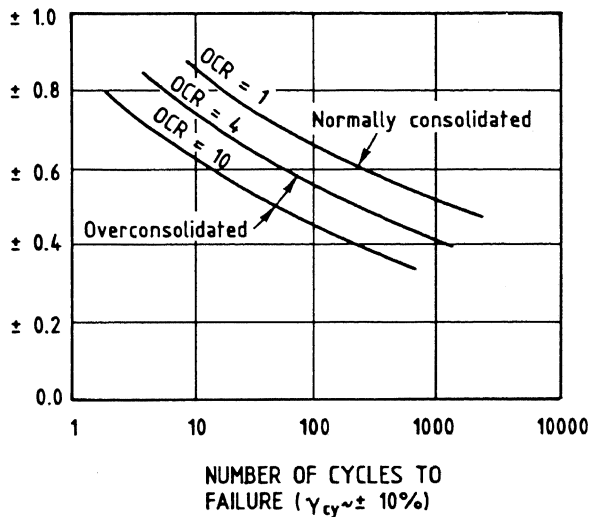


Fig. 48. Number of cycles to failure for undrained symmetrical cyclic simple shear loading on Drammen clay with various overconsolidation ratios.  $\tau_{hf}$  is the undrained static shear strength from tests with approx. 2 hrs. to failure.

The effect of the average shear stress on the number of cycles to failure, is illustrated in Fig. 49. The figure shows the number of cycles to failure for different stress paths and various combinations of average and cyclic shear stresses. If the average shear stress distribution in the soil is calculated, and if the storm loading is simplified to a certain number of equivalent cycles of the maximum wave in the storm, both  $\tau_a$  and  $N$  will be known for all the elements. Depending on  $\tau_a$ ,  $N$  and the assumed stress path for each element along the potential failure surface, the cyclic shear stress,  $\tau_{cy}$ , which will cause failure can be determined from Fig. 49. The cyclic strength to be used in the stability analysis will be  $\tau_a + \tau_{cy}$  for each of the elements. (In the above it is assumed that  $\tau_a$  in the various elements along the potential failure surface remains constant throughout the storm. In reality, however, some stress distribution will occur, and there will be some changes in  $\tau_a$ .)

A real storm is as mentioned composed of waves with varying heights and periods. The soil elements beneath a platform will therefore be subjected to an arbitrary variation in cyclic shear stress from one cycle to another.

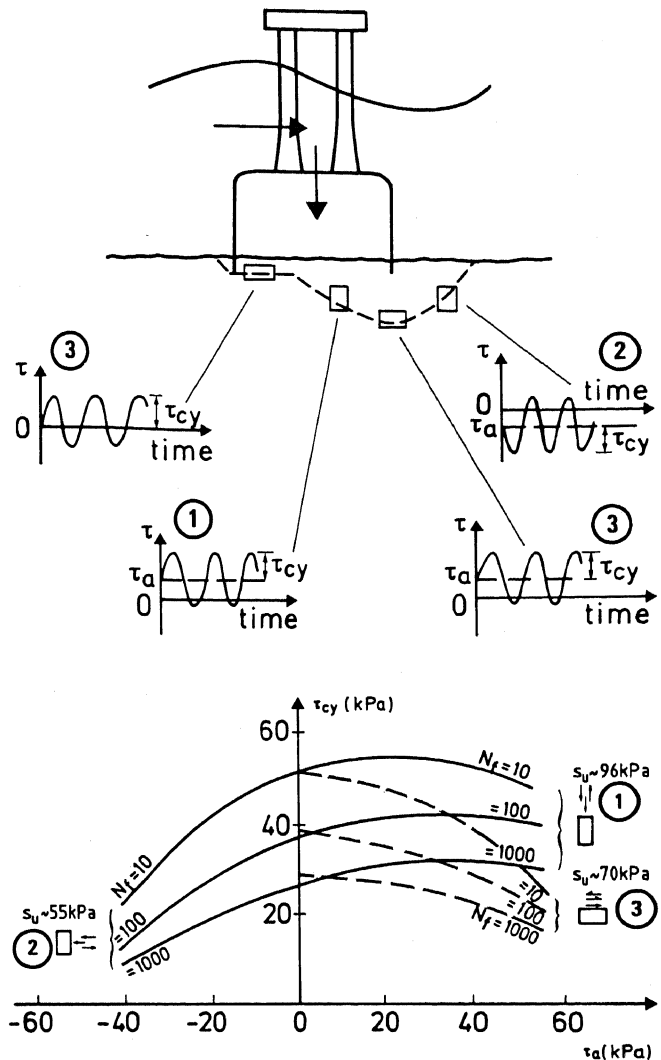


Fig. 49. Example of cyclic strengths for various stress paths and shear stress combinations (Andersen, 1983).  $s_u$  is the undrained static shear strength.

In practice it is not possible to simulate all relevant cyclic load histories in the laboratory. Usually, therefore the laboratory tests are run with one constant cyclic shear stress throughout the test. To be able to use these tests to predict the soil strength for real storm loading, procedures have been developed to predict soil behaviour under varying cyclic shear stresses, from tests employing constant cyclic shear stress. One such procedure uses the cyclic shear strain as a memory of the effect of cyclic loading (Andersen, 1976; Andersen et al., 1978). This procedure is based

on so-called "strain contour diagrams" constructed from cyclic tests with constant cyclic shear stress. Examples of contour diagrams are shown in Fig. 50 which is valid for cyclic simple shear loading with zero average shear stress. Separate diagrams have to be established for other stress paths and other combinations of cyclic and average shear stresses.

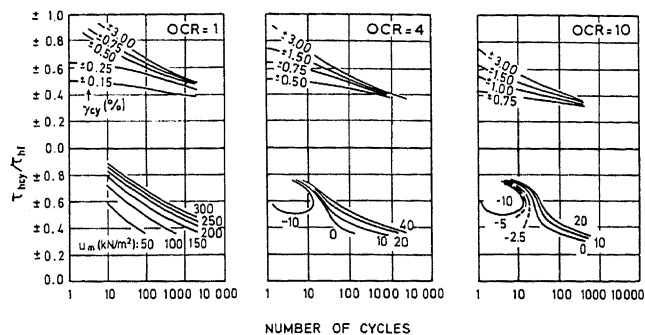


Fig. 50. Countour diagrams for cyclic shear strain and excess pore pressure. Simple shear tests with symmetrical cyclic loading on Drammen clay.  $\tau_{hf}$  is the undrained static shear strength for specimens sheared to failure in approx. 2 hrs. (Andersen et al., 1980).

Figure 51 shows how the "strain accumulation" procedure is used to determine the development of the cyclic shear strain amplitude of a soil element during a 6-hour storm. The assumed cyclic shear stress history is given in Table V. It is assumed that the small waves arrive first and that the maximum wave arrives at the end of the storm when the effect of cyclic loading is most pronounced. The graphs on the left in Fig. 51 show examples of two storms with different maximum cyclic shear stresses. For each of the

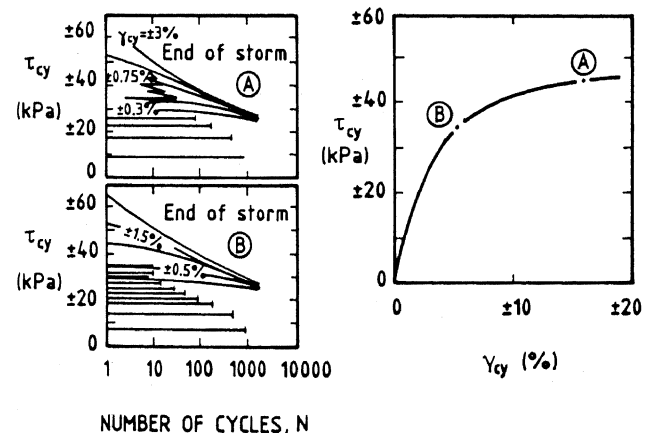


Fig. 51. Maximum cyclic shear strain amplitude as a function of the maximum cyclic shear stress amplitude in a 6-hour design storm (right hand diagram). The construction of points A and B are shown in the diagrams on the left.

two storms the cyclic loading is determined by scaling the load levels for a 6-hour storm in Table V, such that the maximum cyclic shear stress corresponds to 100% in the table.

The maximum cyclic shear strain for each element in Fig. 51 occurs during the cycle with the maximum cyclic shear stress. This maximum cyclic shear strain amplitude is plotted as a function of the maximum cyclic shear stress amplitude on the right hand graph in Fig. 51.

The right hand graph in Fig. 51 shows that if the maximum cyclic shear stress in a storm exceeds a certain critical value, the cyclic shear strain amplitude becomes very large. This critical value is the "cyclic strength" of the clay. This cyclic strength is not a material constant, but depends upon the storm composition and the storm duration. It also depends upon the overconsolidation ratio. Figure 52 shows an example of the ratio between cyclic strength and conventional undrained static strength for a simple shear element. The cyclic strength is valid for the 6-hour storm in Table V.

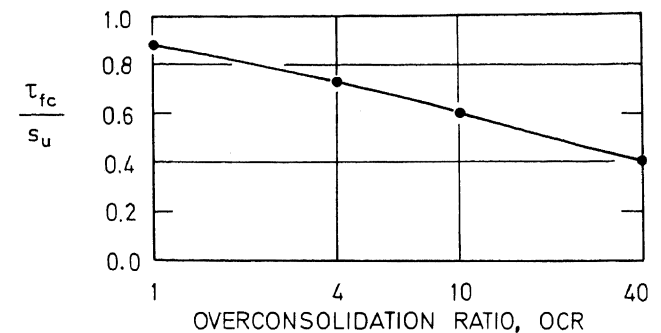


Fig. 52. Cyclic strength normalized with respect to the undrained static shear strength.  $s_u$  is the undrained static shear strength for 2 hours to failure prior to cycling (Andersen et al., 1982).

Diagrams like the one in Fig. 52 may also be established for other stress paths and various values of the average shear stress. It should be kept in mind that in the general case, the cyclic strength to be used in a stability analysis is equal to the sum of  $\tau_a$  and  $\tau_{cy}$  at failure.

The values in Figs. 51 and 52 are evaluated for a 6-hour storm. As mentioned previously, the clay foundation may be undrained for a longer period than a 6-hour storm. The effect of storm duration on the cyclic strength of plastic Drammen clay is presented in Fig. 53. The results in Fig. 53 show that it is important to base the analyses on a correct storm duration figure.

Another procedure for predicting soil behaviour under varying cyclic shear stress from tests with constant cyclic shear stresses, is to use the cyclically induced excess pore pressure as a parameter instead of the cyclic shear strain. For sands where it is important to incorporate partial drainage, this pore pressure accumulation procedure may be most suitable. For clays



the other hand, it is difficult to perform pore pressure measurements in cyclic laboratory tests with a high degree of accuracy. Since there is not likely to be significant drainage during a storm, it is recommended that strain accumulation procedure be used for clays. For most practical purposes it is the cyclic shear modulus and the cyclic shear strength that are of primary importance. These parameters will be determined directly from the strain accumulation procedure without involving the uncertain pore pressures.

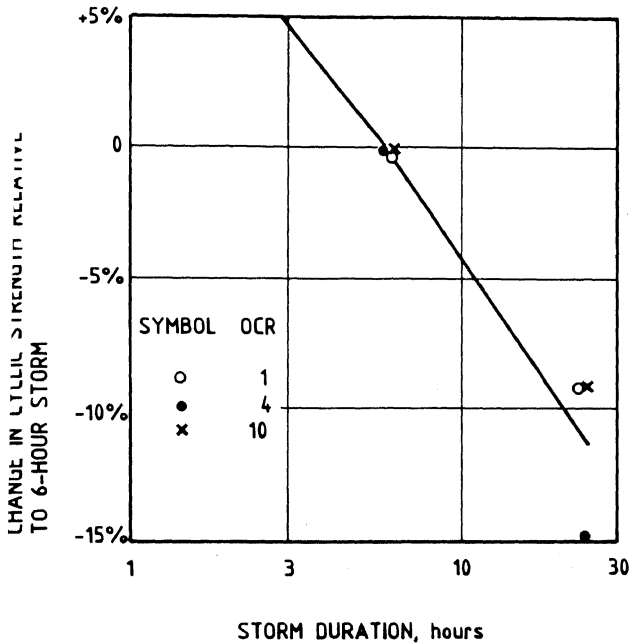


Fig. 53. Effect of storm duration on cyclic strength of Drammen clay. Based on constant volume, simple shear tests (Andersen et al., 1982).

Undrained Shear Strength Reduced for Effect of Undrained Cyclic Loading

Reduction in undrained static strength due to cyclic loading can also be determined from laboratory tests. The laboratory tests are then first subjected to undrained cyclic loading. Afterwards they are loaded to failure by undrained monotonic static loading.

Examples of results from static tests on clay specimens with and without previous undrained cyclic loading are shown in Fig. 54. Both the undrained static shear strength and the undrained static shear modulus are reduced by the cyclic loading. An example of reduction in undrained static shear strength as a function of cyclic shear strain which occurred during cyclic loading, and the number of cycles, is presented in Fig. 55.

For design purposes, the reduced undrained static shear strength can be evaluated by first determining the cyclic shear strain amplitudes in the soil beneath the platform during the design wave at the end of the design storm.

These cyclic strains can be obtained from the finite element analysis used to calculate cyclic displacements or from other simplified methods. When these cyclic strains are known, the reduction in undrained static strength can be determined from diagrams of the type in Fig. 55.

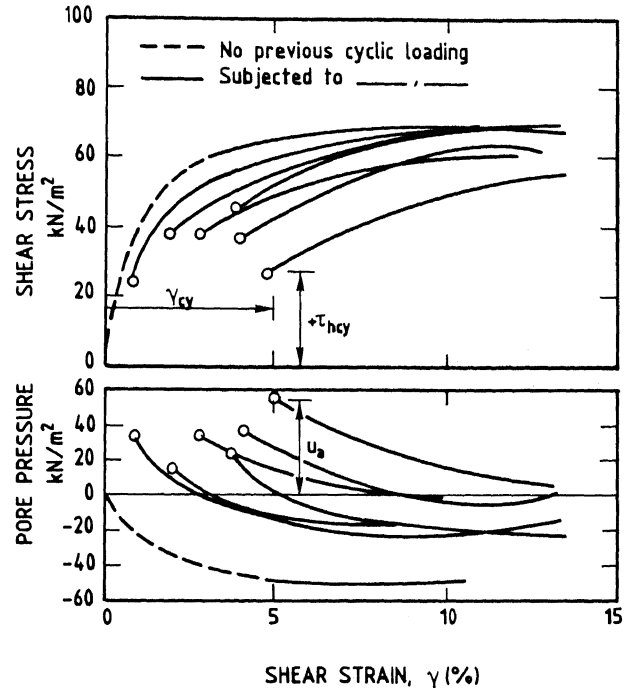


Fig. 54. Results from undrained static simple shear tests on specimens with and without previous undrained cyclic loading. Drammen clay with OCR = 4 (Andersen et al., 1980).

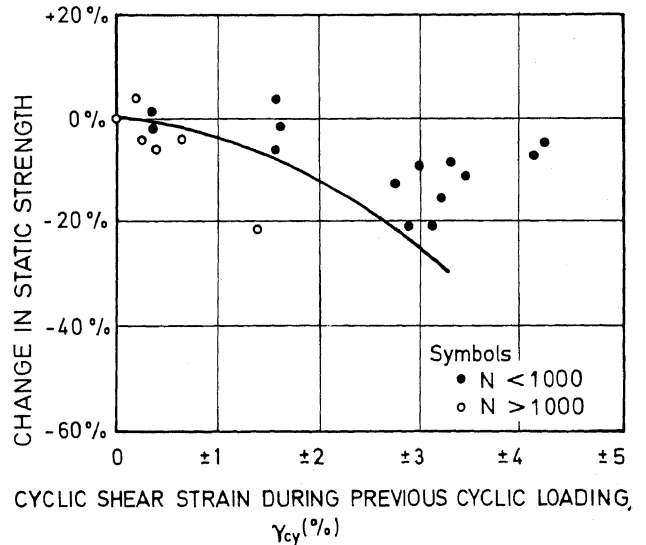


Fig. 55. Reduction in undrained static shear strength due to undrained cyclic loading. Simple shear tests on Drammen clay with OCR = 4 (Andersen, 1976).

For sands where partially drained states may occur, it may be more convenient to work with pore pressures and effective stresses (e.g. Smits et al., 1978; Rahman et al., 1977).

The static laboratory tests are often run to failure in approx. 2 hours with a constant rate of strain. Andersen et al. (1982) have shown that strain-controlled loading gives a shear stress variation with time which is close to the first quarter of a sinusoidal variation. Constant rate of strain tests may thus be a reasonable approximation of the wave force loading in situ. The time to failure in situ, however, would be much shorter than 2 hours and closer to 5 seconds. The effect of this difference in time to failure is presented for some clays in Fig. 56. For plastic clays the effect of time to failure may be quite significant, and ideally the laboratory tests should be run with the same time to failure as is required in situ.

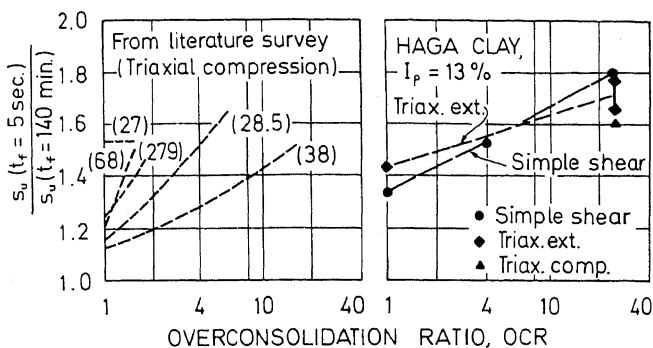


Fig. 56. Increase in undrained static shear strength when time to failure  $t_f$ , is reduced from 140 minutes to 5 seconds. Numbers in parentheses indicate plasticity,  $I_p$ , in percent (Andersen et al., 1982).

Stability Analyses Based on Static Strength which is Reduced for the Effect of Cyclic Loading

For foundation design of gravity platforms in the North Sea, it has been the practice to perform the stability analyses by calculating the safety against failure due to the single characteristic wave force, assuming that it arrives at the end of the storm. The static strength reduced to account for the effect of cyclic loading from all the other waves in the storm is taken to represent soil strength. A load coefficient,  $\gamma_f$ , of 1.0 has been applied to the cyclic wave forces when evaluating the effect of cyclic loading from the waves in the storm. However, a load coefficient,  $\gamma_{f,100}$  of 1.3 is applied to the forces from the single characteristic wave when performing the stability analysis. In total stress analyses based on reduced undrained static shear strengths, a material coefficient  $\gamma_m$  of 1.3 is required.

In the case when horizontal sliding is the critical failure mode, the critical horizontal design force,  $H$ , will be:

$$H = \frac{s_u^A \cdot A}{\gamma_m \cdot \gamma_{f,100}}$$

where:

$s_u^A$  is the static strength reduced to account for the effect of cyclic loading

$A$  is the foundation area

In the case of horizontal sliding there is no difference between working with partial safety coefficients and a lump safety factor, and the product  $\gamma_m \cdot \gamma_{f,100} = 1.69$  is equivalent to working with a lump safety factor,  $SF$ , of 1.69 i.e.:

$$H = \frac{s_u^A \cdot A}{\gamma_m \cdot \gamma_{f,100}} = \frac{s_u^A \cdot A}{SF}$$

This way of analysing the stability means that the safety factor is applied to cover uncertainties in the undrained shear strength and the design force. No safety factor is applied to cover uncertainties in the forces from the other waves in the storm when evaluating the effect of cyclic loading on the static shear strength. It may be argued, however, that the forces from smaller waves are just as uncertain as the design wave forces and that a load coefficient should be applied to the forces from all the waves in the storm. The consequences of uncertainties in the forces from all the waves are illustrated by an example:

Figure 57 shows the results from analyses of platforms where horizontal sliding is the critical failure mode. The analyses are made for platforms on clay with different overconsolidation ratios. The platforms are designed according to current practice, meaning that the material coefficient,  $\gamma_m$ , is 1.3. In order to see the consequences of uncertainties in the storm, all the wave forces in the storm have been increased by a certain percentage in excess of the design values, and the corresponding material coefficient has been calculated.

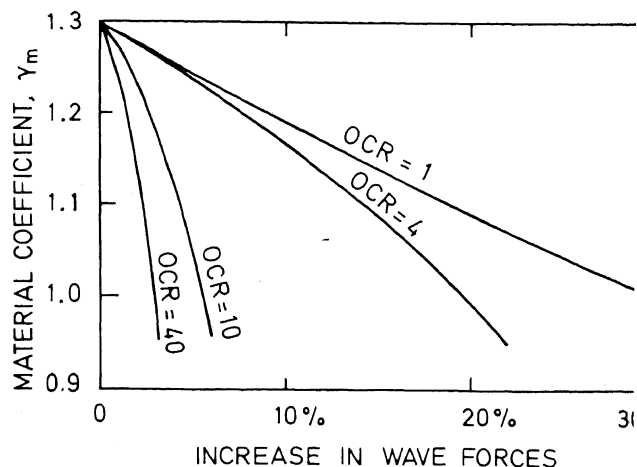


Fig. 57. Effect of increases in wave forces on a platform which is designed with static strength analyses according to current practice. The diagram is valid for Drammen clay and for platforms where horizontal sliding is the critical failure mode (from Andersen et al., 1982).

Figure 57 shows that for normally consolidated clays the wave forces can be increased by 30% before the material coefficient drops to 1.0. For higher overconsolidation ratios, however, only small increases in wave forces lead to reductions in the material coefficient from 1.3 to 1.0. For OCR = 10, for instance, this drop occurs for a 5% increase of the wave forces in a storm.

These results indicate that when making stability analyses based on static strength reduced to account for the effect of cyclic loading, the margin of safety against uncertainties in storm loading depends dramatically upon the overconsolidation ratio and this margin of safety is undesirably low for highly overconsolidated clays. This is the case both when working with lump safety factors and when working with partial safety coefficients.

As will be shown later, stability analyses based on cyclic shear strength will be better suited to account for the uncertainties in wave forces. First, however, the influence of rate effect on the shear strength and on the calculated bearing capacity will be shown.

As mentioned before, the static tests are often brought to failure in about 2 hours with a constant rate of deformation. The actual wave loading, however, is of a much shorter duration and in cases where the wave loads are the main driving forces, it would be more appropriate to run the static tests to failure in 5 to 10 seconds. For plastic clays, the undrained static strength increases significantly with increasing time to failure. For lean clays, the effect is less pronounced, and for sands it is negligible. The effect of rate of loading on the measured undrained soil strength is shown for some clays in Fig. 58.

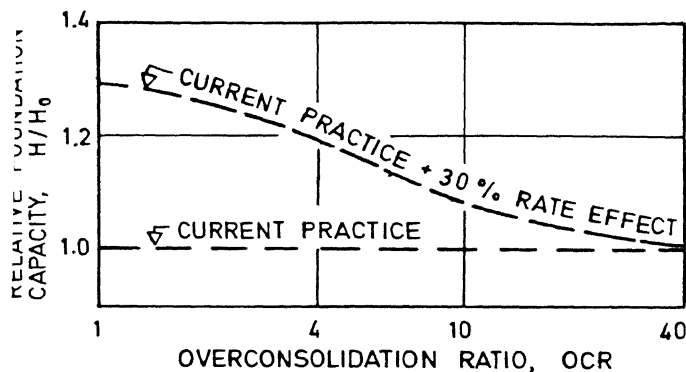


Fig. 58. Influence of 30% strain rate effect on foundation capacity.  $H$  is the horizontal design force that can be carried by the foundation (Andersen et al., 1982).

The influence of rate effect on the foundation capacity, computed according to current practice, is illustrated by means of an example. It is assumed that the strength increases by 30% when the time to failure is reduced from 2 hours to 5 seconds. It is also assumed that the same numerical values of  $\gamma_f$  and  $\gamma_m$  are required as for the conventional 2 hours to failure. This may be subject to discussion, since the specification of material coefficients ought to be closely

linked with the selection of soil strength values. Figure 58 shows that for OCR = 1, the foundation capacity increases with the same percentage as the strength increase. However, for high OCRs the calculations show that the calculated foundation capacity is little influenced by the rate effect.

### Stability Analyses Based on Cyclic Shear Strengths

For the more recent platforms, stability analyses based on cyclic shear strengths have been included in addition to analyses with static shear strengths (Foss et al., 1978; Andersen et al., 1982). The choice of numerical values for the material and load coefficients (or for the lump safety factor) is more open for discussion in this case. The material coefficient should be applied to the cyclic shear strength, and it seems reasonable to apply the value of 1.3 as for the static strength. When deciding upon the numerical value of the load coefficient, however, it must be kept in mind that the load coefficient in this case is applied to the forces from all the waves in the storm and not only to the force from the single design wave.

Figure 59 shows the results of cyclic strength analyses compared to analyses with reduced static strengths according to current practice. The results of the cyclic strength analyses are shown for various values of the product  $\gamma_m \cdot \gamma_f$  (= SF in the case of horizontal sliding). The diagram shows that in the case with no rate effect, and if a material coefficient of 1.3 and a load coefficient of 1.0 are applied, the cyclic strength analyses will be governing for overconsolidation ratios higher than 3.5.

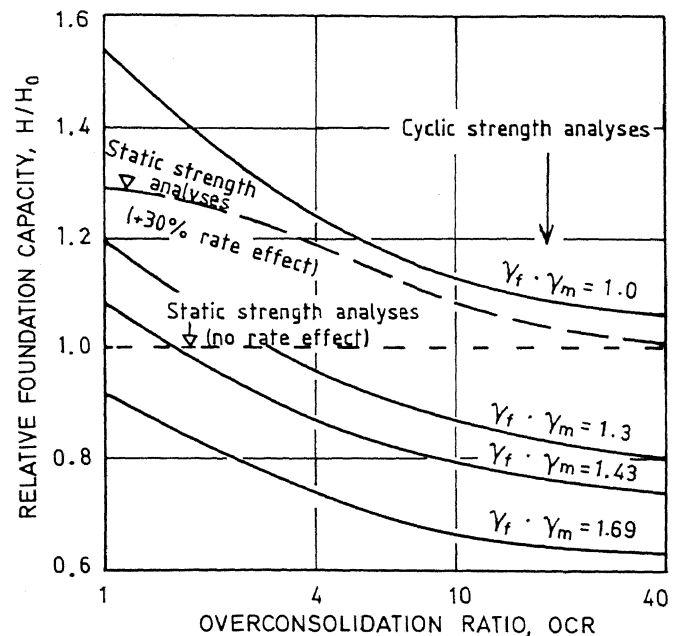


Fig. 59. Comparison between static and cyclic strength analyses. Valid for Drammen clay and for cases where horizontal sliding is the critical failure mode. The influence may be less for deep-seated failure modes.

It is believed that the cyclic strength analysis will lead to a more consistent safety level independent of the overconsolidation ratio, and it is recommended that cyclic strength analyses should be included in addition to or instead of the static strength analysis in cases where the wave forces are the main driving forces. The numerical value of the load coefficient (or the lump safety coefficient, SF) must be decided upon by the regulatory authorities.

Effect of Storms Prior to the Design Storm

In design it is usually assumed that the design storm arrives early during the first major storm season before any other significant storm loading has occurred. In reality, however, the platform will probably experience smaller storms accompanied by drainage before the design storm arrives. This precycling/drainage will influence the soil behaviour under subsequent undrained storm loading. The foundation engineer must therefore investigate whether this may deteriorate the soil and make it more unfavourable if the design storm arrives at a later time than usually assumed.

With sands, laboratory tests have shown that repeated cyclic loading accompanied by drainage may reduce the tendency to cyclically induced excess pore pressure considerably. Bjerrum (1973) presented results from laboratory tests on very dense sand which showed that the rise in excess pore pressure per cycle decreased by a factor of 10 - 100 if the specimens were first precycled with a low cyclic shear stress and then allowed to drain (Fig. 60). The precycling

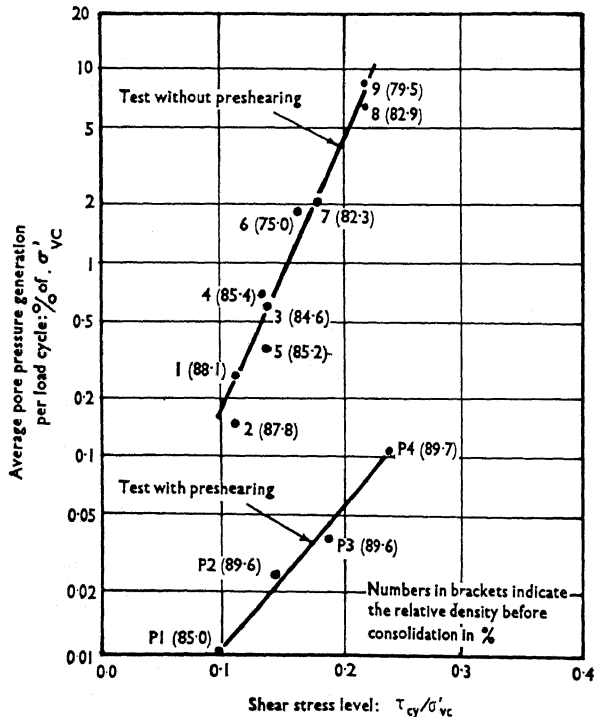


Fig. 60. Pore pressure rise per cycle observed in undrained simple shear tests with cyclic loading on fine sand samples prepared with relative densities of 80% (Bjerrum, 1973).

corresponded roughly to a summer storm for the sand beneath a typical North Sea gravity platform.

This effect of precycling and drainage may have important practical implications for gravity platforms on sand. If the platform is installed early in the summer, it will most likely be subjected to a small amount of wave loading which will precycle the sand beneath the platform and, since drainage is likely to occur fairly rapidly, make it more resistant to subsequent undrained cyclic loading.

For a sand with a reasonably high permeability, it is also likely that some drainage occurs during the first, less critical part of the design storm. The beneficial precycling/drainage effect may thus actually occur during the first part of the design storm.

The possibility of a beneficial precycling/drainage effect ought to be considered in the foundation design of gravity platforms on sand, both for laboratory testing where some precycling and drainage might be applied prior to the undrained testing, and when evaluating soil properties for the calculations. Neglecting this effect may lead to unnecessary conservatism.

With clays, laboratory tests have shown that precycling and drainage may be beneficial for normally consolidated clays and lead to smaller pore pressure generation during subsequent cyclic loading (Fig. 61). For overconsolidated clays, however, laboratory tests have shown that precycling and drainage may be unfavourable and lead to softening of the clay and greater generation of pore pressure due to cyclic loading (Fig. 62).

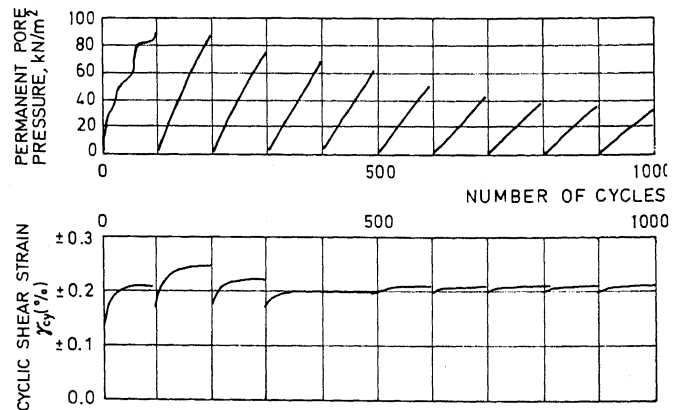


Fig. 61. Cyclically induced excess pore pressures and cyclic shear strains during consecutive series of undrained cyclic loading. Drainage between each series. Simple shear tests with symmetrical, constant cyclic loading on normally consolidated Drammen clay (Andersen et al., 1977).

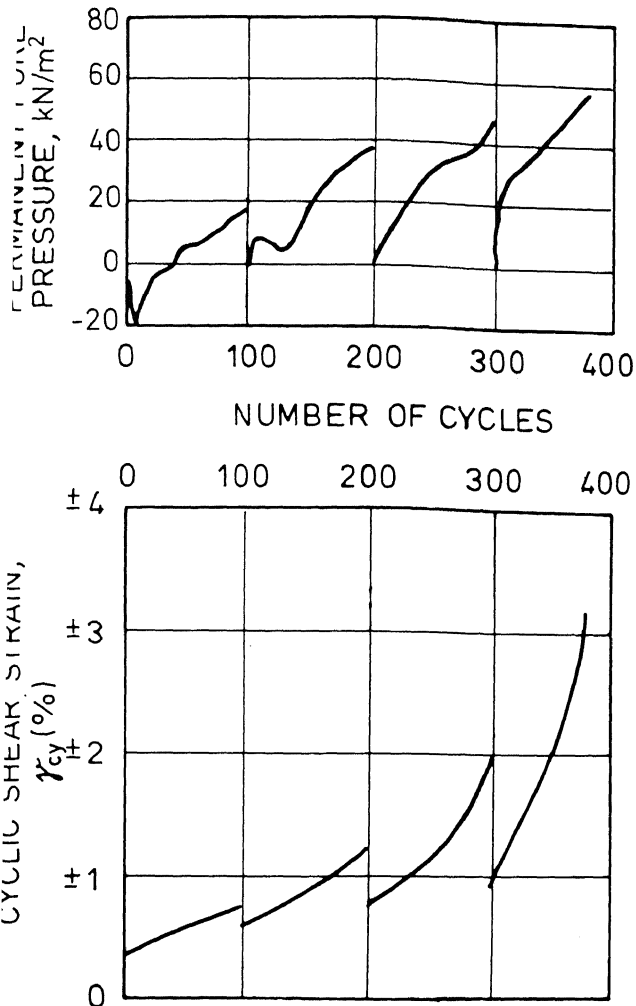


Fig. 62. Cyclically induced excess pore pressures and cyclic shear strains during consecutive series of undrained cyclic loading. Drainage between each series. Simple shear tests with symmetrical constant cyclic loading on Drammen clay with OCR = 4 (Andersen et al., 1977).

With normally consolidated clays the cyclically induced pore pressure will drain away very slowly, and one cannot rely on the beneficial effect occurring before the design storm arrives. For overconsolidated clays, where there may be a negative effect of precycling/drainage, the consolidation of the soil due to the weight of the platform will occur in parallel with the precycling/drainage. Provided the platform is designed with the assumption that the design storm arrives before significant consolidation has occurred, it is believed that the beneficial effect of consolidation due to the weight of the platform will dominate over the negative effect of precycling/drainage. For platforms on clay the effect of precycling/drainage is believed to have less practical importance than for platforms on sand.

Field observations of cyclically induced pore pressures for consecutive storm periods, with time intervals long enough for drainage to occur between the storms, would have shed more light on the effect of precycling/drainage on four-

dation behaviour. Unfortunately, such measurements are not available at present.

#### SOIL STIFFNESS FOR DYNAMIC ANALYSES AND CALCULATION OF CYCLIC DISPLACEMENTS

##### General

The cyclic wave forces will lead to cyclic deformations in the soil and cyclic displacements of the platform. The cyclic displacements have to be calculated to evaluate the stresses in oil wells, pipe line connections, etc. They also have to be calculated to ensure that cyclic displacements and accelerations higher up in the platform do not cause discomfort for the crew or damage the equipment on board.

The dynamic behaviour of the platform under cyclic wave action also has to be analysed to make sure that the natural period of the platform is not too close to the periods of waves with high energy. In all cases dynamic amplification of the wave forces has to be calculated and taken into account in design. The stiffness of the soil under cyclic loading is an important parameter in dynamic platform analysis. The soil is often represented in the dynamic analysis by equivalent springs.

The calculation of cyclic displacements and soil spring stiffnesses is based on the cyclic stress-strain properties of the soil. The analyses have to consider the same factors as mentioned in the beginning of the section on stability, i.e. type of loading, wave load period (inertia effects, rate effects on soil properties), consolidation, influence of cyclic loading on soil properties, drainage, precycling/drainage and for tripod platforms load distribution on and interaction between the pods. Detailed discussion of the effect of these factors will not be included in the following. Their effect on stress-strain properties and the calculation of cyclic displacements and stiffnesses will in general be similar to their effect on shear strength and the calculation of bearing capacity. In the following the main emphasis will be given to platforms on clay. With sand the effect of drainage may have a favourable influence and has to be considered.

##### Analysis Procedure

The cyclic displacements and spring stiffnesses may be calculated by the finite element method. Figure 63 shows a typical model. The finite element analysis accounts for stress distribu-

#### SOIL STIFFNESS

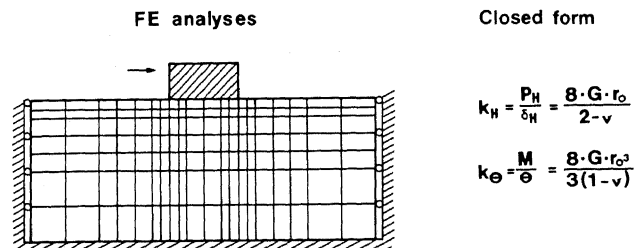


Fig. 63. Finite element model and some simple closed form solutions for calculating soil stiffness under cyclic wave loading.

tions and may also account for soil layering and non-linear stress-strain properties. Proper modelling of these factors is essential. This will be exemplified by the plate loading test results presented later. As in the case of stability analyses, it is usually assumed that the design wave arrives at the end of the design storm when the effect of cyclic loading is most severe. When evaluating the effect of cyclic loading on the soil properties, a soil foundation of clay is assumed to be undrained during the storm. For sands, however, the effect of drainage during the storm must be considered. As in the case of stability analyses, it is believed to be appropriate both for clay and sand to assume that the soil foundation remains undrained during the single design wave, unless the sand is very permeable.

In the finite element analysis the problem has often been approximated by a plane strain model. For undrained conditions, this will underestimate the soil stiffness. For storm loading on a typical North Sea gravity platform a low soil stiffness will be conservative with respect to cyclic displacements and dynamic behaviour.

The finite element analysis may be performed with elastic-plastic cyclic soil models where the stress-strain relationship depends on the number of cycles. Every load cycle is applied and followed in the analysis. Computer programs capable of doing this exist (e.g. Prévost, 1981). However, there are uncertainties in such computations, and in the modelling of the complex constitutive soil model which is required. Experience concerning the quality of the results from such calculations is also limited. In addition, such analyses are so costly that it may be prohibitive to analyse more than a few load cycles.

An alternative is to use a simplified, less costly approach where the relationship between the cyclic shear stress and cyclic shear strain amplitudes is modelled (Andersen et al., 1978). This relationship will also depend upon the number of cycles, and also in this case a realistic soil model has to be established. How this can be accomplished will be shown in a later section. Such simplified finite element analyses were used to back-calculate the cyclic displacements of the Condeep Brent B platform (Fig. 65) and the agreement between calculations and measurements was encouraging.

Approximate values of cyclic displacements and spring stiffnesses may also be calculated by closed form solutions (e.g. Gazetas, 1983). However, these formulas have a limited ability to account for soil layering and non-linear stress-strain properties, and must be used with caution.

#### Tripod Platforms

For tripod platforms special consideration has to be given to the distribution of the horizontal force on the various pods and to interaction between the pods through the soil. Movement of one pod will lead to movements of the soil underneath the other pods, as indicated in Fig. 64. This force distribution and interaction must be taken into account in the analyses used to determine cyclic displacements and soil spring stiffnesses.

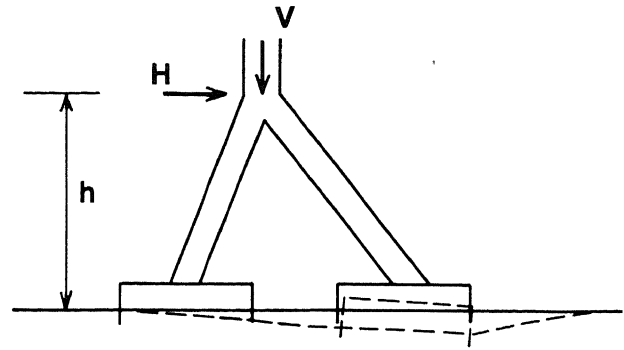


Fig. 64. Illustration of interaction between the pods through the soil for a tripod platform under cyclic wave loading.

#### Field Observations of Cyclic Displacements and Dynamic Behaviour

Several of the North Sea gravity platforms have been instrumented with accelerometers to ensure that the cyclic displacements and the dynamic behaviour are in agreement with the design assumptions. The measurements on the Condeep Brent B platform constitute the most complete measurements and interpretation of such accelerometer data. Observations were made during several major storms the second winter after the platform had been installed. The soil was the fully consolidated under the weight of the platform. The most severe of the storms had a significant wave height of 10.3 m. The maximum wave forces in this storm were estimated to constitute a moment of  $8.5 \cdot 10^6$  kNm (43% of design moment) and a horizontal force of  $1.51 \cdot 10^5$  kN (30% of the horizontal design force).

Figure 65 shows observed cyclic horizontal and rotational displacement of the platform at sea bed elevation as a function of wave forces. The displacements were found by integrating the measured accelerations. The highest standard deviation of cyclic horizontal platform displacement at sea-bed elevation was found to be approx. 1 mm, corresponding to a maximum amplitude of approx. 4 mm. The highest standard deviation of horizontal deck displacement was found to be approx. 15 mm corresponding to a maximum amplitude of approx. 60 mm (Hansteen, 1979).

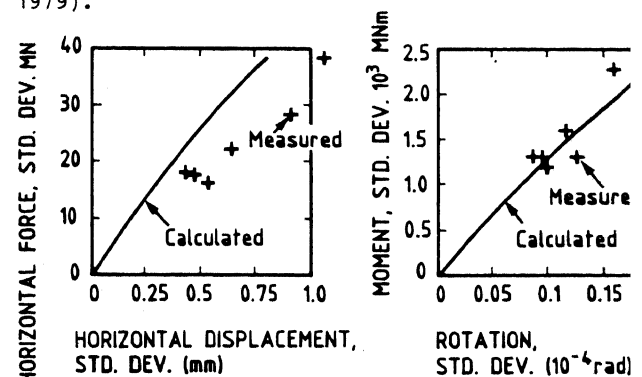


Fig. 65. Comparison between measured and calculated standard deviations of cyclic displacements (Andersen and Aas, 1979).

n Fig. 66 the observed cyclic displacements at sea-bed elevation are extrapolated to the design force values by a combination of measurements and calculations. The figure shows that if the design storm, with a horizontal design wave force of  $5.1 \cdot 10^5$  kN and a moment of  $2 \cdot 10^7$  Nm, arrives before the soil consolidates under the weight of the platform, it is expected to cause a cyclic horizontal displacement of 90 mm and a rotation of  $6.5 \cdot 10^{-4}$  radian corresponding to a cyclic vertical displacement of approx. 0 mm at the platform periphery. Theoretical calculations have shown that if the cyclic horizontal displacements reach a value of approx. 50 mm, yielding may occur in the oil wells underneath the platform (Andersen et al., 1982). The figure further indicates that the consolidation will have a beneficial effect and reduce the predicted cyclic horizontal and rotational platform displacements at sea-bed elevation to roughly one third of those before consolidation.

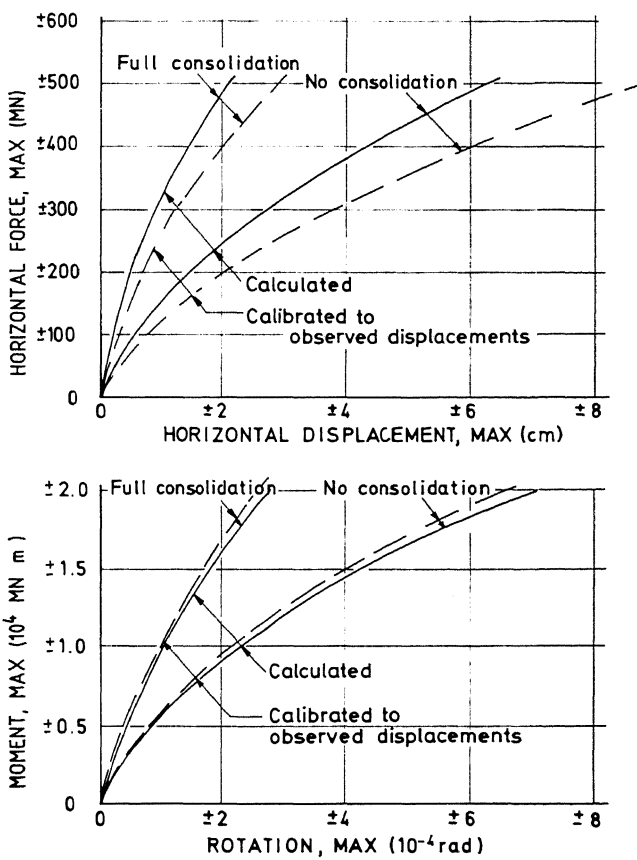


Fig. 66. Expected cyclic displacements at sea-bed elevation during storm for the Brent B Condeep platform. Design forces are a horizontal force of 50 000 t and a moment of  $2 \cdot 10^6$  tm (from Andersen and Aas, 1980).

The equivalent soil shear modulus for an homogeneous elastic halfspace, back-calculated from the measured cyclic displacements, was found to be 150 MPa for horizontal displacements and 250 MPa for rotations. It is important, however, to be aware that these measurements were made after

the soil had consolidated and under less severe storm loading than the design storm. The extrapolations in Fig. 66 indicate that the equivalent shear stiffnesses to be used for a design storm arriving soon after platform installation (no consolidation) is only 10 - 25% of the measured ones.

Figure 67 shows acceleration spectra for the first three modes as calculated from the measured accelerations during the major storm the second winter. The resonance periods are 1.78, 1.72 and 1.19 seconds and are reasonably well below the wave periods. For structures in deeper water, however, the resonance periods may increase to more than 4 seconds. This becomes very close to the periods for the smaller waves and may lead to high amplification of the forces from the small waves. Since there is a large number of small waves, this may mean that fatigue becomes an important design consideration.

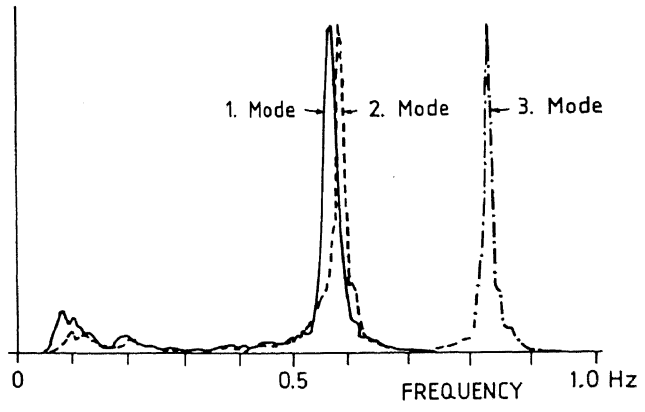


Fig. 67. Acceleration spectra for the Brent B Condeep platform as calculated from measured accelerations (Hansteen, 1979). The two first modes of 1.78 and 1.72 seconds represent bending in the two horizontal directions. The third mode of 1.19 seconds is torsion about the vertical axis.

Experience from Plate Loading Tests

The plate loading tests on stiff, overconsolidated clay, mentioned in the section on stability, give valuable information concerning the calculation of cyclic displacements and soil spring stiffness. The plate tests so far interpreted with respect to displacements and stiffness, are tests employing undrained monotonic static loading. However, the conclusions that will be drawn from these tests in the following are equally valid for cyclic behaviour.

For simplicity, the interpretation has concentrated on the behaviour at 50% of the failure loads. Results from tests with vertical loading as well as from tests with combined vertical, horizontal and moment loading have been analysed. The average normalized secant shear stiffness,  $G_{50}/s_u$ , has been back-calculated for an equivalent homogeneous elastic halfspace and found to be in the range 115 to 150, depending upon the type of loading. The undrained strength used in the normalization is the average strength back-calculated from the measured failure load.

The normalized secant shear modulus measured in laboratory tests at 50% of the undrained strength, is in the range  $G_{50}/s_u = 10 - 25$  depending upon type of test and overconsolidation ratio. The laboratory tests were consolidated to the in situ stresses and subjected to the same type of loading (stress controlled) and the same time to failure as in situ.

The laboratory tests thus give a soil stiffness which at 50% of the failure value is 5 - 15 times smaller than the average stiffness back-calculated from the plate loading tests. This difference is probably due to the fact that the major part of the soil beneath the plates is subjected to a shear stress which is significantly smaller than 50% of the shear strength and that the shear modulus increases strongly with decreasing shear stress. Simplified finite element analyses showed that if the shear stress distribution in the soil, the non-linearity of the soil modulus and the influence of the stress path were accounted for, reasonable agreement between measured and calculated displacements were achieved. In the case of the plate subjected to horizontal and moment loading, the results showed that it may be important to perform three-dimensional analyses. In this case two-dimensional plane strain analyses overestimated the displacements and underestimated the stiffness by a factor of 1.67.

Soil Representation in Simplified Finite Element Analyses

The soil properties used to calculate cyclic displacements and soil spring stiffnesses must as mentioned be determined from laboratory tests which are representative for the soil elements beneath the platform. The stress situation beneath the platform is very complex, and it is impossible to simulate all possible stress situations in laboratory tests. However, triaxial and simple shear tests represent some important elements (Fig. 47), and such tests are usually included in a laboratory test program for the foundation design of gravity platforms. These tests ought to be subjected to combinations of static and cyclic shear stresses representative of the stress conditions beneath the platform.

To calculate cyclic displacements and soil spring stiffnesses, it is also important to know the soil modulus outside the zone immediately beneath the platform. The stresses and strains there will be relatively small, and the accuracy of ordinary triaxial and simple shear tests may not be good enough. Resonant column tests should therefore be included to determine the soil modulus at small stress and strain levels.

In this presentation results from cyclic laboratory tests on Drammen clay will be used to show some typical stress-strain behaviour of various soil elements and to indicate how to determine a representative soil model for use in the simplified finite element analysis described previously.

Figure 68 shows the stress-strain behaviour of Drammen clay under different cyclic loading conditions in the laboratory. Figure 68a shows that symmetrical cyclic loading in the simple

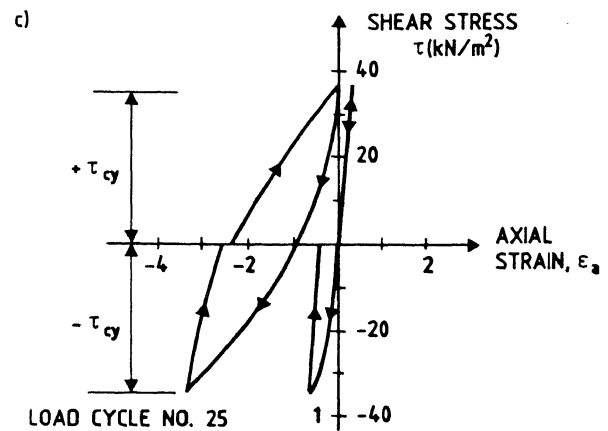
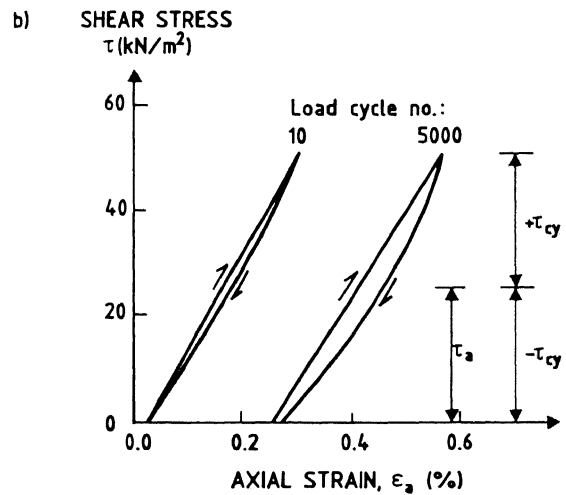
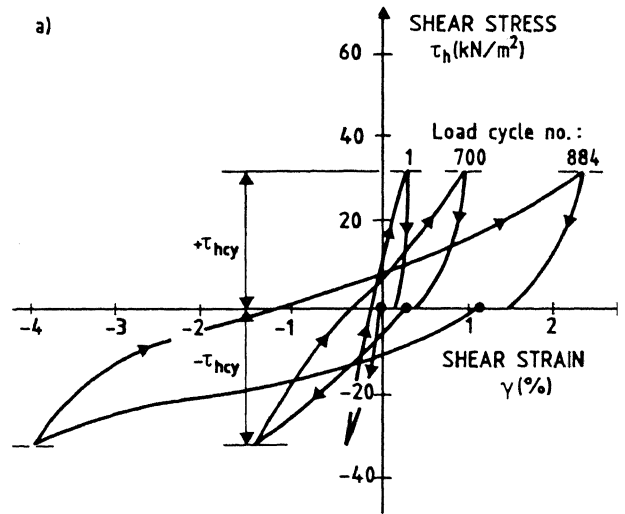


Fig. 68. Stress-strain behaviour of Drammen clay under various cyclic loading conditions (OCR 0.4).  
a) Symmetrical simple shear loading  
b) Non-symmetrical triaxial loading  
c) Symmetrical triaxial loading.



hear apparatus causes relatively symmetrical cyclic shear strains. The cyclic shear amplitude increases and the secant shear modulus increases with the number of cycles. This is due to the pore pressure build-up which is generated by the cyclic loading.

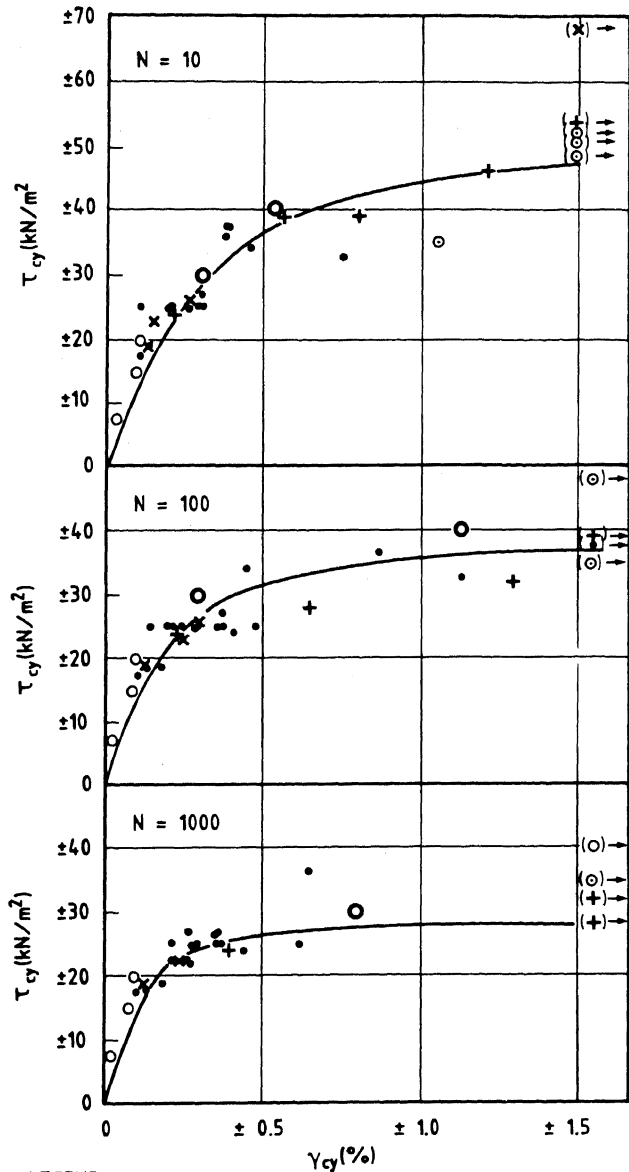
Figure 68b shows that if the cyclic shear stress is not symmetrical, the predominant behaviour may be an increase in the permanent strain with number of cycles and a relatively small increase in the cyclic shear strain amplitude.

Figure 68c shows that in the triaxial tests, there may be a permanent shear strain development even if the shear stress is symmetrical about zero. This is different from the simple shear test results which showed a symmetrical strain response. The reason for the permanent strain in this triaxial specimen is that the undrained extension shear strength is lower than the compression strength of the specimen. A symmetrical stress will therefore lead to a higher degree of strength mobilization on the extension side than on the compression side.

The three examples in Fig. 68 show that it is important to model the type of loading correctly when trying to determine the stress strain behaviour or the modulus in situ from laboratory tests. It also shows that the stress strain behaviour is complex and complicated to formulate in a general material model.

However, for calculating cyclic displacements and soil spring stiffnesses, it is the cyclic shear modulus which is of primary interest. Figure 69 shows that for Drammen clay the cyclic shear strain amplitude is essentially only a function of the cyclic shear stress amplitude and the number of cycles. Both simple shear and triaxial tests under various loading conditions are included.

Figure 69 represents a simplified picture of the cyclic soil behaviour which needs further investigation. For instance, the data do not contain results from tests with average shear stresses in excess of 35% of the undrained shear strength. Such tests would probably plot somewhat less favourably in the diagram. There may also be soils with properties which do not plot as favourably as the data in Fig. 69, even at low values of  $\tau_a$ . However, until more information becomes available, it seems reasonable to assume that the cyclic secant shear stiffness of a soil element is governed only by the cyclic shear stress amplitude and the number of stress cycles and that it is independent of both stress path and average shear stress. This simplifies the soil modelling in the analysis considerably and means that the shear modulus determined from simple shear tests can be used for the whole foundation.



**LEGEND:**

- × One-way simple shear
- + Two-way simple shear
- Triax  $\tau_{cons} = 0.35 \cdot s_u$ , one-way
- Triax  $\tau_{cons} = 0.35 \cdot s_u$ , two-way
- ⊖ Triax  $\tau_{cons} = 0$ , two-way
- Triax  $\tau_{cons} = 0$ , one-way

Fig. 69. Relationship between cyclic shear stress and cyclic shear strain amplitudes after 10, 100 and 1000 cycles. The plots include triaxial and simple shear tests with symmetrical and non-symmetrical undrained cyclic loading. Valid for Drammen clay with OCR = 4 (Andersen et al., 1978).

Figure 70 shows an example of cyclic secant moduli determined in simple shear tests. The ordinary laboratory tests do not give accurate results at small shear stresses, and the variation below a shear stress ratio of 0.25 is determined by interpolation to the initial modulus values determined from resonant column tests. It is obvious from this figure that even for one type of test the soil modulus is not a constant, but significantly dependent on parameters like cyclic shear stress ratio,  $\tau_{cy}/s_u$ , overconsolidation ratio and number of cycles.

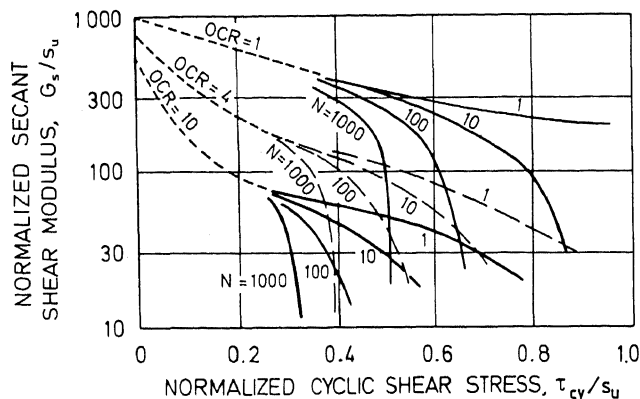


Fig. 70. Secant shear modulus,  $G_s$ , for cyclic loading on Drammen clay. Based on stress-controlled simple shear tests (Andersen et al., 1980) and resonant column tests (Rivette, 1981).  $s_u$  is the undrained static simple shear strength for 2 hours to failure.

For typical North Sea gravity platforms it is conservative to assume high cyclic displacements and low soil spring stiffnesses when analysing storm loading conditions. As in the case of stability analyses, it is therefore often assumed that the design wave arrives at the end of the design storm when the effect of cyclic loading is most severe. The stability section presented a procedure for deriving the cyclic shear strain amplitude as a function of the cyclic shear stress amplitude for design waves arriving at the end of a storm. Such relationships are presented in Fig. 71. This relationship can be put into mathematical form and used as a soil model in the simplified finite element analysis. Details of the mathematical modelling and determination of soil parameters for this model are found in Andersen (1983).

The assumption that the design wave arrives at the end of the design storm will, as mentioned, give conservative values for cyclic displacements and soil spring stiffnesses for typical North Sea gravity platforms. For dynamic analyses it may be more realistic to use the expected average soil spring stiffness in the design storm (e.g. NPD, 1979). One definition of average soil spring stiffness is that it is equal to the ratio between standard deviations of wave forces and cyclic displacements at the interface between the soil and the platform. These average soil spring stiffness values can be calculated on the basis of the same principles as described above. Details are presented in Andersen (1983).

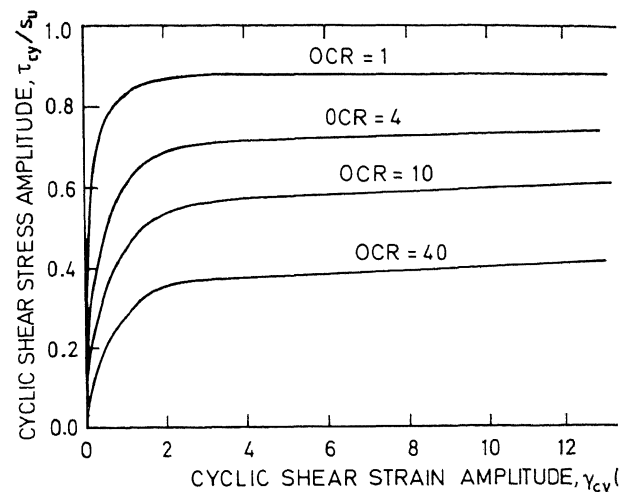


Fig. 71. Cyclic shear strain as a function of cyclic shear stress under the design wave forces. The maximum wave is assumed to occur at the end of a 6-hour storm. Based on constant volume, simple shear loading on Drammen clay.  $s_u$  is the undrained strength for 2 hours to failure (Andersen et al., 1982).

#### Earthquake Analyses

Earthquake analyses also require a foundation soil stiffness for the dynamic analyses of the platform under such loading conditions. Earthquake analyses are described by Selnes (1981). The earthquake analyses are normally performed with other computer programs and with other soil parameters than those used for storm loading analyses.

The main reason for mentioning soil spring stiffness for earthquake analyses here, is to emphasize that the soil spring stiffness to be used in the dynamic analyses of earthquakes may be quite different from the one calculated for storm analyses.

The soil properties for calculating the soil spring stiffness for earthquake analyses can be determined from the same laboratory tests which are used to calculate the soil spring stiffness for storm loading. However, the following differences between earthquake and wave loadings may lead to very different resulting foundation soil spring stiffnesses:

- Type of loading. The dominating earthquake loading consists of movements propagated from the bedrock upwards through the soil. The whole soil foundation is influenced by this loading and not only a zone close to the platform as is the case with storm loading. Since the cyclic soil modulus is non-linear and depends upon the cyclic shear stress level, this means that for earthquake loading there will be a lower modulus than for wave loading in the soil away from the platform.
- The maximum cyclic shear stress may not be the same for the design earthquake and the design storm. Since the soil stiffness is non-linear and depends upon the cyclic shear stress level, this will also influence the resulting soil stiffness.

Duration (no. of cycles). An earthquake has a much shorter duration than a storm. The number of significant cycles may be 100 times higher in a storm than in an earthquake. The effect of cyclic loading may therefore be different in the two cases.

Load frequency. The earthquake load period is of the order of 0.1 to 0.01 times the load period for waves. This will influence the cyclic soil behaviour. It also means that inertia effects are important and must be taken into account in the analyses.

In the case of storm loading, it is normally unfavourable to use a low soil stiffness in the dynamic analysis of the platform. In dynamic analyses for earthquake loading, however, it is more uncertain whether a high or a low soil spring stiffness is unfavourable. A range of soil spring stiffness values must therefore be considered in the earthquake analyses.

An example with calculated soil spring stiffnesses for dynamic storm and earthquake analyses for a typical North Sea gravity platform is presented in Fig. 72 (Hansteen, 1983). In this case the soil spring stiffnesses for storm loading are even lower than the lower bound value determined for earthquake loading.

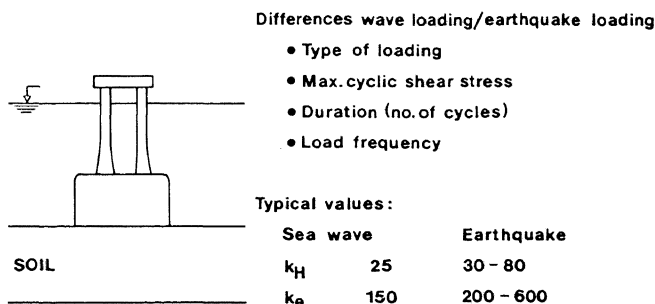


Fig. 72. Differences between wave loading and earthquake loading. Comparison between soil stiffness values for wave load analyses and earthquake analyses for a typical platform.

## SETTLEMENTS AND PERMANENT DISPLACEMENTS

### General

After installation the submerged weight and the environmental loads will cause permanent deformation in the soil beneath and outside the platform. This may cause the following permanent platform displacements:

- vertical settlement
- differential settlement
- lateral displacements

There will also be displacement of the seafloor outside the platform associated with the above platform displacements.

The permanent displacements will cause stresses in oil wells, pipelines etc. Overloading of these elements may have serious consequences, and stresses induced in them by the soil deformation must be evaluated. These stresses will depend on the distribution of displacements with depth in addition to the total displacement. The oil wells, the pipelines etc. are installed some time after the platform has been installed, and only the displacements occurring after this time will induce stresses in them. It is therefore of interest to know the time sequence of the displacements. The time sequence of the vertical settlement is also needed to evaluate the increase in soil strength and stiffness due to consolidation under the weight of the platform. The vertical settlement will also reduce the free-board between the deck and the sea.

To provide the necessary information, the geotechnical design analyses have to include calculations of the settlements and the other permanent displacements. Both total values, variations with depth and time sequences are of interest.

The vertical settlement of a gravity platform may be separated into different components. These components are not independent mechanisms. Several of them occur simultaneously and influence each other. However, a separation into the components listed in Table VI may be useful when attempting to predict settlement.

The first three components will also occur in the case of a structure on land. Components 4 and 5, however, are caused by cyclic loading and seldom occur to the same extent on land as offshore. The cyclic loading may lead to increase in the settlement compared to a structure with only static loading. This is illustrated by the settlement records in Figs. 73 and 74. Both examples are for structures on stiff, overconsolidated clays. For structures without cyclic loading, the long-term settlement (after consolidation is completed) usually plots as a straight line in a semi-logarithmic plot as shown in Fig. 73. This means that the settlement rate decreases with time. For structures with cyclic loading, however the settlement often does not slow down, but continues at the same rate. This is illustrated in Fig. 74 which shows that the settlement curve bends downwards in the semilogarithmic plot. Similar observations have been made on other structures.

Differential settlement may take place due to lateral variations in soil properties beneath the platform or non-symmetrical permanent or cyclic base loads. Differential settlements must in particular be given attention in the case of tripod platforms, where non-symmetrical cyclic base loads will occur.

Permanent lateral displacement may be caused by non-symmetrical horizontal loads due to preferred wind, current and wave directions.

TABLE VI. Vertical Settlement Components for an Offshore Gravity Platform

Load	Settlement Component
S t a t i c	1a. Initial settlement. (Shear strains under undrained conditions due to application of static load.)
	1b. Undrained creep (shear strains under undrained conditions due to the sustained load from the weight of the platform. (Continuation of component 1a.)
	2. Consolidation settlement. (Volumetric strains due to pore pressure dissipation under the weight of the platform.)
o n l y	3. Secondary settlement. (Volumetric and shear strains under drained conditions and constant effective stresses.)
	4a. Local plastic yielding and redistribution of stresses during cyclic loading. (Undrained.)
C y c l i c  l o a d	4b. Shear strains caused by cyclically induced excess pore pressures and the corresponding reductions in effective stress and soil stiffness. (Undrained.)
	5. Volumetric strains due to dissipation of the cyclically induced excess pore pressures.

Analysis procedures

With vertical settlement, components 1, 2 and 3 (Table VI) occur under constant static load and can be evaluated by the same procedures used for structures on land. Even if there are uncertainties related to the calculation of these components, the procedures are relatively well established for calculating both total settlement, distribution with depth and time sequence. Since many of the existing platforms in the North Sea are founded on stiff to hard clays, it may just be mentioned that the data from

measured settlements of buildings on overconsolidated London and Gault clay has been utilized to supplement settlement calculations based on parameters from oedometer tests. Fr back-calculation, Butler (1975) found an equivalent Young's modulus of  $E = 130 \cdot s_u$  and a Poisson's ratio of  $\nu = 0.1$  to give good correlation with measured settlements. The measured settlements included both settlement component 1 and 2 (Table VI).

The vertical settlement due to cyclic loading (components 4 and 5) is more difficult to calculate. This is a load situation which seldom occurs to the same extent on land, and there is no generally accepted calculation methods to predict these settlement components. In the

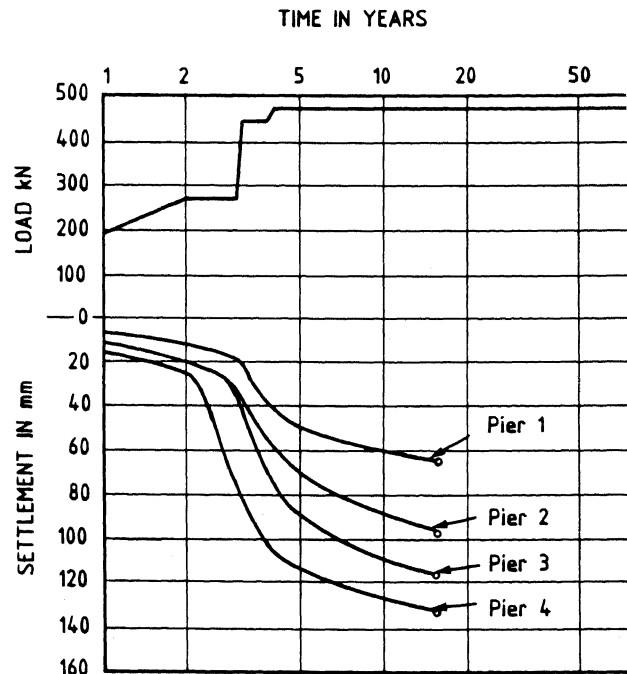
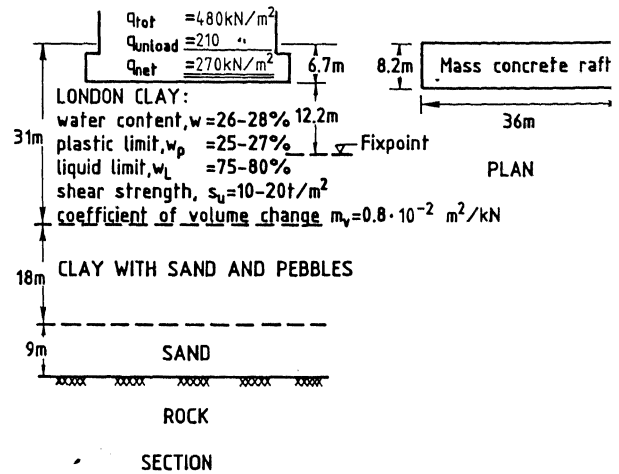


Fig. 73. Settlement record for the Waterloo Bridge, London. After Cooling and Gibson, 1955 (reproduced from Bjerr 1966).

ase of the existing North Sea gravity plat-  
orms, the predictions of these settlement com-  
onents have been made on an empirical basis, by  
ssuming that the rate of vertical settlement  
fter the end of consolidation will be 10 - 15  
n/year. This figure includes settlement com-  
onents 3, 4 and 5 (Table VI). However, this  
npirical design practice cannot be uncritically  
sed to predict settlement of gravity platforms  
n general. It is limited to single base plat-  
orms on stiff clays and dense sands in water  
pths less than 150 m and is not valid for con-  
itions with soft clay, greater water depths and  
her platform geometries (e.g. tripod  
latforms).

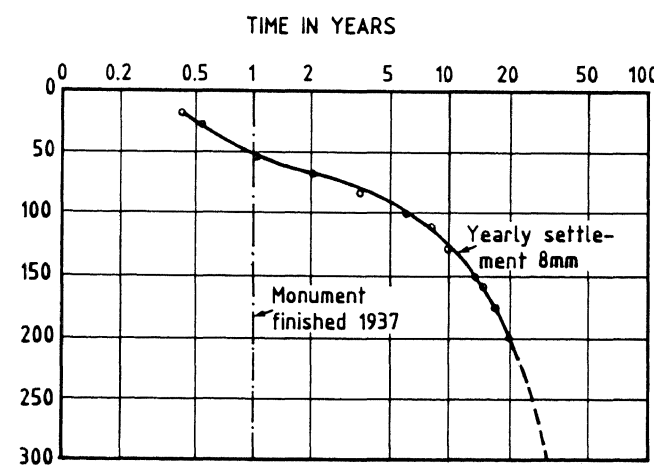
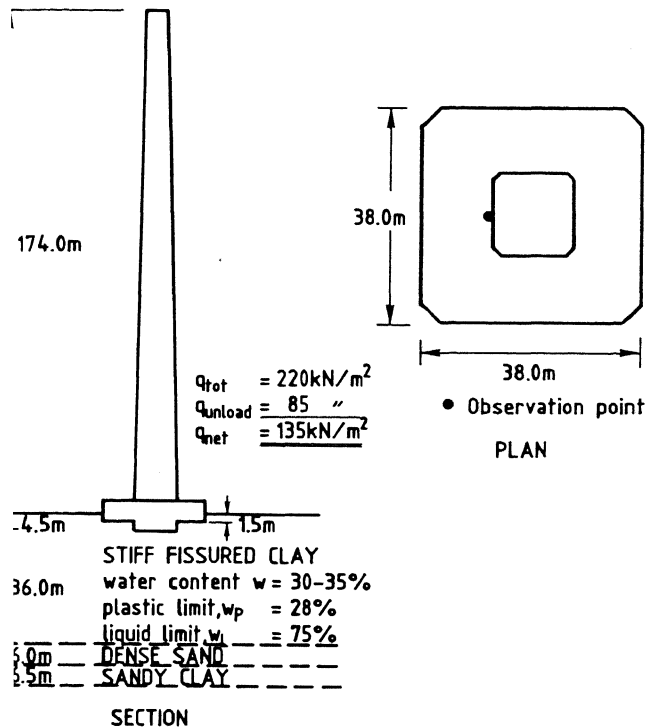


Fig. 74. Settlement record for the San Jacinto Monument, Texas, which is subjected to cyclic wind loading. After Dawson, 1974 (reproduced from Bjerrum, 1966).

One way of calculating the settlement due to cyclic loading under undrained conditions (components 4a and 4b), would be to perform finite element analyses with elastic-plastic cyclic soil models where the stress-strain curve depends upon the number of cycles. Every load cycle should then be applied and followed in the analyses. Computer programmes capable of doing this exist (e.g. Prevost et al., 1981). However, as mentioned in the section on cyclic displacements and soil stiffnesses, there are uncertainties involved in such computations, and they may be very costly.

An alternative calculation approach is to perform more simplified finite element analyses along the same lines as the simplified finite element analyses described to calculate cyclic displacements and soil spring stiffnesses.

The volumetric strains due to dissipation of the cyclically induced pore pressure (component 5) may be calculated in the same way as conventional consolidation settlement, but with the reloading compressibility taken into account. The stress change causing settlements is set equal to the cyclically induced excess pore pressure.

The differential settlement associated with static loading (i.e. settlement components 1, 2 and 3) may be evaluated by the same procedures as used to calculate the average vertical settlements provided data about lateral variation in soil properties and any unequal distribution of the vertical load are available.

The differential settlement due to non-symmetrical cyclic base loads are more difficult to calculate. Calculation procedures as described for calculating settlement due to cyclic loading (components 4 and 5, Table VI) should be considered. Differential settlement due to non-symmetrical loading due to preferred wind, current and wave directions may be evaluated from simplified finite element analyses.

The permanent lateral displacements may also be evaluated from simplified finite element analyses provided data about non-symmetrical horizontal loads due to preferred wind, current and wave directions are available.

Settlement Analysis of Tripod Platforms

Tripod platforms are more susceptible to differential settlements due to their non-symmetrical cyclic base loads, and this must be given special consideration.

In the static load case, consideration also has to be given to the interaction between the pods through the soil (Fig. 75). This may cause a tendency for some rotation of the pods. If the platform is rigid, this will induce forces in the structure. This effect may be evaluated by finite element analyses.

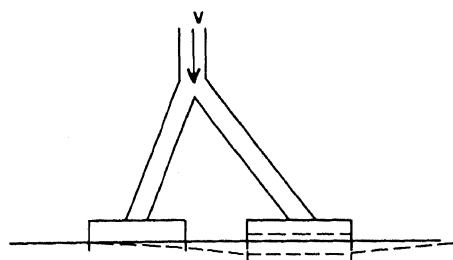
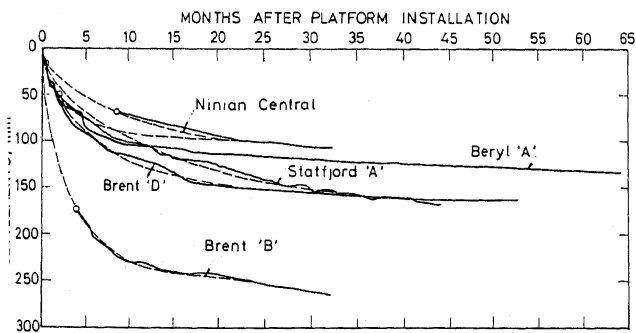


Fig. 75. Illustration of interaction between the pods through the soil for a tripod platform during vertical settlement.

#### Field Observations of Vertical Settlement

Settlement has been measured for most of the gravity platforms in the North Sea. A summary of some of the settlement records is presented in Fig. 76. These records are all for platforms on stiff to hard overconsolidated clays and dense sands. More details about the settlement records may be found in Clausen et al. (1975), Andersen and Aas (1979), Eide et al. (1979), Lunne et al. (1981) and Lunne and Kvalstad (1982). For most platforms the settlement measurements did not start until some months after the platform had been installed. The settlement records have therefore been extrapolated back to time equal to zero by means of one-dimensional consolidation theory. The settlement at the end of consolidation has been in the range of 80 to 230 mm. These numbers and the settlement records in Fig. 76 do not include the initial settlement. Figure 77 shows a more detailed interpretation of the settlement of the Condeep Brent B platform. The initial settlement has in this case been estimated by means of theoretical calculations.



g. 76. Summary of measured settlement for 5 North Sea gravity platforms (excluding initial settlement).

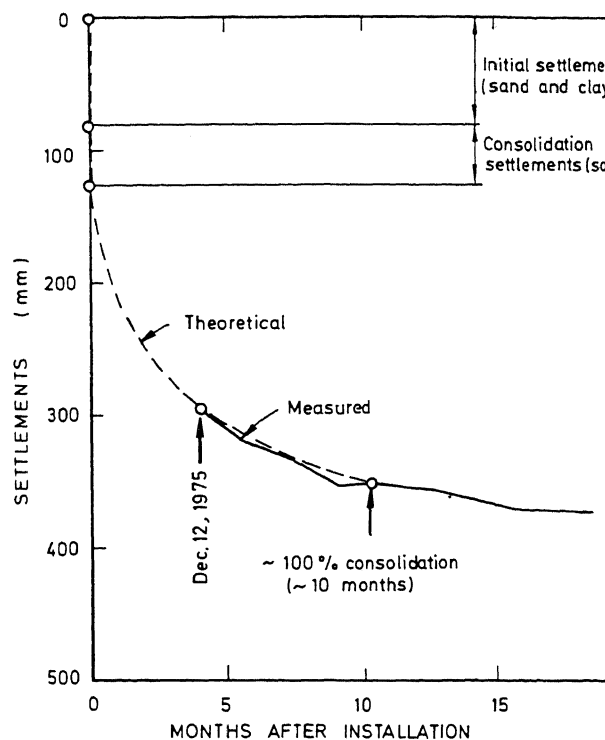
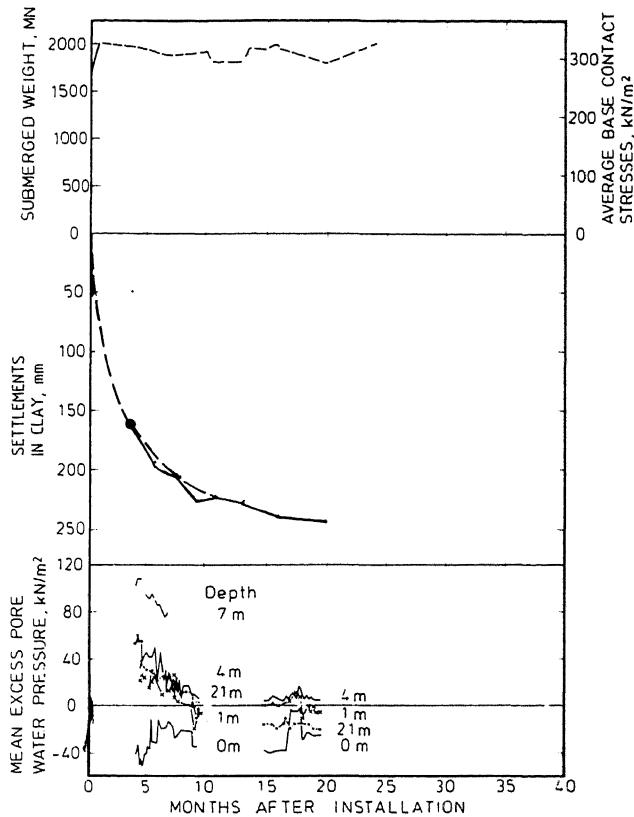


Fig. 77. Interpretation of the settlement observations of the Brent B Condeep platform (from Andersen and Aas, 1980).

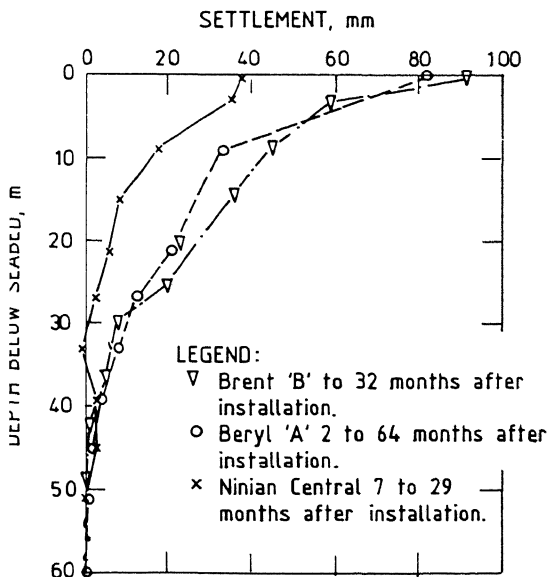
Back-calculation of this settlement gives an estimated value of  $E/s_u$  in the range 100 to 1. to be used together with  $\nu = 0.1$  to calculate the sum of initial and consolidation settlement (Lunne et al., 1981). As mentioned, Butler (1975) found  $E = 130 \cdot s_u$  for London and Gault clay. Lunne et al. (1981) also back-calculate a constrained modulus,  $M = k \cdot s_u$ , to calculate the consolidation settlement and found values  $k$  in the range 190 to 280, with an average of 250. They also found that the agreement with constrained moduli measured from the reloading branch in oedometer tests was reasonably good.

The time required for consolidation is not always well defined because the foundation soil contain layers of both sand, silt and clay which consolidate at different rates. However, the time required for consolidation has been estimated from the time-settlement curves and when available, from pore pressure measurements. An example of settlement and pore pressure record is given in Fig. 78. The equilibrium pore pressure values are slightly below zero due to the influence of the underbase drainage system

The consolidation time for platforms on soil consisting mainly of dense sand varies from almost instantaneous consolidation for the Ekofisk tank on a 26 m thick upper sand layer 8 to 10 months for platforms with 10 m thick upper sand layers. For the Condeep Brent B platform on 45 m thick layer of clay interbedded with sand layers and with sand beneath 45 m, consolidation time is approx. 10 months. For the Statfjord A platform on mainly soil con-



g. 78. Time history of settlement, pore pressure and vertical load for the Condeep Brent B platform.



g. 79. Distribution of measured vertical settlement with depth for three platforms.

sisting of clay, the observed consolidation time is approx. 40 months. The predicted consolidation times depends upon the assumed thickness of the layer and on drainage conditions, but in general consolidation occurs faster than predicted (Lunne et al., 1981).

The settlement records seem to indicate that the settlement which occurs after consolidation is completed (components 3, 4 and 5 in Table VI), occurs with a rate in the range of 3 to 13 mm/year. This agrees favourably with the design assumptions of 10 - 15 mm/year.

Settlement distribution with depth has been measured on three platforms. Figure 79 shows that roughly 70% of the total settlement actually occurs in the upper 14 m. However, the settlement distribution with depth depends strongly on the soil layering.

#### Field Observations of Differential Settlement

Differential settlement recorded on four of the platforms has been in the range 0.01 to 0.05, corresponding to differential settlement of up to 90 mm across a 100 m diameter base. The measurements cover time periods of 15 to 64 months, but for two of the platforms the measurements did not start immediately after installation.

These measurements are all from single base platforms. For tripod platforms higher differential settlement might be expected due to the non-symmetrical cyclic base loads.

#### Field Observations of Permanent Lateral Displacements

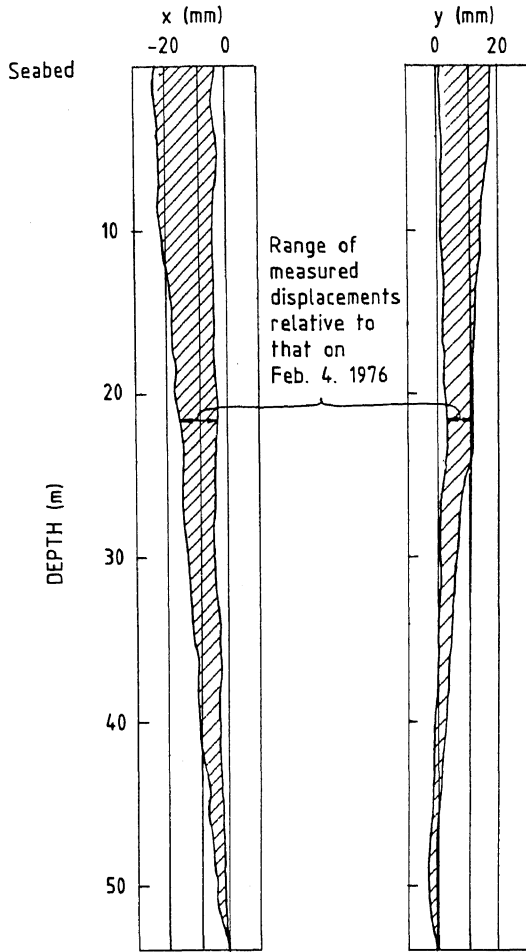
Permanent lateral displacement has been measured on three platforms. Figure 80 shows the measurements from the Condeep Brent B platform. The measurements do not cover the very first storm, but do include storms with wave forces of up to 45% of the design forces. The measured displacements have been small - less than 28 mm, which may be of the same order as the accuracy of the measurements. Similar results have been obtained from the measurements on the two other platforms.

#### BASE CONTACT STRESSES AND STRESSES ON SKIRTS

##### General

As mentioned in the section on installation, the foundation analyses have to predict distribution of normal and shear stresses on the base and the skirts. The stress distribution has to be known in order to design the base and the skirts such that they will be strong enough to withstand the expected stresses. During the operation phase the cyclic stresses induced by the wave forces have to be calculated. It is also necessary to evaluate how the non-uniform stresses which developed during installation will be redistributed during the operational phase. The submerged weight carried by the skirts may with time be transferred to the base, causing increased base contact stresses.

### DISTRIBUTION OF LATERAL DISPLACEMENT WITH DEPTH



### LATERAL DISPLACEMENT IN THE HORIZONTAL PLANE AT THE SEABED

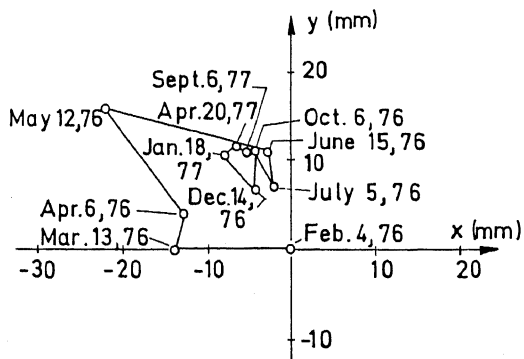


Fig. 80. Measured permanent lateral displacements for the Condeep Brent B platform. The measurements started on February 4, 1976, some 5 months after the platform had been installed (Andersen and Aas, 1979).

The cyclic base contact stresses may be calculated by finite element analyses of the type used to calculate cyclic displacements. The calculation of redistribution of static stress with time, however, is more uncertain, since there are several effects occurring at the same time. Experience from performance observation is therefore very valuable.

### Field Observations of Base Contact Stresses

The base contact stresses have been measured on Condeep platforms with spherical domes. The cyclic base contact stresses measured on the Brent B platform during the most severe storm during the first winter are presented in Fig. 81. This storm is the same as described previously for measured cyclic displacements. The results from finite element analyses are included in the figure. Both calculations and measurements indicate that the cyclic stress distribution is almost linear within the inner 80% of the diameter. The calculations indicate that significant cyclic stress concentrations will occur towards the periphery.

The comparison in Fig. 81 indicates that the measured stresses are of the order of 50% of calculated ones. This is probably because the skirts along the periphery carry a significant

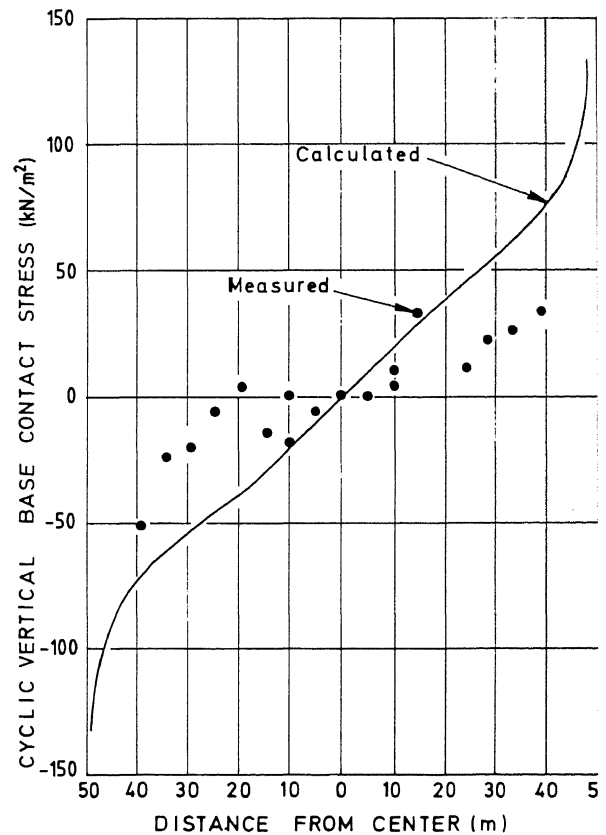


Fig. 81. Measured and calculated cyclic base contact stress variations for the Condeep Brent B platform during a storm with significant wave height 10.3 m (Andersen and Aas, 1979).



rtion of the wave moment. The effect of these irts is not fully accounted for in the calcu- tions. Originally it was anticipated that the asured cyclic base contact stresses could be ed to back-calculate the wave moment perienched by the platform, thus providing a eck on the theoretically predicted wave ment. However, because stress concentrations ar the periphery and forces on the skirts have t been measured, these measurements are not fficient to check the theoretical calculations the wave moment.

e static base contact stress variation for the ndeep Brent B platform is shown in Fig. 82. e figure compares the measured base contact resses on the 19 domes just after grouting tween the platform base and the soil with the resses measured 2 years later. The high resses developed against some domes during stallation seem to remain for a long time. wever, no tendencies to significant long-term creases which may locally overstress the base ve been recorded. The measurements indicate ly modest changes in base contact stresses th time. The stress changes which have curred, have mainly been due to special opera- ons, such as changes in platform weight hanges in deck load and oil storage), outing, use of the underbase drainage system d installation of conductors through the plat- orm base.

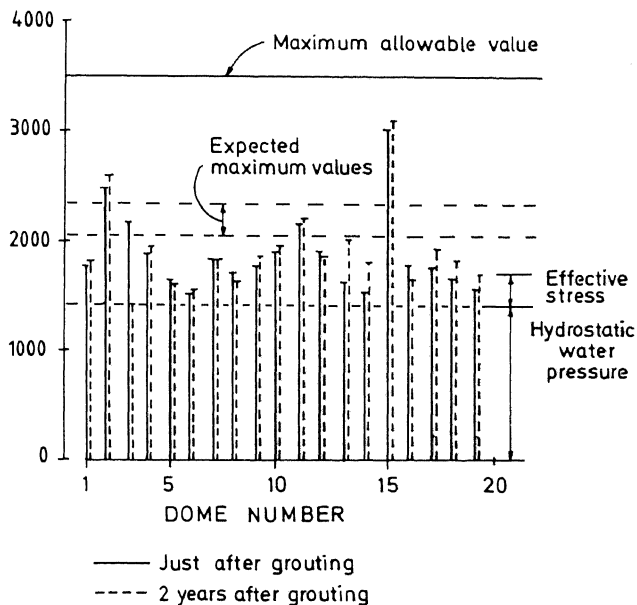


Fig. 82. Measured static base contact stresses beneath the Condeep Brent B platform just after grouting and two years afterwards (Andersen and Aas, 1979).

## PIPING AND EROSION

Waves and currents may cause erosion and piping of the soil around and beneath a gravity platform. Such piping and erosion may damage the soil foundation and must be carefully considered in design.

Whether erosion of the soil surface around the platform will occur or not depends upon the water particle velocity, the soil grading and the transient hydraulic gradients set up in the soil by the cyclic wave moment.

The cyclic wave moment causes cyclic pore pressure changes in the soil. These pore pressures vary from point to point in the soil and cause pore pressure gradients and a tendency for flow of water in the soil and along the interface between soil and platform. Beneath the uplift side of the platform, the gradients cause a tendency to flow from outside the platform in underneath the skirts. At the compression side, the flow tendency is in the opposite direction.

If the gradients are too large they will also lead to piping and erosion along the skirts on the uplift side where there is access to free water from the outside. It is therefore required that the platform does not lift off the ground at the uplift side when subjected to the maximum wave moment. If a crack opens up, water is sucked in and subsequently squeezed out, leading to erosion and possibly serious consequences for the structure. For a platform without skirts, a positive contact pressure is therefore required. Pockets of free water under the structure should not be allowed to remain if it is possible for this water to be squeezed out through the soil and thus lead to erosion in the front of the platform. A structure equipped with skirts can take some suction, depending on the depth of skirts and soil conditions, but each case has to be considered separately.

The potential for piping along the skirts in front of the platform is limited if there are no pockets of free water underneath the platform. However, the gradients may cause some flow and increased pore pressure in the soil outside the front of the platform. This causes reduced effective stresses and increased danger of scour from the soil surface due to currents. It may also cause hydraulic fracturing in the soil.

The gradients in the soil change continuously as a wave passes the platform, and there will be a nonsteady flow in the soil. The pore pressure distribution may be determined from finite element analysis.

The potential problems caused by surface erosion are handled by using scour protection or by designing the foundation in such a way that the platform is safe even if all the soil which is susceptible to erosion is washed away. The majority of platforms are equipped with skirts along the periphery, which protect the soil beneath the platform from erosion. The soil around the platform may be protected from erosion by placing, for instance, a gravel layer outside the platform periphery. If danger of erosion is not fully accounted for, the sea floor must be kept under inspection. Means of preventing further erosion must be available in a short time if tendencies to scour should be detected.

## Field Observations of Erosion

In general, the gravity platforms in the North Sea have not experienced significant erosion (Dahlberg, 1982).

One case in which some erosion has occurred, is the Frigg TP1 platform. This platform has a square base and is situated on dense, fine sand. Originally, it did not have erosion protection. Early after installation in 1976 about 2 m of erosion was observed locally around two corners (Dahlberg, 1982). However, erosion protection by gravel bags and gravel fill effectively stopped further development. Regular inspections have verified that this protection remains effective. The Frigg TP1 case is especially interesting since the Frigg TCP2 platform, which has a circular base and is located only 40 m away, has not experienced erosion. It may therefore be concluded that a square base is more susceptible to scour than a circular base.

The Frigg TP1 and the Frigg TCP2 platforms are both equipped with skirts. A third platform on the Frigg field, the Frigg CDP1 does not have skirts, and a central open space between the base and the platform has not been grouted. With this platform, Dahlberg (1982) reports that divers have observed periodic puffs locally around the periphery, when the sediments were carried in suspension, as the excess pore water escaped due to the hydraulic gradient set up by the cyclic wave action.

The Ekofisk oil storage tank is only equipped with 400 mm high ribs beneath the periphery and has not been grouted either. This platform is placed on dense, silty, fine sand. Scour protection was placed on the sea floor around this platform. The scour protection consisted of a 1.0 to 1.5 m thick, 10 m wide layer of well graded gravel with a maximum grain size of 80 mm. Submarine inspections after a year with severe storms showed that the protection worked satisfactorily, even though the finer grains had been washed out from the upper part of the protective gravel layer.

Platforms on clay have all been equipped with skirts, but have not been surrounded by scour protection. No erosion has been observed around platforms on clay.

## CONCLUSIONS

Each of the 15 gravity structures installed in the North Sea represents an interesting case history regarding the installation phase and the long-term foundation behaviour.

During installation some problems have been experienced:

- skidding of platforms without dowels
- eccentric skirt penetration resistance
- piping below skirt tip level
- delayed skirt penetration after termination of ballasting
- loss of grout out onto the sea-bed during the grouting process
- leakage into the platform during grouting.

None of these problems has been really serious and all the installations are reported to have been successful.

The instrumentation has proved very useful during installation for:

- measuring vertical penetration
- avoiding overstressing of the base by recording dome contact stress
- controlling the effect of the suction which applied to improve penetration and obtain immediate unloading
- improving the installation design for new platforms.

Long term foundation behaviour has also proved to be satisfactory:

- generation of excess pore pressure during storms has been moderate and of the order of magnitude expected
- observed settlement is about as expected
- dynamic motion appears to be in agreement with predictions.

Scour problems have been less than expected. Only one platform with a square base on sand experienced scour at two corners. One platform without skirts on sand has experienced some pumping effects, creating ratholes along the periphery in the predominating storm direction.

The stability of gravity platforms has been analysed employing the following partial safety coefficients:

$$\gamma_f = 1.0 \quad \text{load factor on dead weight}$$

$$\gamma_f = 1.3 \quad \text{load factor on maximum waveloads}$$

$$\gamma_f = 1.0 \quad \text{load factor on other wave loads in 6-hour storm}$$

$$\gamma_m = 1.3 \quad \text{material factor.}$$

The stability analyses have been made in the form of quasi-static analyses with the forces from the design wave and an undrained static shear strength reduced to allow for the effect of cyclic loading. In current design practice the stability is also analysed employing cyclic soil strength values.

For future platforms in greater depths of water the dynamic platform behaviour will become more critical, and the calculation of spring stiffnesses and damping to represent the soil will become more important. Present calculation procedures can be used for these analyses.

If deep-water gravity platforms are installed on soft clays, the cyclically induced settlement may have to be given more attention than in the case with existing platforms.

## KNOWLEDGMENT

The paper is based on accumulated knowledge and experience gained at the Norwegian Geotechnical Institute over the years with offshore foundation activities related to gravity structures. The authors want to express thanks to their colleagues at the Institute for valuable assistance, and specially to K. Høeg and K. Schjetne for careful review of the paper.

## REFERENCES

- Andresen, A., T. Berre, A. Kleven and T. Lunne (1979), "Procedures used to obtain soil parameters for foundation engineering in the North Sea", *Marine Geotechnology*, Vol. 3, No. 3, pp. 201-266, Also publ. in: Norwegian Geotechnical Institute, Publication, 129.
- Bjerrum, L. (1966), "Secondary settlements of structures subjected to large variations in live load", *International Symposium on Rheology and Soil Mechanics, Grenoble 1964*, pp. 460-471, Berlin, Springer, Also publ. in: Norwegian Geotechnical Institute, Publication, 73.
- Bjerrum, L. (1971), "Subaqueous slope failures in Norwegian fjords", Norwegian Geotechnical Institute, Publication, 88, Also publ. in: *International Conference on Port and Ocean Engineering under Arctic Conditions*, 1, Trondheim 1971, Proceedings, Vol. 1, pp. 24-47.
- Bjerrum, L. (1973), "Geotechnical problems involved in foundations of structures in the North Sea", *Géotechnique*, Vol. 23, No. 3, pp. 319-358, Also publ. in: Norwegian Geotechnical Institute, Publication, 100.
- Boon, C., D. Gouvenot, M. Gau and J.P. Geffriaud (1977), "Stability of gravity-type platforms by filling under the raft", *Offshore Technology Conference*, 9. Houston, Texas 1977, Proceedings, Vol. 4, pp. 39-44.
- Bugge, T., R.L. Lien and K. Rokoengen (1978), "Kartlegging av løsmassene på kontinentalsokkelen utenfor Møre og Trøndelag; seismisk profilering", 55 p, Continental Shelf Institute, Norway, Publication, 99.
- Butler, F.G. (1975), "Heavily over-consolidated clays", Review paper: Session III, Settlement of Structures; Conference org. by the British Geotechnical Society, Cambridge 1974, London, Pentech Press, pp. 531-578.
- Clausen, C.J.F., E. DiBiagio, J.M. Duncan and K. Andersen (1975), "Observed behaviour of the Ekofisk oil storage tank foundation", *Offshore Technology Conference*, 7. Houston 1975, Proceedings, Vol. 3, pp. 399-413, Also publ. in: Norwegian Geotechnical Institute, Publication, 108 and in: *Journal of Petroleum Technology*, 1976, March, pp. 329-336.
- Cooling, L.F. and R.E. Gibson (1955), "Settlement studies on structures in England", Institution of Civil Engineers, London, Conference on the Correlation between Calculated and Observed Stresses and Displacements in Structures, Papers, Vol. 1, pp. 295-317.
- Dahlberg, R. (1982), "Observation of scour around offshore structures", *Canadian Conference on Marine Geotechnical Engineering*, 2. Halifax, Nova Scotia 1982, Preprint volume, Session 3.
- Dawson, R.F. (1947), "Settlement studies on the San Jacinto monument", *Texas Conference on Soil Mechanics and Foundation Engineering*, 7. Austin, Texas, Proceedings.
- Andresen, K.H. (1976), "Behaviour of clay subjected to undrained cyclic loading", *International Conference on the Behaviour of Off-shore Structures*, 1. BOSS'76, Trondheim 1976, Proceedings, Vol. 1, pp. 392-403, Also publ. in: Norwegian Geotechnical Institute, Publication, 114.
- Andresen, K.H., S.F. Brown, I. Foss, J.H. Pool and W.F. Rosenbrand (1977), "Effect of cyclic loading on clay behaviour", *Conference (on) Design and Construction of Offshore Structures*, Institution of Civil Engineers, London 1976, Proceedings, pp. 75-79, Also publ. in: Norwegian Geotechnical Institute, Publication, 113.
- Andresen, K.H., O.E. Hansteen, K. Høeg and J.H. Prévost (1978), "Soil deformations due to cyclic loads on offshore structures", *Numerical Methods in Offshore Engineering*, Ed. by O.C. Zienkiewicz, R.W. Lewis and K.G. Stagg, Chichester, Wiley, pp. 413-452, Also publ. in: Norwegian Geotechnical Institute, Publication, 120.
- Andresen, K.H. and P.M. Aas (1980), "Foundation performance", *Shell Brent B Instrumentation Project; Seminar*, London 1979, Proceedings, London, Society for Underwater Technology, pp. 57-77, Also publ. in: Norwegian Geotechnical Institute, Publication, 137.
- Andresen, K.H., J.H. Pool, S.F. Brown and W.F. Rosenbrand (1980), "Cyclic and static laboratory tests on Drammen clay", *American Society of Civil Engineers, Proceedings*, Vol. 106, No. GT 5, pp. 499-529, Also publ. in: Norwegian Geotechnical Institute, Publication, 131.
- Andresen, K.H., S. Lacasse, P.M. Aas and E. Andenæs (1982), "Review of foundation design principles for offshore gravity platforms", *International Conference on the Behaviour of Off-Shore Structures*, 3. Cambridge, Mass. 1982, Proceedings, Hemisphere Publ. Wash. D.C. / McGraw-Hill, London a.o.pl., Vol. 1, pp. 243-261, Also publ. in: Norwegian Geotechnical Institute, Publication, 143.
- Andresen, K.H. and P. Stenhamar (1982), "Static plate loading tests on overconsolidated clay", *American Society of Civil Engineers, Proceedings*, Vol. 108, No. GT 7, pp. 918-934.
- Andresen, K.H. (1983), "Strength and deformation properties of clay subjected to cyclic loading", Norwegian Geotechnical Institute, Report, 52412-8, 54 p.

- Derrington, J.A. (1977), "Construction of McAlpine, sea tank gravity platforms at Ardyne Point, Argyll", Conference on Design and Construction of Offshore Structures, London 1976, Proceedings, pp. 121-130.
- DiBiagio, E., F. Myrvoll and S. B. Hansen (1976), "Instrumentation of gravity platforms for performance observations", International Conference on the Behaviour of Off-shore Structures, 1. BOSS'76, Trondheim 1976, Proceedings, Vol. 1, pp. 516-527, Also publ. in: Norwegian Geotechnical Institute, Publication, 114.
- DiBiagio, E. and K. Høeg (1983), "Instrumentation and performance observations offshore", American Society of Civil Engineers, Conference on Geotechnical Practice in Offshore Engineering, Austin, Texas 1983, Proceedings, pp. 604-625.
- Dybwad, K., E. Åldstedt and R. Lauritzsen (1980), "Feasibility of gravity platforms for 300 m water depth", 27 p., Offshore North Sea Technology Conference and Exhibition, Stavanger 1980, Offshore Field Development for the 1980's, paper, T-II/8.
- Edgers, L. and K. Karlsrud (1982), "Soil flows generated by submarine slides. Case studies and consequences", International Conference on the Behaviour of Off-Shore Structures, 3. BOSS'82, Cambridge, Mass. 1982, Proceedings, Vol. 2, pp. 425-437.
- Eide, O. (1974), "Marine soil mechanics; applications to North Sea offshore structures", 44 p., Offshore North Sea Technology Conference and Exhibition, Stavanger 1974, Proceedings, Technology Volume, Also publ. in: Norwegian Geotechnical Institute, Publication 103, 20 p.
- Eide, O., L.G. Larsen and O. Mo (1976), "Installation of the Shell/Esso Brent B Condeep production platform", Offshore Technology Conference, 8. Houston 1976, Proceedings, Vol. 1, pp. 101-114, Also publ. in: Norwegian Geotechnical Institute, Publication, 113, and in: Journal of Petroleum Technology, Vol. 29, 1977, March, pp. 231-238.
- Eide, O., K.H. Andersen and T. Lunne (1979), "Observed foundation behaviour of concrete gravity platforms installed in the North Sea 1973-1978", International Conference on the Behaviour of Off-Shore Structures, 2. BOSS'79, London 1979, Proceedings, Vol. 2, pp. 435-456, Also publ. in: Norwegian Geotechnical Institute, Publication, 127.
- Eide, O., O. Kjekstad and E. Brylawski (1979), "Installation of concrete gravity structures in the North Sea", Marine Geotechnology, Vol. 3, No. 4, pp 315-368, Also publ. in: Norwegian Geotechnical Institute, Publication, 129.
- Eide, O., A. Andresen, R. Jonsrud and E. Andenæs (1982), "Reduction of pore water pressure beneath concrete gravity platforms", International Conference on the Behaviour of Offshore Structures, 3. BOSS'82, Cambridge, Mass. 1982, Proceedings, Vol., 2, pp. 373-382, Also publ. in: Norwegian Geotechnical Institute, Publication, 143.
- Eide, O. (1983), "Case studies of planning a carrying out site investigations for offsh structure foundations", International Soci for Soil Mechanics and Foundation Engineer Sub-Committee on Site Investigation, Manua Part II.
- Foss, I., R. Dahlberg, T. Kvalstad (1978), "Design of foundation of gravity structure against failure in cyclic loading", Offsho Technology Conference, 10. Houston, Texas 1978, Preprint, Vol. 1, pp. 535-545.
- Foss, I. and J. Warming (1979), "Three gravi platform foundations", International Conference on the Behaviour of Off-Shore Structures, 2. BOSS'79, London 1979, Proceedings, Vol. 2, pp. 239-256.
- Gazetas, G. (1983), "Analysis of machine foudation vibrations: state of the art", International Journal of Soil Dyanmics and Earthquake Engineering, Vol. 2, 1983, No. pp. 2-42.
- Gerwick, B.C. (1975), "Design and constructi of concrete structures in the North Sea", Boston Society of Civil Engineers, Journal Vol. 62, No. 1, pp. 20-24.
- Grouting the Ninian Central Platform's Under (1978), Ground Engineering, Vol. 11, No. 8 pp. 17-24.
- Hackett, B. (1981), "The Feie-Shetland secti A Hydrographic Atlas", Joint project "Den Norske Kyststrøm", University of Bergen, Institute of Geophysics.
- Hansen, J.B. (1980), "A revised and extended formula for bearing capacity", Geoteknisk institut, Copenhagen, Bulletin, 28, pp. 5-
- Hansteen, H. (1983), "Personal communicati
- Hansteen, O.E. (1980), "Dynamic performance' Shell Brent B Instrumentation Project, Seminar, London 1979, Proceedings, London, Society for Underwater Technology, pp. 89- Also publ. in: Norwegian Geotechnical Institute, Publication, 137.
- Hansteen, O.E. (1981), "Equivalent geotechni design storm", 74 p., Norwegian Geotechnic Institute, Internal report, 40007-17.
- Heiberg, S., T. Løken and K. Torsethaugen (1982), "Natural conditions influencing pe leum recovery and field development in Norwegian waters", Offshore Northern Seas Conference and Exhibition, Stavanger 1982. Proceedings paper P/4, 84 p.
- Hovland, M. (1981), "A classification of po mark related featuers in the Norwegian Trench", 28 p., Continental Shelf Institut Norway, Publication, 106.
- Huslid, J.M., O.T. Gudmestad and A. A.-Paul: (1982), "Alternate deep water concepts fo Northern North Sea extreme conditions", International Conference on the Behaviour Off-Shore Structures, 3. BOSS'82, Cambrid: Mass. 1982, Proceedings, Vol. 1, pp. 18-4:

- øeg, K. (1976), "Foundation engineering for fixed offshore structures; state of the art", International Conference on the Behaviour of Off-shore Structures, 1. BOSS'76, Trondheim 1976, Proceedings, Vol. 1, pp. 39-69, Also publ. in: Norwegian Geotechnical Institute, Publication, 114.
- øeg, K. (1982), "Geotechnical issues in offshore engineering", State-of-the-art report, International Conference on the Behaviour of Off-Shore Structures, 3. BOSS'82, Cambridge, Mass. 1982, Also publ. in: Norwegian Geotechnical Institute, Publication 144.
- anbu, N. (1973), "Slope stability computations", Embankment-dam engineering, Casagrande volume, pp. 47-86, New York, Wiley.
- arlsrud, K. and L. Edgers (1982), "Some aspects of submarine slope stability", NATO Workshop on Marine Slides and Other Mass Movements, Algarve, Portugal 1980, Proceedings, New York, Plenum, pp. 61-81.
- jekstad, O., T. Lunne and C.J.F. Clausen (1978), "Comparison between in situ cone resistance and laboratory strength for over-consolidated North Sea clays", Marine Geotechnology, Vol. 3, No. 1, pp. 23-36, Also publ. in: Norwegian Geotechnical Institute, Publication, 124.
- jekstad, O. and F. Stub (1978), "Installation of the Elf TCP-2 Condeep platform at the Frigg field", European Offshore Petroleum Conference & Exhibition, London 1978, Proceedings, Vol. 1, pp. 121-130, Also publ. in: Norwegian Geotechnical Institute, Publication, 124.
- ekstad, O. and T. Lunne (1979), "Soil parameters used for design of gravity platforms in the North Sea", International Conference on the Behaviour of Off-Shore Structures, 2. BOSS'79, London 1979, Proceedings, Vol. 1, pp. 175-192, Also publ. in: Norwegian Geotechnical Institute, Publication, 127.
- casse, S. and T. Lunne (1982), "In situ horizontal stress from pressuremeter tests", Symposium on the Pressuremeter and its Marine Applications, Paris 1982, Paris, Editions Technip, pp. 187-208.
- casse, S. and T. Lunne (1982), "Piezocone tests in two soft marine clays", Presented at: Conference on Updating Subsurface Sampling of Soils and Rocks and their In-Situ Testing, Santa Barbara, Cal. 1982.
- uritzsen, R. and K. Schjetne (1976), "Stability calculations for offshore gravity structures", Offshore Technology Conference, 8. Houston 1976, Proceedings, Vol. 1, pp. 75-82, Also publ. in: Norwegian Geotechnical Institute, Publication, 113.
- uritzsen, R.A. (1983), "Personal communication".
- Lunne, T. and H.D. St.John (1979), "The use of cone penetrometer tests to compute penetration resistance of steel skirts underneath North Sea gravity platforms", European Conference on Soil Mechanics and Foundation Engineering, 7. Brighton, England 1977, Proceedings, Vol. 2, pp. 233-238, Also publ. in: Norwegian Geotechnical Institute, Publication, 128.
- Lunne, T., F. Myrvoll and O. Kjekstad (1981), "Observed settlements of five North Sea gravity platforms", Offshore Technology Conference, 13. Houston 1981, Proceedings, Vol. 4, pp. 305-317, Also publ. in: Norwegian Geotechnical Institute, Report, 52410/S-6, Also publ. in: Norwegian Geotechnical Institute, Publication, 139.
- Lunne, T. and T.J. Kvalstad (1982), "Analysis of full scale measurements on gravity platforms; Final report", Foundation performance during installation and operation of North Sea concrete gravity platforms, Oslo, Norwegian Geotechnical Institute and Det Norske Veritas, 92 p.
- Løken, T. (1976), "Geology of superficial sediments in the northern North Sea", International Conference on the Behaviour of Off-Shore Structures, 1. BOSS'76, Trondheim 1976, Proceedings, Vol. 1, pp. 501-515, Also publ. in: Norwegian Geotechnical Institute, Publication, 114, pp. 45-59.
- Marion, H.A. (1974), "Ekofisk oil storage tank", Symposium on Ocean Engineering, London 1974, Proceedings, pp. 83-94, London, The Royal Institution of Naval Architects.
- McClelland, B. (1975), "Trends in marine site investigations; a perspective", 9 p., Offshore Europe 75 Conference, Aberdeen 1975, Proceedings, Paper OE-75220, London, Spearhead Publications.
- Meyerhof, G.G. (1953), "The bearing capacity of foundations under eccentric and inclined loads", International Conference on Soil Mechanics and Foundation Engineering, 3. Zürich 1953, Proceedings, Vol. 1, pp. 440-445.
- Mizikos, J.P. and P.Y. Hicher (1982), "Synthesis of results from geotechnical instrumentation of two different Frigg field gravity structures (North Sea) as recorded from 1978 to 1981", International Conference on the Behaviour of Offshore Structures, 3. BOSS'82, Cambridge, Mass. 1982, Proceedings, Vol. 1, pp. 262-280.
- Mo, O. (1976), "Concrete drilling and production platforms; review of construction, installation and commissioning", 14 p, Offshore North Sea Technology Conference and Exhibition, Stavanger 1974, Proceedings, technology volume.
- Moeyes, B. and M. Hackley (1983), "Soil investigations in the Troll area", Offshore Northern Seas; Advanced Projects Conference, Stavanger 1983, Proceedings, T6, 37 p.

- Morgenstern, N.R. and V.E. Price (1965), "The analysis of the stability of general slip surface", *Géotechnique*, Vol. 15, No. 1, pp. 79-93.
- New Civil Engineer, Special Feature (1973), North Sea oil, *New Civil Engineer*, No. 65, 38 p.
- Norwegian Geotechnical Institute (1972), "Condeep feasibility study; foundation behaviour", BP Forties Field, Locations FB and FD, Block 21/10, British Sector of the North Sea, Project No. 52406, 122 p.
- Norwegian Petroleum Directorate (1977), "Forskrifter for beregning og dimensjonering av faste bærende konstruksjoner på den norske kontinentalsokkel - Regulations for the structural design of fixed structures on the Norwegian Continental Shelf", Stavanger, Var. pag., Text in Norwegian and English.
- Prévost, J.H., B. Cuny, T.J.R. Hughes and R.F. Scott (1981), "Offshore gravity structures: analysis", *American Society of Civil Engineers, Proceedings*, Vol. 107, No. GT 2, pp. 143-165.
- Rahman, M.S., H.B. Seed and J.R. Booker (1977), "Pore pressure development under offshore gravity structures", *American Society of Civil Engineers, Proceedings*, Vol. 103, No. GT 12, pp. 1419-1436.
- Rivette, C.A. (1981), "Shear modulus determination and shear-strain prediction for Drammen plastic clay", MSc Thesis, University of Kentucky, 183 p.
- Rokoengen, K., M. Løfaldli, L. Rise, T. Løken and R. Carlsen (1982), "Description and dating of a submerged beach in the northern North Sea", To be published in *Marine Geology*.
- Rowe, P.W. and W.H. Craig (1979), "Applications of models to predictions of offshore gravity platform foundation performance", *International Conference on Offshore Site Investigation*, London.
- Ruiter, J. de (1975), "The use of in-situ testing for North Sea soil studies", 10 p., *Offshore Europe 75 Conference*, Aberdeen 1975, *Proceedings*, Paper OE-75219, London, Spearhead Publications.
- Schjetlein, I.O. (1983), "Condeep T300 concrete gravity platform for deep waters", *Offshore Northern Seas; Advanced Projects Conference*, Stavanger 1983, *Proceedings*, T10, 33 p.
- Schjetne, K., K.H. Andersen, R. Lauritzsen and O.E. Hansteen (1979), "Foundation engineering for offshore gravity structures", *Marine Geotechnology*, Vol. 3, No. 4, pp. 369-421, Also publ. in: *Norwegian Geotechnical Institute, Publication*, 129.
- Schjetne, K. and E. Brylawski (1979), "Offshore soil sampling in the North Sea", *International Symposium on Soil Sampling*, Singapore 1979, *Proceedings; State of the Art on Current Practice of Soil Sampling*, pp. 139-156, Also publ. in: *Norwegian Geotechnical Institute, Publication*, 130.
- Selnes, P.B. (1981), "Offshore earthquake geotechnology", *International Conference on Recent Advances in Geotechnical Earthquake Engineering and Soil Dynamics*, St. Louis 1981, *Proceedings*, Vol. 2, pp. 817-823; Vol. 3, pp. 1117-1132, Also publ. in: *Norwegian Geotechnical Institute, Publication*, 140, 1982, with the title: *Geotechnical problems in offshore earthquake engineering*.
- Smits, F.P., K.H. Andersen and G. Guddehus (1978), "Pore pressure generation", *International Symposium on Soil Mechanics Research and Foundation Design for the Oosterschelde Storm Surge Barrier - (Symposium on) Foundation Aspects of Coastal Structures*, Delft 1978, *Proceedings*, Vol. 1, pp. II.3.1-II.3.16, Also publ. in: *Norwegian Geotechnical Institute, Publication*, 125.
- Stenhamar, P. and K.H. Andersen (1982), "Fundamenters bæreevne på leire reduseres ved sykklisk belastning", *Bygg*, Vol. 30, No. 7, p. 26, Also publ. in: *Norwegian Geotechnical Institute, Publication*, 141.
- Tryggestad, S. (1983), "Environmental conditions at the Troll field with special emphasis on ocean currents", *Offshore Northern Seas; Advanced Projects Conference*, Stavanger, 1983, *Proceedings*, T7, 56 p.
- Werenskiold, K. (1976), "Maritime operations relative to construction of large concrete offshore structures", *Conference (on) Design and Construction of Offshore Structures*, Institution of Civil Engineers, London 1976, *Proceedings*, pp. 97-105.
- West, R.G. (1969), "Pleistocene geology and biology with especial reference to the British Isles", London, Longmans, 377 p.
- Zuidberg, H.M. (1974), "Use of static cone penetrometer testing in the North Sea", *European Symposium on Penetration Testing*, ESOPT, Stockholm 1974, *Papers*, Vol. 2.2, pp. 433-436.
- Zuidberg, H.M. (1975), "Seacalf: A submersible cone-penetrometer rig", *Marine Geotechnology*, Vol. 1, No. 1, pp. 15-32.